



UNIVERSITY OF NAIROBI

COLLEGE OF BIOLOGICAL AND PHYSICAL SCIENCES

SCHOOL OF PHYSICAL SCIENCES

DEPARTMENT OF METEOROLOGY

**EMPIRICAL ANALYSIS OF SEASONAL RAINFALL
VARIABILITY AND ITS ASSOCIATED EFFECTS ON MAJOR
FOOD CROP YIELDS IN RWANDA**

BY

PROSPER AYABAGABO

REG №: I56/89684/2016

SUPERVISORS: Dr. OPIJAH Franklin J.

Dr. GREATREX Helen

**A RESEARCH DISSERTATION SUBMITTED IN PARTIAL FULFILLMENT OF THE
REQUIREMENTS FOR THE AWARD OF MASTER'S DEGREE IN METEOROLOGY
OF THE UNIVERSITY OF NAIROBI**

DECEMBER 2018

ACKNOWLEDGEMENT

I am highly grateful to Almighty God for his protection, guidance and blessings in all. Secondly, I am deeply indebted to the International Centre for Tropical Agriculture (CIAT) for their sponsorship through the CCAFS/USAID Climate services for Agriculture project for Master's degree studies in Meteorology. Moreover, I am sincerely grateful to the Government of Rwanda through Rwanda Meteorology Agency for the study leave. Special thanks goes to my supervisors, Dr. Opijah Joseph Franklin from the University of Nairobi, Department of Meteorology and Dr. Helen Greatrex from the International Research Institute for Climate and Society (IRI), USA and all the academic and non –academic staff of the department of Meteorology, University of Nairobi. I am indebted to any other person who contributed in any other way towards the achievement of this research project.

DEDICATION

To my beloved family:

My wife, MUTATSINEZA Sophie and our daughter, INEZA AYABAGABO Chloe for their patience during my absence and words of encouragement.

To my beloved Parents:

My father, MUGABOWAKIGELI F. Xavier and mother, MUJAWAMARIYA Drocelle for instilling in me discipline and hard work at an early age, and their words of encouragement.

To all my brothers, sisters and friends.

ABSTRACT

Droughts are common in the lowland areas in the east of Rwanda while floods are frequently observed in the high grounds to the west and north of the country, which may lead to severe negative effects on agriculture during extreme climate conditions.

This study aims at investigating how the variability in seasonal rainfall affects the yield of the major food crops in the country.

The daily gridded rainfall dataset known as ENACTS dataset for a period of 37 years (1981 to 2017) and crop yields data for 12 years (2006 to 2017) on maize and 9 years (2009 to 2017) on beans were used. The data were analyzed using rotated empirical orthogonal function in order to delineate near homogeneous rainfall zones over Rwanda. Furthermore, the analysis of the temporal variability of rainfall onset and/cessation, rainfall amount, frequency and intensity were carried out for each delineated zones. Later, maize and beans temporal variability were studied. Finally, the relationship between rainfall and crop yields were investigated using correlation and regression techniques. Again, the onset/cessation of rainfall in each delineated zone was computed and a standardized precipitation index was calculated in order to understand temporal variability of rainfall amount and frequency. Mann – Kendall and Sen’s slope estimates statistics was computed in order to quantify the magnitude of change in rainfall and its trend

The results indicated that there are ten near homogeneous rainfall zones during the short rains season and nine near homogeneous rainfall zones during the long rains for the 37 years period of seasonal rainfall datasets from 1981 to 2017 over Rwanda. The early onset was found in the zones surrounding the high mountains of Crete Congo Nile, which is in agreement with the migration of the ITCZ during the short and long rains season. The mean seasonal length exceed three months over the western and below two months over the eastern during the long rains season. A shortage in crop yields were recorded over studied zones of Rwanda from 2014 to 2017 with extreme shortage during 2016 and 2017 years. A strong and significant correlation between monthly rainfall amount and crop yields was found over the central plateau (Rugobagoba and Gisanga stations) of Rwanda which means that sufficient rainfall amount for food production is available. A drying trend in rainfall was found over almost all rainfall zones. Strategies to improve on food security needs to be envisaged in all zones especially those with more drying trends.

TABLE OF CONTENTS

DECLARATION	i
ACKNOWLEDGEMENT	ii
DEDICATION	iii
ABSTRACT	iv
LIST OF FIGURES	viii
LIST OF TABLES	xiii
LIST OF ACRONYMS	xv
CHAPTER ONE	1
1.0 INTRODUCTION.....	1
1.1 Background of the study	1
1.2 Statement of the Problem	2
1.3 Objectives.....	3
1.4 Justification of the Study.....	3
1.5 Area of Study	3
1.6 Limitations of the Study.....	5
CHAPTER TWO	6
2.0 LITERATURE REVIEW	6
2.1 Rainfall Mechanisms over East Africa.....	6
2.2 Rainfall Patterns over Rwanda.....	8
2.3 Rainfall influences on Crop yield across sub-Saharan Africa.....	10
2.4 Rainfall influences on Crop yield across Rwanda	12
2.5 Temperature and Precipitation Indices.....	12
2.5.1 Standardized Precipitation index	13

CHAPTER THREE	15
3.0 DATA AND METHODOLOGY.....	15
3.1 Data	15
3.1.1 Definition of season.....	16
3.1.2 Data Quality Control	16
3.2 Methodology	16
3.2.1 Empirical Orthogonal Function analysis	16
3.2.2 Analysis of Onset and Cessation of Rainfall	18
3.2.3 Standardized Precipitation Index Analysis.....	19
3.2.4 Analysis of the Magnitude of Variability	20
3.2.4.1 Mann-Kendall test for Analysis of Trends	20
3.2.4.2 Sen’s Slope Estimator.....	21
3.2.5. Analysis of the Temporal Variation of Rainfall and Yields of Beans and Maize	23
CHAPTER FOUR.....	25
4.0 RESULTS AND DISCUSSIONS.....	25
4.1 Data Quality Control.....	25
4.1.1 Mass Curve Analysis	25
4.1.2 Normality Test.....	28
4.2 Near-homogeneous Seasonal Rainfall Zones during Short and Long rainfall Seasons over Rwanda.....	29
4.3 Temporal Variability of Onset and Cessation from 1981 to 2017	35
4.4 Rainfall Amount and Frequency	57
4.5 Mann Kendall and Sen’s Slope Statistics.....	69
4.6 Analysis of Rainfall and Crop Yields for Maize and Beans	72
CHAPTER FIVE	87

5.0 CONCLUSIONS AND RECOMMENDATIONS	87
5.1 Conclusions	87
5.2 Recommendations	88
5.2.1 Recommendations for Weather and Climate Scientists	88
5.2.2 Recommendations for Policy Makers.....	88
5.2.3 Recommendations for End users	89
REFERENCES	90
APPENDICES	96
STATISTICAL TECHNIQUES	96
A: Homogeneity and Normality Tests of Climate Data.....	96
A.1: The double Mass curve Method	96
A.2 The Shapiro-Wilk's (w) Normality test.....	96
B: Normalized departures.....	97
C. Procedure and Formula for computation of SPI.....	97

LIST OF FIGURES

Figure 1: The new climate zones of Rwanda based on Climatic Data from 1996 to 2011 (Henninger, 2013).....	5
Figure 2: The elevation in meters (a) and Annual Mean Rainfall in mm (b) Maps for Rwanda (sources: Internet and Muhire <i>et al</i> , 2014).....	9
Figure 3: Double Mass curve for Ntendezi and Gisakura during the Short rains season from 1981 to 2017	26
Figure 4: Double Mass curve for Busoro and Ruhuha locations during the Short rains season from 1981 to 2017.....	26
Figure 5: Double Mass curve for Gisanga and Shyogwe during the long rains season from 1981 to 2017	27
Figure 6: Double Mass curve for Gatumba and Rwankuba during the long rains season from 1981 to 2017	27
Figure 7: Derived near homogeneous rainfall zones during Short rains season from 1981 to 2017 over Rwanda. Stars represent meteorological stations	33
Figure 8: Derived near homogeneous rainfall zones during long rains season from 1981 to 2017 over Rwanda. Stars represent meteorological stations	34
Figure 9: Temporal variability and trend of rainfall Onset days for Save Paroisse location during the short rains season from 1981 to 2017	38
Figure 10: Temporal variability and trend of rainfall Onset days for Kibuye location during the Short rains season from 1981 to 2017.....	38
Figure 11: Temporal variability and trend of rainfall Onset days for Ntendezi locations during the short rains season from 1981 to 2017	39
Figure 12: Temporal variability and trend of rainfall Onset days for Tamira location during the Short rains season from 1981 to 2017.....	39
Figure 13: Temporal variability and trend of rainfall Onset days for Cyinzuzi location during the Short rains season from 1981 to 2017.....	40
Figure 14: Temporal variability and trend of rainfall Onset days for Rugobagoba location during the short rains season from 1981 to 2017	40
Figure 15: Temporal variability and trend of rainfall Onset days for Rwamagana location during the Short rains season from 1981 to 2017.....	41

Figure 16: Temporal variability and trend of rainfall Onset days for Gabiro location during the Short rains season from 1981 to 2017.....	41
Figure 17: Temporal variability of rainfall Onset days for Busoro location during the Short rains season from 1981 to 2017	42
Figure 18: Temporal variability and trend of rainfall Onset days for Bukora location during the Short rains season from 1981 to 2017.....	42
Figure 19: Temporal variability and trend of rainfall Onset days for Gatumba location during the long rains season from 1981 to 2017	43
Figure 20: Temporal variability and trend of rainfall Onset days for Rwankeri_Nyabihu location during the long rains season from 1981 to 2017.....	43
Figure 21: Temporal variability and trend of rainfall Onset days for Rwamagana location during the long rains season from 1981 to 2017	44
Figure 22: Temporal variability and trend of rainfall Onset days for Mushubi location during the long rains season from 1981 to 2017	44
Figure 23: Temporal variability and trend of rainfall Onset days for Gisanga location during the long rains season from 1981 to 2017	45
Figure 24: Temporal variability and trend of rainfall Onset days for Gikonko location during the long rains season from 1981 to 2017	45
Figure 25: Temporal variability and trend of rainfall Onset days for Gatunda location during the long rains season from 1981 to 2017	46
Figure 26: Temporal variability and trend of rainfall Onset days for Butare Aero location during the long rains season from 1981 to 2017	46
Figure 27: Temporal variability and trend of rainfall Onset days for Ntaruka location during the long rains season from 1981 to 2017	47
Figure 28: Temporal variability and trend of rainfall Cessation days for Ntendezi location during the Short rains season from 1981 to 2017.....	47
Figure 29: Temporal variability and trend of rainfall Cessation days for Kibuye location during the Short rains season from 1981 to 2017.....	48
Figure 30: Temporal variability and trend of rainfall Cessation days for Tamira location during the Short rains season from 1981 to 2017.....	48

Figure 31: Temporal variability and trend of rainfall Cessation days for Save Paroisse location during the Short rains season from 1981 to 2017	49
Figure 32: Temporal variability and trend of rainfall Cessation days for Cyinzuzi location during the Short rains season from 1981 to 2017.....	49
Figure 33: Temporal variability and trend of rainfall Cessation days for Rugobagoba location during the Short rains season from 1981 to 2017	50
Figure 34: Temporal variability and trend of rainfall Cessation days for Rwamagana location during the Short rains season from 1981 to 2017	50
Figure 35: Temporal variability and trend of rainfall Cessation days for Gabiro location during the Short rains season from 1981 to 2017.....	51
Figure 36: Temporal variability and trend of rainfall Cessation days for Busoro location during the Short rains season from 1981 to 2017.....	51
Figure 37: Temporal variability and trend of rainfall Cessation days for Bukora location during the Short rains season from 1981 to 2017.....	52
Figure 38: Temporal variability and trend of rainfall Cessation days for Gatumba location during the Long rains season from 1981 to 2017.....	52
Figure 39: Temporal variability and trend of rainfall Cessation days for Rwankeri location during long rains season from 1981 to 2017	53
Figure 40: Temporal variability and trend of rainfall Cessation days for Rwamagana location during long rains season from 1981 to 2017.....	53
Figure 41: Temporal variability and trend of rainfall Cessation Days for Mushubi location during long rains season from 1981 to 2017	54
Figure 42: Temporal variability and trend of rainfall Cessation days for Gisanga location during long rains season from 1981 to 2017	54
Figure 43: Temporal variability and trend of rainfall Cessation days for Gikonko location during long rains season from 1981 to 2017	55
Figure 44: Temporal variability and trend of rainfall Cessation days for Gatunda location during long rains season from 1981 to 2017	55
Figure 45: Temporal variability and trend of rainfall Cessation days for Butare Aero location during long rains season from 1981 to 2017.....	56

Figure 46: Temporal variability and trend of rainfall Cessation days for Ntaruka location during long rains season from 1981 to 2017	56
Figure 47: Temporal variability and trend of SPI for Gatumba location during long rains season from 1981 to 2017.....	58
Figure 48: Temporal variability and trend of SPI for Rwankeri_Nyabihu location during long rains season from 1981 to 2017	58
Figure 49: Temporal variability and trend of SPI for Rwamagana location during the long rains season from 1981 to 2017	59
Figure 50: Temporal variability and trend of SPI for Mushubi location during the long rains season from 1981 to 2017	59
Figure 51: Temporal variability and trend of SPI for Gisanga location during the long rains season from 1981 to 2017	60
Figure 52: Temporal variability and trend of SPI for Gikonko location during the long rains season from 1981 to 2017	60
Figure 53: Temporal variability and trend of SPI for Gatunda location during the long rains season from 1981 to 2017	61
Figure 54: Temporal variability and trend of SPI for Butare Aero location during the long rains season from 1981 to 2017	61
Figure 55: Temporal variability and trend of SPI for Ntaruka location during the long rains season from 1981 to 2017	62
Figure 56: Temporal variability and trend of SPI for Ntendezi during the Short rains season from 1981 to 2017	62
Figure 57: Temporal variability and trend of SPI for Kibuye location during the Short rains season from 1981 to 2017	63
Figure 58: Temporal variability and trend of SPI for Tamira location during the Short rains season from 1981 to 2017	63
Figure 59: Temporal variability and trend of SPI for Save Paroisse location during the Short rains season from 1981 to 2017	64
Figure 60: Temporal variability and trend of SPI for Cyinzuzi location during the Short rains season from 1981 to 2017	64

Figure 61: Temporal variability and trend of SPI for Rugobagoba location during the Short rains season from 1981 to 2017	65
Figure 62: Temporal variability and trend of SPI for Rwamagana location during the Short rains season from 1981 to 2017	65
Figure 63: Temporal variability and trend of SPI for Gabiro location during the Short rains season from 1981 to 2017	66
Figure 64: Temporal variability and trend of SPI for Busoro location during the Short rains season from 1981 to 2017	66
Figure 65: Temporal variability and trend of SPI for Bukora location during the Short rains season from 1981 to 2017	67
Figure 66: Temporal variability of Maize yields during the Short rains season (Season A for Agriculture) from 2006 to 2017	72
Figure 67: Temporal variability of Maize yields during the Long rains season (Season B for Agriculture) from 2007 to 2017	73
Figure 68: Temporal variability of Beans yields during the Short rains season (Season A for Agriculture) from 2009 to 2017	74
Figure 69: Temporal variability of Beans yields during the Long rains season (Season B for Agriculture) from 2010 to 2017	74

LIST OF TABLES

Table 1: Weather Conditions classification based on SPI values (WMO_1090, 2012).....	20
Table 2: Test of Normality for representative stations during the short rains season from 1981 to 2017 (Lon: Longitude and Lat: Latitude)	28
Table 3: Test of Normality for representative stations during the long rains season from 1981 to 2017 (Lon: Longitude and Lat: Latitude)	29
Table 4: Eigenvalues and Variance explained for the Short rains season from 1981 to 2017 over Rwanda	30
Table 5: Eigenvalues and Variance explained for the Long rains season from 1981 to 2017 over Rwanda	31
Table 6: Mean Onset and Cessation Dates for the short rains season from 1981 to 2017 over all delineated zones (Lon: Longitude and Lat: Latitude).....	36
Table 7: Mean Onset and Cessation Dates for the long rains season from 1981 to 2017 over all delineated zones (Lon: Longitude and Lat: Latitude).....	37
Table 8: The Percentage Frequency for the Short rains season from 1981 to 2017 based on SPI classifications over the representative stations over Rwanda	68
Table 9: The Percentage Frequency for the long rains season from 1981 to 2017 based on SPI classifications over the representative stations over Rwanda	69
Table 10: Mann - Kendall trend Test and Sen's slope estimates over Rwanda for the Short rains season from 1981 to 2017 over the representative stations	70
Table 11: Mann - Kendall trend test and Sen's slope estimates for rainfall during the long rains season from 1981 to 2017 over Rwanda.....	71
Table 12: Monthly (September, October, November, December) Rainfall Contribution on Maize and Beans Yields during the short rains from 2006 – 2017 over Rwanda	75
Table 13: Test of significance of the monthly (September, October, November and December) rainfall contribution on Maize and Beans yields during the short rains from 2006 to 2017	76
Table 14: Monthly (March, April, May) Rainfall contribution on Maize and Beans yields during the long rains from 2007 – 2017 over Rwanda.....	77
Table 15: Test of significance of the monthly (March, April, May) rainfall contribution on Maize and Beans yields during the long rains from 2007 to 2017	78

Table 16: Significance of the Pearson’s Correlation of the relationship between seasonal rainfall amount and crop yields during the short rains season from 2006 to 2017 over Rwanda	79
Table 17: Significance of the Pearson’s Correlation of the relationship between seasonal rainfall amount and crop yields during the long rains from 2007 to 2017 over Rwanda.....	80
Table 18: Significance of the Pearson’s Correlation of the relationship between rainfall Intensity and crop yields during the short rains season from 2006 to 2017 over Rwanda	81
Table 19: Significance of the Pearson’s Correlation of the relationship between rainfall intensity and crop yields during the long rains season from 2007 to 2017 over Rwanda	82
Table 20: Pearson’s Correlation between rainfall frequency and crop yields during the short rains season from 2006 to 2017 in Rwanda.....	83
Table 21: Pearson’s Correlation between rainfall frequency and Crop yields during the long rains season from 2007 to 2017 in Rwanda.....	84
Table 22: Significance of the Pearson’s Correlation of the relationship between season length and crop yields during the short rains season from 2006 to 2017 over Rwanda	85
Table 23: Significance of the Pearson’s Correlation of the relationship between season length and crop yields during the long rains season from 2007 to 2017 over Rwanda	86

LIST OF ACRONYMS

BAMS: Bulletin of American Meteorological Society

ENACTS: Enhancing National Climate Services

ENSO: El Niño – Southern Oscillation

EOF: Empirical Orthogonal Function

GDP: Gross Domestic Product

IOD: Indian Ocean Dipole

IRI: International Research Institute for Climate and Society

ITCZ: Inter Tropical Convergence Zone

FAO: Food and Agriculture Organization

MAM: March - April - May

MIDIMAR: Ministry of Disaster Management and Refugee Affairs of Rwanda

MINAGRI: Ministry of Agriculture

MER: Monthly Effective Rain

NADSS: National Agriculture Decision Support System

NDMC: National Drought Mitigation Center

MJO: Madden Julian Oscillation

NISR: National Institute of Statistics of Rwanda

NISR_SAS: National Institute of Statistics of Rwanda_ Seasonal Agriculture Survey

OND: October –November- December

PDSI: Palmer Drought Severity Index

QBO: Quasi-Biennial Oscillations

SAS: Seasonal Agriculture Survey

SON: September -October- November

SPI: Standardized Precipitation Index

SSA: Sub- Saharan Africa

SSTs: Sea Surface Temperatures

WMO: World Meteorological organization

WRCC: Western Regional Climate Center

CHAPTER ONE

1.0 INTRODUCTION

This chapter describes the background of the study, the statement of the problem, the main objectives of the research study, justification, the area of study and the limitations of the study.

1.1 Background of the Study

Subsistence agriculture, which mainly depends on rainfall, sustains the Rwandese citizens. The importance of agriculture to the Rwandese population, which was estimated to be 10,515,973 people in 2012 (NISR, 2014) and with an annual growth rate estimated at 2.6%, means increased demand for food and livelihood in the future.

The security of Rwandese citizens' livelihoods has in the past been affected by the space and time variability of rainfall, including extreme rainfall events. Extreme convective precipitation events combined with prolonged wet spells caused flash floods, widespread inundations and landslides. Severe floods associated with the El Niño episode of 1997/1998 damaged so badly the plantations and biodiversity in the basins of Nyabarongo and Akanyaru rivers of Rwanda (Nile Basin Initiative, 2008). The floods caused deaths of 108 people in the northwestern areas of Rwanda in May 2002. In 2007, floods displaced more than 456 families and hundreds of hectares of crops were destroyed in Bigogwe, Nyabihu district (Nile Basin Initiative, 2008). In September 2008, about 2,000 ha were destroyed and 500 families were displaced as a result due to heavy rainfall accompanied with strong winds. This affected 8 out of 12 sectors of the Rubavu district in the north west of Rwanda (Nile Basin Initiative, 2008). The floods and landslides of April to June 2016 led to 118 deaths and damaged 5157 ha of plantations, especially in the northern parts (Gicumbi, Burera and Gakenke District) and western part (Karongi, Ngororero, Nyabihu, Rutsiro and Rubavu Districts) of Rwanda (MIDIMAR, 2016).

The gaps in station measurements hampers the investigation of recent trends in rainfall over Rwanda. The central plateau of Rwanda indicated a drying trend whereas the highlands area and the area surrounding the Lake Kivu had wetter trend from 1935 to 1992 (Muhire *et al*, 2014). Henninger (2013), showed a drying trend over most parts of Rwanda using a relatively small period from 1996 to 2011. He indicated that a strong reduction exists over the northern highlands whereas

constant trend exists over Lake Kivu only compared with the period from 1931 to 1960. Due to the observed changes in rainfall and temperature, Henninger (2013) delineated six climate zones instead of the formerly known four climate zones in Rwanda. Long meteorological time series are necessary to arrive at results that are more conclusive on the optimal number of climatic zones over the country.

1.2 Statement of the Problem

Food security in Rwanda depends largely on rain-fed agriculture since rainfall influences agricultural productivity in the country. The agricultural sector contributes up to 32% of the country's GDP (NISR, 2017). For this reason, analyzing seasonal rainfall pattern like near homogeneous rainfall zones and seasonal rainfall characteristics such as the onset and cessation, intensity and frequency, amount and trends of rainfall is expected to contribute to planning in agriculture as well as the management of water resources and other sectors that depend on rainfall like hydropower production.

The high percentage of missing values in the observed rainfall datasets is a problem in rainfall analysis. A new blended rainfall dataset at high resolution that covers the study area was implemented.

All sectors of the economy of any country are affected by enhanced and depressed rainfall events, which characterize the seasonal rainfall variability. Floods and droughts linked with enhanced and depressed rainfall events severely affects agricultural productivity. These occur at various timescales such as daily, dekadal, monthly or seasonal timescales. Moreover, enhanced food demand is linked with the growth rate of the population. Therefore, strategies to cope with time variability of rainfall for increased food production need to be formulated and implemented. The shortage of the main food crops like maize and beans leads to hunger and the associated effects in families. Therefore, there is a need to reduce the negative effects resulting from the temporal and spatial variability in seasonal rainfall that leads to crop failure through the provision of sufficient weather/climate information in order to achieve food security.

1.3 Objectives

The lack of enough information on the extreme climate events and its linked effects leads to higher vulnerability of communities. Hence, this study sought to contribute on the reduction of vulnerability to extreme climate events.

The overall objective of this study was to determine the effects of seasonal rainfall variability on the variabilities in the yields of beans and maize in Rwanda through empirical analysis techniques.

The specific objectives below were pursued as a means to realize the overall objective.

1. To identify homogeneous climatic rainfall zones in the country.
2. To determine the temporal variability of seasonal rainfall based on its onset and cessation, amount, intensity and frequency.
3. To determine the temporal variability of the beans and maize yields.
4. To determine the effect of temporal seasonal rainfall variability on the temporal variability in crop yields.

The null hypothesis tested was that there exists no relationship between temporal seasonal rainfall variability and the temporal variability in crop yields.

1.4 Justification of the Study

The study is expected to contribute to policy making and planning in agriculture to ensure food security in the near future as well as provide a way of reducing the vulnerability of Rwandese citizens to extreme climate events that are usually associated with the lack of enough information on the characteristics of extreme climate events and their linked effects. The study would contribute to knowledge on seasonal rainfall zones and characteristics. Hence, contribute to improved seasonal yields forecasting.

1.5 Area of Study

Rwanda is located in the southwestern part of the Lake Victoria Basin under the equatorial tropical East Africa. The country is situated between the latitudes 1° 04'S and 2° 51'S and longitudes, 28° 45'E and 31° 15' E. Rwanda borders with the Democratic Republic of Congo to the west, which has the second highest frequency of thunderstorm and lightning activities characterized by

extended deep convection (BAMS, 2016), Uganda to the North, Tanzania to the East and Burundi to the South.

Rwanda has the total surface area of 26,338 km² and a succession of quite large hills and valleys that host its inland rivers from both the Congo and Nile Basin.

The double passage of the Inter Tropical Convergence Zone (ITCZ) over Rwanda due to its location near the equator causes two rainfall regimes. The “short rains” season start from September to December whereas the “long rains” start from March to May. The total precipitation per year ranges from 800 mm to 1600 mm. The drier areas are closer to the border between Rwanda and Tanzania to the east and the wet areas being located at the windward slopes of the Nile-Congo watershed mountains Muhire *et al.*, (2014). Henninger (2013) discussed the four climate zones delineated traditionally over Rwanda, proved that they are not updated with the recent warming trends, and delineated new six climate zones using a dataset from 1996 to 2011. The lowlands and swamps of eastern Rwanda had the hot and relatively dry savanna climate, the central highlands had the temperate climate, the Nile-Congo Watershed Mountains had the cool and humid climate and finally, the Lake Kivu had the land-lake climate based on rainfall and temperature data of the climate normal period from 1931 to 1960. Figure 1 below indicates the new climatic zones based on the 1996 to 2011 climatic dataset by Henninger (2013).

The principal local sources of moisture for rains over Rwanda includes the Lake Victoria Basin and the Congo Air masses. The anomalies from the equatorial tropical Indian Ocean SSTs, Congo convection and equatorial tropical Atlantic as well as the Pacific Ocean fluctuations were linked to the seasonal rainfall in East Africa in several other research studies like Ogallo *et al* (1988); Goddard &Graham (1999); Eliakim (2002) and Omondi *et al* (2012).

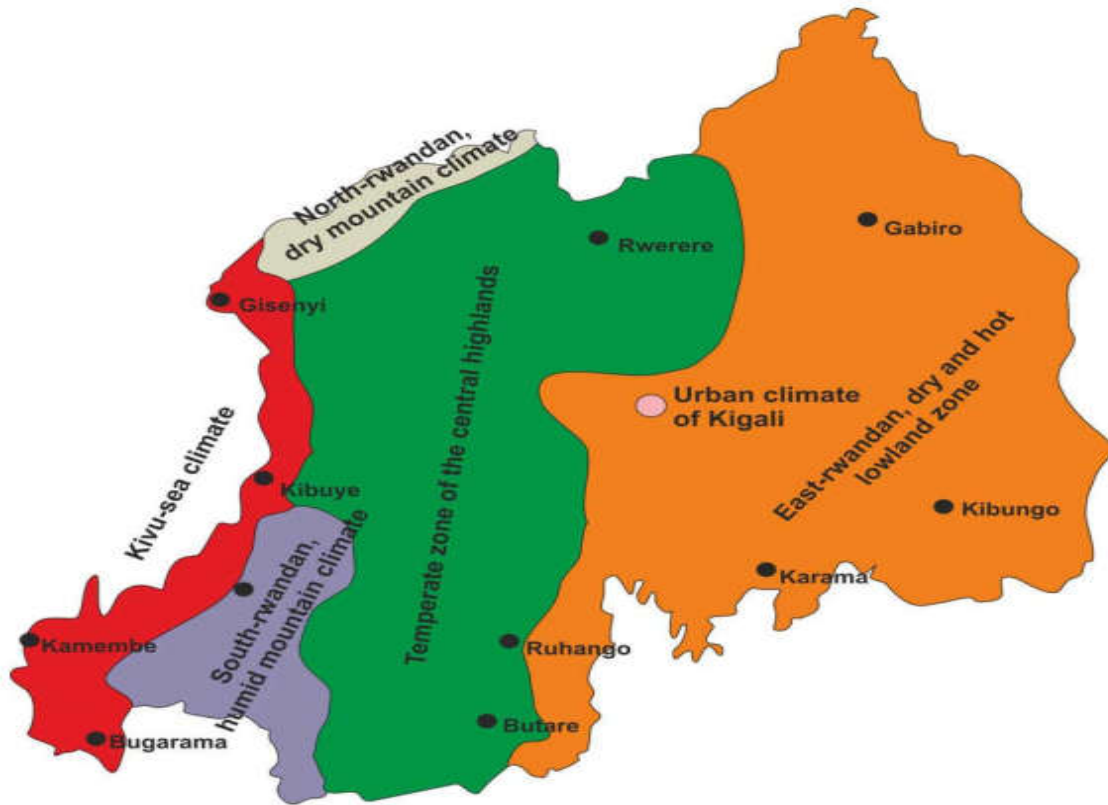


Figure 1: The new climate zones of Rwanda based on Climatic Data from 1996 to 2011 (Henninger, 2013)

1.6 Limitations of the Study

This study investigated the near homogeneous rainfall zones over Rwanda for the period from 1981 to 2017 without taking into account topographical variations using gridded rainfall, ENACTs dataset over the study area. The ENACTs dataset were not validated against the stations observations data during this study.

This study analyzed only maize and beans crop yields in relations with rainfall characteristics for the period from 2006 to 2017 and from 2009 to 2017 respectively. The phonological stages data were not available which leads to its omission in the analysis and this implies that the rainfall effects on crop growth were not analyzed. Crop yields depends on other climatic factors like Temperature, relative humidity, strong winds and non-climatic factors like pests and diseases which were not analyzed in this study.

CHAPTER TWO

2.0 LITERATURE REVIEW

2.1 Rainfall Mechanisms over East Africa

East Africa exhibits a dry annual mean climatology and an annual cycle of two seasons, with the long rains season from March to May and the short rains season from October to December. The systems that control rainfall over this area are occasionally associated with enhanced or depressed rainfall leading to floods or droughts (Camberlin et al, 2009).

The ENSO episode has a determinant role in the monthly and seasonal rainfall patterns over East Africa in some months. The relatively wet conditions were observed during El Niño years' October to December rainfall season and in the following year, March to May season (Indeje *et al*, 2000). In addition, the short rains season following the El Niño year suffer from depressed rainfall events.

The East African seasonal rains variability is associated with the strength of the quasi-permanent high-pressure cells around Africa, namely, the Mascarene high, the St. Helena high, The Azores high and the Arabian high; the ITCZ and the linked monsoonal inflow. These factors interact to develop the meridional and zonal axes of convection in that region. The enhanced meridional axes of convection generates intensified rainfall in Congo basin and the surrounding areas including Rwanda (Eliakim, 2002). In addition, the turn over east-west circulation of the Atlantic Ocean is thought to interact with ENSO in order to modulate the Congo convection. The convection in Congo modulates the rainfall in East Africa through the supply of latent heat and moisture that drive all weather systems. Hence, improved rainfall activity in the Congo basin and East Africa takes place.

In terms of rainfall trend, there exists a significant declining trend in total rainfall for wet days (days with rainfall amount greater than 1mm) over the Greater Horn of Africa (Omondi *et al*, 2013).

The climate of tropical Africa is partly controlled by the variability in SSTs over the Atlantic and Indian Oceans at the inter-annual timescale. The effect of local uptake of global climate signals over the East Africa is observed through rainfall intensification or reduction due to positive or

negative SSTs anomalies respectively (Eliakim, 2002). Warmer SSTs in the western tropical Indian Ocean produces decelerating low-level westerly convergence and moisture transport over the central East Africa whereas Cooler SSTs produces accelerating low-level easterly divergence over the same area (Goddard and Graham, 1999).

The warmer SSTs in the low latitude western Indian Ocean produces enhanced convective heating over those areas. Therefore, anomalous cyclonic circulations set off over the Southeast Africa. Hence, it produces the low-level flow from southeast and moisture transport divergence over southern Africa that leads to reduction of rainfall in that region. This leads to moisture transport convergence and enhancement of rainfall over the Central East Africa (Goddard and Graham, 1999).

The cooler SSTs in the low latitude western Indian Ocean produces reduced convective heating over those areas. Therefore, anomalous anticyclonic circulation set off over the southeast Africa. Hence, it produces the low-level flow from northwest and moisture transport convergence over southern Africa that leads to enhanced rainfall in that region. This leads to moisture transport divergence and reduction of rainfall over the Central East Africa. These two mechanisms form a dipole pattern between the central-eastern and southern African (Goddard and Graham, 1999).

There is a tendency to generate anomalous downward vertical motion and low-level flow of easterlies over near equatorial Africa and the tropical Indian Ocean as a result of warmer SSTs in the central and eastern tropical Pacific Ocean. These lead to suppression of convection in the near equatorial Indian Ocean and Africa. Therefore, a shift of the ITCZ towards the pole over the western Indian Ocean is observed. These changes in the flow pattern produces divergent flow towards the equator and rainfall suppression over southern Africa as well as over the Central East Africa (Goddard and Graham, 1999).

Again, there is a tendency to generate anomalous upward vertical motion and low-level flow of westerlies over near equatorial Africa and the tropical Indian Ocean as a result of cooler SSTs in the central and eastern tropical Pacific Ocean. These lead to intensification of convection in the near equatorial Indian Ocean and Africa. Therefore, a shift of the ITCZ towards the equator over the western Indian Ocean is recorded. These changes in the flow pattern produce convergent flow

towards the pole and enhanced rainfall over southern Africa as well as over the Central East Africa. (Goddard and Graham, 1999).

The formation of a steep slope between the Congo basin and East Africa during the episodes of convergence between the low-level westerlies from the Atlantic Ocean and low-level easterlies from the Indian Ocean because of the interaction between the east-west section of the zonal wind leads to high rainfall events over the Congo (Eliakim, 2002). This pattern enhance the low-level convergence over western Rwanda. The local factors like topography dominate the modulation of seasonal rainfall rather than large-scale factors in high rainfall variability (Eliakim, 2002).

2.2 Rainfall Patterns over Rwanda

Rwanda exhibits a temperate climate despite its location near the equator but most of the central plateau and eastern lowlands areas of Rwanda are semi-arid. The rain shadow area resulting from the western mountains are the origins of the dryness in the Eastern lowlands. The rainfall variability in space has been linked to the highly variable topography and large inland rivers in Rwanda. In addition, the rainfall amounts correlate significantly with the elevation of a given station over Rwanda during the long rains season with a low correlation with SSTs over the Indian Ocean (Ngarukiyimana *et al*, 2017). Figure 2 indicates the topography in meters and annual rainfall in millimetres patterns over Rwanda.

The decrease of rainfall with topography from west to east (Figure 2) especially during October of the short rains season and February suggest an Atlantic monsoon influence and, the homogeneous spatial rainfall distribution agrees with the Inter tropical front or ITCZ mechanism for rainfall (Ilunga *et al*, 2004). The variability of rainfall in time over Rwanda happens on diurnal, dekadal, monthly, intra-seasonal/seasonal and interannual timescales. The variability at interannual timescale has depicted extreme rainfall events like floods and droughts with severe effects on agriculture and other sectors of the economy. The synoptic scale systems that control the rainfall include the ITCZ, which displays two distinct branches mainly meridional and zonal arms. The meridional arm dominate over the country with westerly lower tropospheric winds from the Congo Airmass that enhances precipitation mainly over the western and central parts of Rwanda. The annual patterns of rainfall (Figure 2b) over Rwanda from 1935 – 1992 is given below:

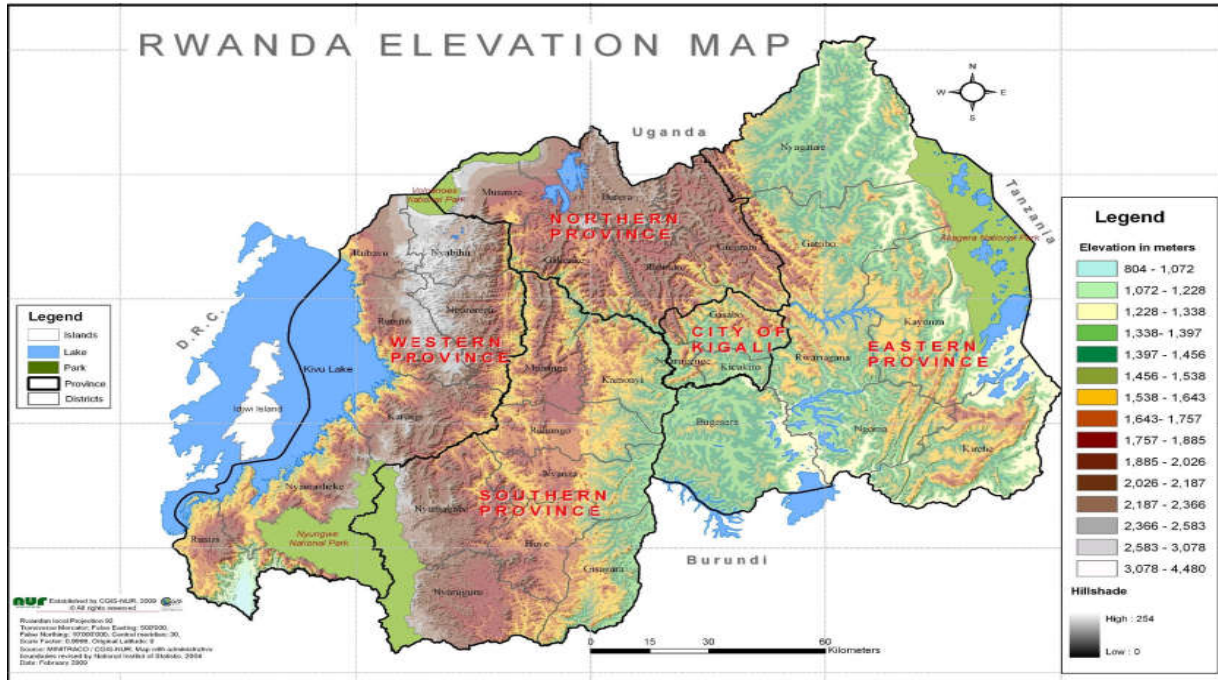


Figure 2a: The elevation map of Rwanda in meters (<http://cgis.ur.ac.rw/content/rwanda-elevation-map>, valid on 5th, December 2018)

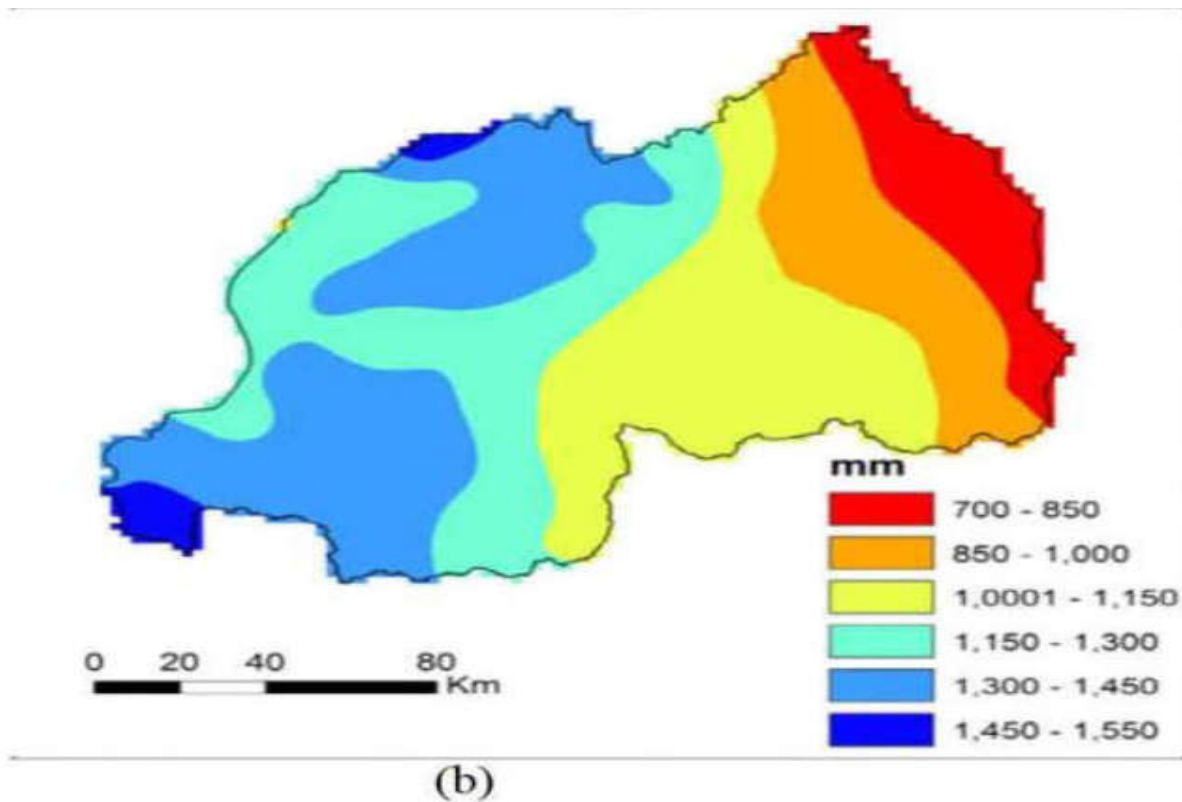


Figure 2b: Annual Mean Rainfall (in mm) distribution for Rwanda (Muhire *et al*, 2014)

In order to understand the temporal variability of rainfall over Rwanda, below are some examples and cases. Sebaziga (2014) examined the association between MJO, wet and dry spells over Rwanda and the results indicated that daily rainfall and MJO indices have moderately significant level of association. Again, findings indicated that a considerable number of wet spells during long rains season occurs between the third week of March and the second week of May while the rainfall peaks were depicted in the first two weeks of March that mark the beginning of the season with the rains starting from western, southern, northern, central and eastern parts respectively. During this study, rainfall onset and cessation for long rains were compared with these to comprehend their variability.

Ndabarasa (2015) determined monthly and seasonal rainfall variability coefficient and found out that dry months had more than 110% of coefficient of variability against 50% of coefficient of variability for wet months and the short rains season had lower coefficient of variability in comparison to the long rains season. Muhire *et al* (2014) found out that from 1935 to 1962, La Niña episodes were better linked to relatively drier conditions, while from 1935 to 1992, El Niño episodes were more linked to wetter conditions; non-ENSO events were strongly linked to drier conditions in the same period. However, for the entire period of study and at all weather stations, the strong relationship between rainfall anomalies and the ENSO events were not identified. Consequently, the long rains variability over Rwanda cannot be explained alone using the ENSO episodes (Muhire *et al*, 2014). Furthermore, during the El Niño events, the frequency of floods tends to be higher whereas during La Niña events, droughts are frequent (Muhire *et al*. 2014). For example, during the La Nina episode of 1999/2000, the east and southeastern part (e.g. Bugesera District) of Rwanda suffered from a crop failure due to drought. The background state of climate in teleconnection to the ENSO episodes is altered by the SSTs anomalies over the Atlantic and Indian Oceans (Omondi *et al.*, 2012). Again, the correlation between ENSO and rainfall events has been non-stationary over time. The drought and floods episode happened in non-ENSO years. These were considered to comprehend the rainfall patterns over Rwanda.

2.3 Rainfall Influences on Crop Yield Across Sub-Saharan Africa

The research evidence shows that crop yields are likely to be severely affected by climate change in many sub-Saharan African countries (Gachene *et al*, 2015). The reliance on rainfall for growing crops made cereal systems vulnerable to climate change and variability in this region.

There is a projected decrease in production growth for cereal by 3.2% in 2050 because of climate change in sub-Saharan Africa for a range of crops. Maize is the principal staple crop relied on in sub-Saharan Africa countries. Maize occupy around 27 million of hectares of the arable land. The 30% of the total arable land used for growing cereals in SSA countries is occupied by maize especially West Africa had 30.9 % of the land for cereals, Central Africa had 8.8%, East African maize occupied, 30.9 % of arable land for cereals whereas Southern Africa maize occupied 29.4% of the area under cereal production. In particular, the crop occupied 62.1% of the total area under cereal production in central Africa (FAO, 2010). In addition, the analysis of calculated and simulated crop yields showed a decrease by more than 10% by 2055 in sub-Saharan African countries (Gachene *et al*, 2015). The impacts of climate change on yields is attributed to the rising frequency of extreme climate events; the elevated carbon dioxide CO_2 ; the interactions between the temperature, and rainfall as well as with soil nutrients; and increased vulnerability of crops to weed competitions, insect, pests and disease. In addition, the agricultural production is limited more by rainfall and water availability than temperatures according to several studies in sub-Saharan Africa. However, modelling the effects of climate change on yields are limited by the ability of models to predict the present day variability of climatic events. In addition, the maize and bean yields are severely affected on seasonal timescales with poor performance of seasonal rainfall like any other crop.

The low yields are generally linked to stress from rainfall deficit, inherent low soil fertility, soil erosion, weeds, pests, diseases, low available input, low input use and lack of improved seed varieties (Gachene *et al*, 2015).

Climate change affects various crops differently and the largest negative yield effects is projected on wheat, followed by sweet potatoes even though the SSA region grows little. The millet and sorghum's stronger resistance to high temperature indicated slightly high simulated yields under climate change (Gachene *et al*, 2015). Thus, the adaptation strategies such as improved germplasm with high resistance to drought and heat stress as well as improved management practices are required in order to address the crop yields in a changing climate over sub-Saharan Africa. Among other countries in East Africa, Rwanda is also subjected to a changing climate in either rainfall amount, rainfall onset/cessation with severe effects on crop yields.

2.4 Rainfall Influences on Crop Yield Across Rwanda

The major food crops in Rwanda include maize, rice, banana, Irish potatoes, sweet potatoes, beans and cassava. The total arable land in Rwanda is 1.4 million hectares that corresponds to 52% of the total land (Ngabitsinze, 2014). Beans (19.8%) rank third in all crops for the total cultivated land after banana (23.2%), cassava (20.8%) followed by the maize during short rains season of 2015/2016, followed by sorghum (9.9%) and then maize (5.1%) during long rains seasons (NISR_SAS2016, 2016). The implementation of the crop intensification program by the Government of Rwanda through the Ministry of Agriculture enhanced the production in maize from 2008. The annual maize production is valued at between 80,000 to 170,000 metric tons with a grain yield of 1.2t/ha (Ngabitsinze, 2014). Both maize and beans are grown in all agro ecological zones of Rwanda. Current studies indicate declining trends in yields will be due to a decrease in mean rainfall in the near future. Muhire *et al* (2015) implemented the simulation of major food crop yields by stochastic weather generator from 2011 to 2050 through incorporation of climate and soil data. He indicated that most appropriate areas for beans, cassava, maize and sweat potatoes are located in the central plateaus and southwest areas of Rwanda except Irish potatoes that are more appropriate for the north – western part of the country. The predicted increase in yields for the indicated food crops lies only in the central plateau of Rwanda. It is expected that the south – western part will record an increase in beans, cassava and sweat potato yield in the short rain seasons. Due to the decreasing trends in mean rainfall and number of rainy days, the decrease in food crop yields is expected over the eastern low lands. During the long rains season, there exist an increase in the predicted yields for beans, maize and Irish potatoes that correlate with an increase in mean rainfall and number of rainy days. Floods, landslides and waterlogged of land due to heavy rains in the north west of Rwanda will affect negatively the yields over there. In this study, near present seasonal rainfall amount in terms of an index and intensity are analyzed in relation to maize and beans yield.

2.5 Temperature and Precipitation Indices

The variability of meteorological surface variables like temperature and precipitation at for example, hourly or daily frequency, requires adequate monitoring so that it contributes greatly in studying climate extremes based on explicitly defined indices (e.g.: McKee *et al*. 1993; Zhang *et al* 2011; Zwiers *et al* 2013). The observed effects of temperature and rainfall on society or

ecosystem mark the reason for studying the temperature and precipitation indices. The studied indices include:

- (i) Quantities in absolute values like maximum and minimum monthly temperature and the maximum precipitation in a year;
- (ii) How often is a fixed threshold like rainfall amount greater than 1mm per day exceeded in a season or on annual basis;
- (iii) How often does a relative threshold like the 95th percentile of daily precipitation in a year exceed above or reduce below it. The threshold is determined from a climatology base period like 1971 to 2000; and
- (iv) Unitless indices like the ratio of annual rainfall that is produced by the rainfall event greater than the 95th percentile of daily precipitation amounts. The threshold is determined from a fixed base period.

2.5.1 Standardized Precipitation Index

McKee *et al.* (1993, 1995) developed the SPI to be an index for moisture supply conditions that performs better compared to the Palmer Drought Severity index (PDSI). The SPI was designed using statistical probability to be an invariable indicator of drought in space so that it allows comparison in space and time. The potential of the SPI led to its adoption by the World Meteorological Organization (WMO). The standardized departure from or with respect to a rainfall probability distribution function is used to express the SPI values. SPI can be applied in various interpretations, for example, to apply this index for agricultural or meteorological purposes, dekads or months period can be used, and for water supply and management purpose, the longer periods of years can be used (Wu *et al.*, 2005).

The calculation of SPI is based on a number of probability distribution functions such as the two parameters gamma distribution; the three parameters Pearson Type III; the three parameters generalized extreme value; the four parameters Kappa and the five parameters Wakeby. The maximum likelihood method is used to estimate parameters in the two-parameter gamma distribution. This is very crucial because using a different probability distribution function would generate different SPI values, even with the same input. Blain *et al.*, 2015 published reasons of the inadequacy of gamma probability density function for SPI computation. However, an evaluation of the monthly precipitation probabilities indicated that gamma distribution was among the more

appropriate function to describe these probabilities. For example, the two parameter gamma probability distribution were used by the U.S. National Drought Mitigation Center (NDMC); Western Regional Climate Center (WRCC); and the National Agricultural Decision Support System (NADSS) calculate the SPI (Wu *et al*, 2007). These motivated the author to use the two-parameter gamma PDF. The two-parameter gamma model has also been implemented in the SPI software distributed by the National Agricultural Decision Support System (NADSS, nadss.unl.edu). This study computed all SPI values based on the two-parameter gamma probability density function (Kumar *et al*, 2009).

Due to its ability to standardize precipitation for a given location and time of interest, the SPI has been widely used for research and operational applications (Wu *et al.*, 2001, Wu *et al.*, 2007). In addition, the standardization also gives a means to determine the unusual probability of the drought episode and the probability to get enough precipitation amount that terminate the drought.

The record length of data limits the computation of SPI value. Hence, more than 50 years of data is recommended for SPI computation but a minimum possible of 30 years can be used. The extreme values of SPI may only be accurate for the long period of rainfall records reaching to 80 years of data or more (Wu *et al.*, 2005).

The SPI is affected by normalization procedure like the selection of probability distribution function that is used as discussed above. Generally, decisions to adjust missing data have a direct effect on the magnitude of computed indices for drought based on precipitation like the SPI. In addition, the true distribution of precipitation data is distorted by the means of space and time averaging that tend to smooth the data. Hence, precipitation data required careful handling and aggregation prior to the calculation of the SPI where monthly totals were added to provide seasonal rainfall totals. In this study, rainfall amounts are expressed in terms of SPI. A full derivation of the SPI is included in Appendix C.

CHAPTER THREE

3.0 DATA AND METHODOLOGY

This chapter comprises the data and the methodology used to achieve the general and the specific objectives of the study.

3.1 Data

This study involved two types of data, namely: rainfall dataset and crop yields data. The rainfall data without missing values i.e. Enhancing National Climate Services (ENACTS) dataset was selected among other rainfall datasets from Rwanda Meteorology Agency (Meteo Rwanda). The ENACTS dataset is an initiative led by the International Research Institute for Climate and Society (IRI) of Columbia University (Dinku *et al*, 2014), aimed at enhancing the availability, access and use of climate information by working directly with the National Meteorological and Hydrological Agency (Dinku *et al*, 2016).

The ENACTS data is created through three steps: Assessment of available stations data, data quality check, and merging satellites data with available stations or rain gauge data. In this process, availability of ENACTS climate data is achieved by quality control of the data from national meteorological observations networks and later, combined with satellites' rainfall estimates, digital elevation models for rainfall and climate reanalysis for temperature. Processed data and derived products are available on the websites of the NMHA and can be downloaded for other applications. In this study, a 5 km x 5 km daily gridded rainfall for Rwanda for 1981-2017 were obtained from Meteo Rwanda.

Crop yields data was collected from both the Ministry of Agriculture of Rwanda (MINAGRI) and National Institute of Statistics of Rwanda (NISR) for the period of 2007 – 2013 and 2014 – 2017 respectively. The first was collected from crop assessment reports while the latter is from seasonal agriculture survey (SAS) report. The differences in methodology of data collection caused a slight reduction in the number of for the 2014 and 2015 yields records as a result of introducing strata in the calculation of crop yields. The six locations for each season were selected randomly depending on the availability of crop yields data in the near homogeneous rainfall zones for rainfall influence on maize and beans yields studies.

The maize and beans were selected among other main crops of Rwanda due to the fact that these crops are grown in both seasons and their studies together with seasonal rainfall can be implemented. In addition, the yields data was tabulated from each yearly crop assessment and seasonal agriculture survey report.

3.1.1 Definition of Season

There exists two major rainfall seasons in Rwanda, namely: the short rains season, locally known as *Umuhindo* extending from September to December and the long rains season, locally known as *Itumba* extending from March to May. According to Ilunga *et al* (2004), the month of September is considered drier over the eastern low lands. Hence, the short rains season exhibits a 3-month pattern over this area. However, rainfall amount analysis was carried out separately for every 3 months i.e., September to November and October to December for short rains season and March to May for long rains season. This would help in understanding how the months of September or December contribute to the overall index.

3.1.2 Data Quality Control

The data analysis first involved statistical data quality control and tests of homogeneity for selected rainfall data using double mass curve (Gonzalez – Rouco *et al*, 2000; Mugume *et al*, 2016) and Shapiro’s normality test. The double mass curve reflects the measure of how one station’s seasonal cumulative rainfall compares to another neighboring station. For very similar cumulative rainfall, the line of best fit is a straight line and all points lie on the line with no outliers. The normality test helps to understand how the seasonal rainfall is distributed along the mean in a normal distribution. The station with non-normally distributed values caused by uneven distribution of observed rainfall along the mean was crosschecked to comprehend the extreme cases.

3.2 Methodology

The methods used to achieve the study objectives are presented and discussed in this section

3.2.1 Empirical Orthogonal Function Analysis

The Empirical Orthogonal Function (EOF) was carried out to delineate the homogeneous rainfall zones over Rwanda. The method consisted of finding the interrelation between space and time variables in order to depict the underlying structure of these variables. The EOF was used due to the combination of space and time trends in rainfall data. EOF provide unique answer, which does

not dependent on any hypothesis about the data distribution. Principal component analyses were implemented, firstly, to depict the dynamics of seasonal rainfall from 1981 to 2017 over Rwanda by combining time and space variables. Secondly, to reduce the rainfall data dimension where a few factors are used to explain a certain percentage of variance. Thirdly, to minimize the redundancy in the rainfall data and later for data compression and filtering the atmospheric noise in the data. The main goal of EOF was to decompose a continuous space-time field $X(s, t)$, where s and t denote space and time variables respectively.

While performing principal component analysis, a linear combination of variables in the dataset is assumed to exist. Another assumption is that components with higher variance explain meaningful dynamics in the data whereas components with a lower variance explain the noise. The outcome of a factor analysis are uncorrelated components expressed in terms of several orthogonal lines of best fit to the dataset. The first component is expressed as the linear combination of variables such that the greatest variance in the dataset lay on the first axis. The second component lay on the second axis with the second greatest variance, and so on. Eigenvectors were combined with values across all variables. This combination between the components and the original variables is called the component's eigenvalue. In multiple variable spaces, component loadings were defined by the correlation between the components and the original variables. The percentage variance explained by the component in a variable was obtained from the component loadings. The square of the component loadings gave the amount of explained variation in a similar way for Pearson's coefficient of correlation.

In atmospheric sciences, there exist a common practice of delineating homogeneous climate zones like in Sanogo *et al* (2015), Diro *et al*, 2011, Basalirwa *et al* (1999) and Basalirwa *et al* (1995). The rotated empirical orthogonal function was used to identify zones of similar rainfall trends and patterns using gridded rainfall data from 1981 to 2017 over Rwanda. The rotated EOF is known to provide more understandable physical interpretation than the original EOF. The EOF Analyses were done on standardized seasonal rainfall data for both the short rains and the long rains seasons for the period of study.

The "Scree" test criterion (O'Lenic and Livezey, 1988) were used to judge the number of components to rotate orthogonally in order to properly delineate Rwanda into near homogeneous

rainfall zones. The orthogonal rotation dropped all the EOFs after the steep decline in the percent variance explained to more or less constant values.

Suppose that X is a matrix of $P \times N$ seasonal rainfall data, P is the number of seasons and N is the number of stations. That matrix was decomposed into linear functions of P temporal and N spatial vectors so that the rainfall observation X_{ij} on season i at station j is given as follows:

$$X_{ij} = \sum_{k=1}^n c_{ik} e_{kj} \Leftrightarrow X = ce \quad (3.1)$$

In (3.1), c_{ik} is the element for season i in the k^{th} time vector and e_{kj} is the element for station j in the k^{th} space vector.

The result from the analysis of EOF are given by a matrix of covariance or correlation coefficients that stands for the transformed coefficients or eigenvectors written in the order of variation from the highest to the lowest coefficient. The total variance for each component was accounted for as an eigenvalue. Hence, the spatial variability of the 37 years rainfall data were reproduced at large using a few of the space vectors. The interpretation was done in terms of physical mechanisms that generate rainfall.

The EOF technique found a new set of variables that depict most of the observed variance from the rainfall dataset through the linear combination of original variables (Jolliffe, 2002 and Hannachi *et al*, 2007). The rotated EOF method is better suited to complex terrain climate of Rwanda due to its robustness in physical interpretation. The gaps in station data in the 1990s are disadvantageous in manual and automatic weather stations records, which prove why gridded rainfall was considered.

3.2.2 Analysis of Onset and Cessation of Rainfall

The onset of rains or the start of rainfall season, OD, was defined as the 1st day of a five-day period from 1st of September or 1st March for short and long rains respectively with at least a total rainfall of 20 mm recorded. The onset days for the short and long rains season was calculated for individual years as in Adelekan & Adegebo, 2014; Mensah *et al*, 2016 using the definition below:

- (i) At least 20 mm of rainfall recorded in the period of five (5) consecutive days of observation

(ii) At least three days in five received rainfall not less than 1 mm. The start day must be a rainy day.

(iii) The 30 days following the start day must not have a dry period of seven days or more.

Again, the onset was calculated using Fuzzy logic approach as given by the Equation (3.2):

$$OD = D \frac{(20-F)}{R}, \quad (3.2)$$

In Equation (3.2), OD represents the onset date, D is the total number of days in the first month of the season with effective rain (Monthly Effective Rain, MER means the accumulated rainfall totals that are equal to or exceed 20 mm). F is the accumulated rainfall totals of earlier month in mm and R is the accumulated rainfall within MER.

The rainfall cessation was defined based on the following criteria:

(i) The period of five (5) consecutive days with total rainfall less than 20 mm

(ii) The period of three (3) days out of five (5) days with rainfall less than 1mm (three dry days in five)

(iii) The period of five (5) days were followed by at least seven (7) dry days.

Alternatively, the cessation day were computed using Fuzzy logic approach (Mensah *et al*, 2016) as given by the Equation (3.3):

$$CD = b + 275 \quad (3.3)$$

In the Equation (3.3), CD denotes the cessation date. The number of days in which there exist a maximum improvement of the pre-season moisture is denoted by the letter b . CD was defined as any day after which there are more than 7 consecutive days of rainfall with amount below 50% of the soil water requirements from the 1st of December or the 1st of May.

3.2.3 Standardized Precipitation Index Analysis

The standardized precipitation Index (SPI) was based on the probability of rainfall for any timescale. The probability of observed seasonal rainfall for the last 37 years was transformed into an index that was used to provide moisture conditions and help assess the drought or rainfall shortage severity.

The long-term gridded rainfall data from 1981 to 2017 was used to compute the SPI sums for each delineated near homogeneous rainfall zone. The long-term record was fitted into a gamma probability distribution function, and later transformed into a normal distribution so that the mean SPI for each location during the last 37 years period is zero (WMO, 2012). Positive SPI values indicated that rainfall greater than the median rains occurred while negative values indicated that rainfall lesser than median rains occurred for a given rainfall zone. The Table 1 below indicates the weather condition classification suggested by WMO based on SPI values. The SPI is a normalized index. Hence, it was used to indicate both wet and dry climates in the same way. Again, the SPI can be used to monitor wet conditions. During this dissertation project, the SPI for one month (SPI -1), and SPI for three-months (SPI-3) were calculated to reflect crop stress, short and medium term moisture conditions. The classification approach shown in Table 1 below defined weather conditions based on SPI values according to WMO (2012).

Table 1: Weather Conditions classification based on SPI values (WMO_1090, 2012)

SPI Values	Class of SPI
2.0 or more	Extremely wet
1.5 to 1.99	Very wet
1.0 to 1.49	Moderately wet
-0.99 to 0.99	Near normal
-1.0 to -1.49	Moderately dry
-1.5 to -1.99	Severely dry
-2 and less	Extremely dry

3.2.4 Analysis of the Magnitude of Variability

3.2.4.1 Mann-Kendall Test for Analysis of Trends

The analyses of the seasonal rainfall trend form 1981 to 2017 over Rwanda were determined using the Mann-Kendall test (Sanogo *et al*, 2015; Ahmad *et al*, 2015; Ganguly *et al*, 2015; da Silva *et al*, 2015; Nsubuga *et al*, 2014). The Mann-Kendall (Mann 1945; Kendall 1975) were calculated using Equation (3.4) as:

$$S = \sum_{i=1}^{n-1} \sum_{j=i+1}^n \text{sgn}(x_j - x_i) \quad (3.4)$$

In Equation (3.4), n denotes the number of data points while x_i and x_j are the data values in the time series i and j , where ($j > i$) respectively, and $sgn(x_j - x_i)$ is the sign function as:

$$sgn(x_j - x_i) = \begin{cases} +1 & \text{if } (x_j - x_i) > 0 \\ 0 & \text{if } (x_j - x_i) = 0 \\ -1 & \text{if } (x_j - x_i) < 0 \end{cases} \quad (3.5)$$

The variance was computed as:

$$Var(S) = \frac{n(n-1)(2n+5) - \sum_{i=1}^P t_i(t_i-1)(2t_i+5)}{18} \quad (3.6)$$

In Equation (3.6) n denotes the number of data points, P stands for the number of tied groups, the sign (Σ) denotes the summation of all tied groups, and t_i denotes the number of data values in the P^{th} group. The summation part was ignored in the case of missing tied groups in the data. A tied group is defined as a group of sample data with equal values.

During this study, the sample size was given by $n = 37$. Hence, the standard normal test statistic Z_s was computed using Equation (3.7) as follows:

$$Z_s = \begin{cases} \frac{S-1}{\sqrt{Var(S)}} & \text{if } S > 0 \\ 0 & \text{if } S = 0 \\ \frac{S+1}{\sqrt{Var(S)}} & \text{if } S < 0 \end{cases} \quad (3.7)$$

The positive values of Z_s denote an increasing trend while negative Z_s values denote a decreasing trend. The specific significance level of $\alpha = 0.05$ was used to test the trends. The null hypothesis of no trend in rainfall data was rejected and a significant trend exists in the time series for $|Z_s| > Z_{1-\frac{\alpha}{2}}$. The value of $Z_{1-\frac{\alpha}{2}}$ was obtained from the standard normal distribution table. The null hypothesis for no trend was rejected for $|Z_s| > 1.96$ at the 5% significance level.

3.2.4.2 Sen's Slope Estimator

The determination of the magnitude of trends for 37 years rainfall data was done using the Sen's slope estimator. The nonparametric procedure developed by Sen (1968) was used to estimate the magnitude of the slope in a sample of n pairs of rainfall data from 1981 to 2017 for each delineated

near homogeneous rainfall zone. The Sen's slope estimator has been widely used in hydro-meteorological time series (Kundu *et al*, 2015, Sanogo *et al*, 2015, da Silva *et al*, 2015). The Sen's slope estimator approach quantify the slope of the trend using a linear model whose residual's variance must be constant in time. The linear model is expressed using Equation (3.8):

$$Q_i = \frac{X_j - X_k}{j - k} \text{ for } i = 1, \dots, N \quad (3.8)$$

In Equation (3.8) X_j and X_k are the data values at time j and k with ($j > k$). In case of only one date in each time period, then

$$N = \frac{n(n-1)}{2} \quad (3.9)$$

In Equation (3.9), n is the number of observations. If there were multiple observations in one or more period, $N < \frac{n(n-1)}{2}$ was considered.

After the calculation, the N values of Q_i were ranked from the smallest to the largest, and the median of slope or Sen's slope estimator were computed as:

$$Q_{median} = \begin{cases} Q_{[\frac{(n+1)}{2}]}, & \text{if } n \text{ is odd} \\ \frac{Q_{[\frac{n}{2}]} + Q_{[\frac{(n+2)}{2}]}}{2}, & \text{if } n \text{ is even} \end{cases} \quad (3.10)$$

In Equation (3.10), the sign of Q_{median} reflects data trend, while its value indicates the steepness of the trend. The confidence interval of Q_{median} at specific probability was determined in order to decide whether the median slope was statistically different from zero. The confidence interval was calculated at the significance level of $\alpha = 0.05$ and the time slope was computed as follows:

$$C_\alpha = Z_{1-\frac{\alpha}{2}} \sqrt{Var(S)} \quad (3.11)$$

In Equation (3.11), $Var(S)$ is the variance and the standard normal distribution table provided the $Z_{1-\frac{\alpha}{2}}$ value. The lower and upper limit of the confidence interval, Q_{min} and Q_{max} were the M_1^{th} largest and $(M_2 + 1)^{th}$ largest values of the n ordered slope estimates. Moreover, the values of M_1 and M_2 were calculated as, $M_1 = (n - C_\alpha) / 2$ and $M_2 = (n + C_\alpha) / 2$ for the limits. When the lower and upper limits have similar sign, the slope Q_{median} had a value statistically different from zero.

3.2.5. Analysis of the Temporal Variation of Rainfall and Yields of Beans and Maize

The variability of yields of maize and beans as a function of time for a specific delineated zone were studied during both the short and the long rains season. Later, the standardized anomalies in crop yields were correlated with the standardized precipitation index, rainfall frequency, rainfall intensity and the length of the season for the available crop yields dataset.

Quantitative analysis of the relationship between rainfall and crop yield was carried out using correlation and regression techniques. The Pearson's correlation coefficient, R and multivariate linear regression analysis were done to establish the linear relationship between the rainfall and crop yields. The Pearson's correlation coefficient was determined to measure the strength of the linear relationship between maize or beans' yield variability and rainfall variability where -1 and $+1$ denotes, respectively, complete indirect and direct dependency of the two variables and 0 denotes the complete independency between variables.

The Pearson's coefficient of correlation was computed using the Equation (3.12) below, in which x represents the predictor variable (rainfall) and y represents the response variable (maize and beans' yields).

$$r = \frac{\sum(x_i - \bar{x})(y_i - \bar{y})}{\sqrt{\sum(x_i - \bar{x})^2 \sum(y_i - \bar{y})^2}} \quad (3.12)$$

The regression model between the rainfall anomalies and yields' anomalies was implemented in order to confirm how much variation of the response variable could be expressed by the predictor variable using the linear Equation (3.13):

$$\Delta y = a + (\alpha \cdot \Delta P_1) + (\beta \cdot \Delta P_2) + (\gamma \cdot \Delta P_3) + (\delta \cdot \Delta P_4) \quad (3.13)$$

In Equation 3.13, Δy is the variability in yield due to variability in seasonal rainfall amount either in the short or long rains season for each delineated rainfall zone, a is the regression coefficient and, α , β and γ are coefficients of the monthly rainfall during either the short or the long rains season. Similarly, ΔP_1 , ΔP_2 and ΔP_3 are the variability in monthly rainfall for the first, second and third months respectively.

Finally, the coefficient of determination, which is the square of the Pearson's correlation coefficient, was calculated to get the percentage of the variance in crop yields explained by the

variability in rainfall for each delineated zone and season. The test of significance of the correlation between rainfall, beans and maize yields were done using the student t test.

CHAPTER FOUR

4.0 RESULTS AND DISCUSSIONS

This chapter summarizes the outcome from various analysis methods used in order to accomplish the overall and specific objectives of the study.

4.1 Data Quality Control

The gauge datasets were quality-controlled through testing them for homogeneity and normality. This study used more than 200 gridded rain gauge datasets for both seasons. The selection of near homogeneous rainfall zones and the representative stations was done through a rotated principal component analysis that generated 24 components in terms of spatial and temporal patterns. The stations with high squared component loading were selected to represent a factor or a component and the latter correlated with each other and seasonal rainfall to determine how many homogeneous rainfall zones are required. As a result, 10 stations and 9 stations were used to represent 10 and 9 near homogeneous rainfall zones for short rains and long rains, respectively.

4.1.1 Mass Curve Analysis

A double mass curve analysis was performed and the results proved a small deviation from cumulative rainfall between two stations' data on selected stations during both short and long rains season. The selected stations represent the wetter and the drier zones during the short rains season while the selected stations for the long rains season represent the central region that is considered for continuous suitable climate to major food crops by some authors like Muhire *et al* (2014). The double mass curve indicates how good the cumulative values of one station approach the cumulative value of a neighboring station. In addition, the number of outliers indicates the level of discrepancy of two cumulative values. Figure 3 to Figure 6 show the mass curves for selected stations. The figures indicated the line of best fit passing through zero on a scatter plot between two cumulative seasonal rainfall values of two stations in each for four delineated zones as an example. Simultaneously, Gisakura and Ntendezi stations on Figure 3 and Busoro and Ruhuha stations on Figure 4 exhibited nearly homogeneous cumulative rainfall in the last 37 years from 1981 to 2017 during the short rains season.

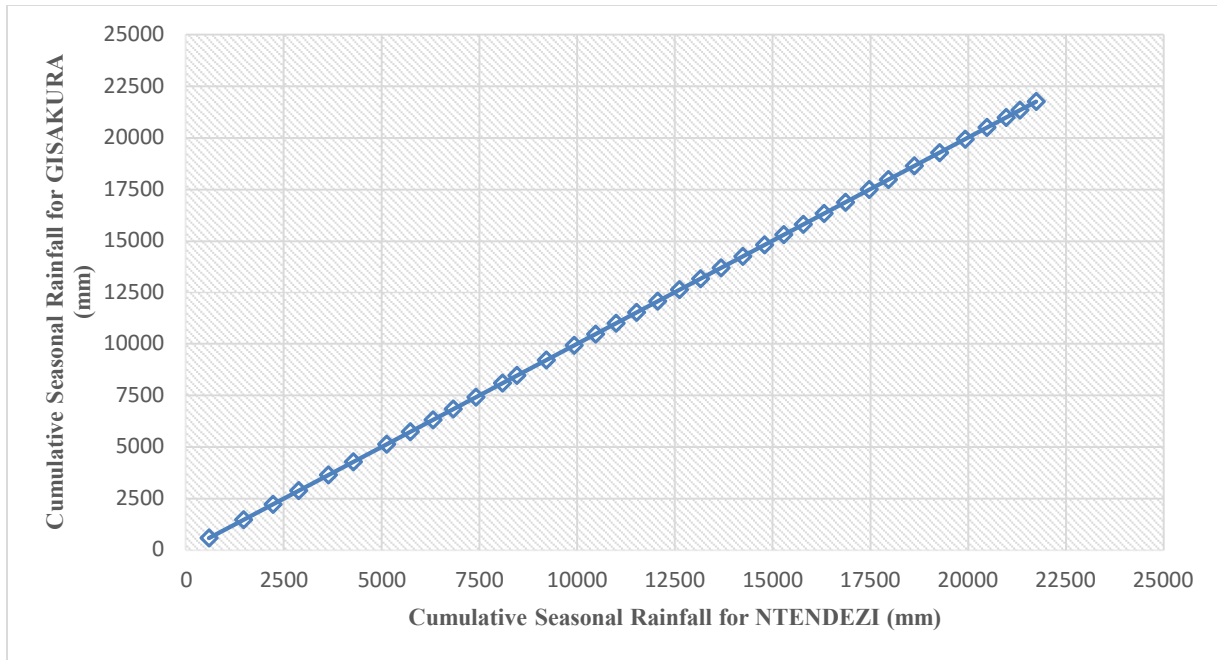


Figure 3: Double Mass curve for Ntendezi and Gisakura during the Short rains season from 1981 to 2017

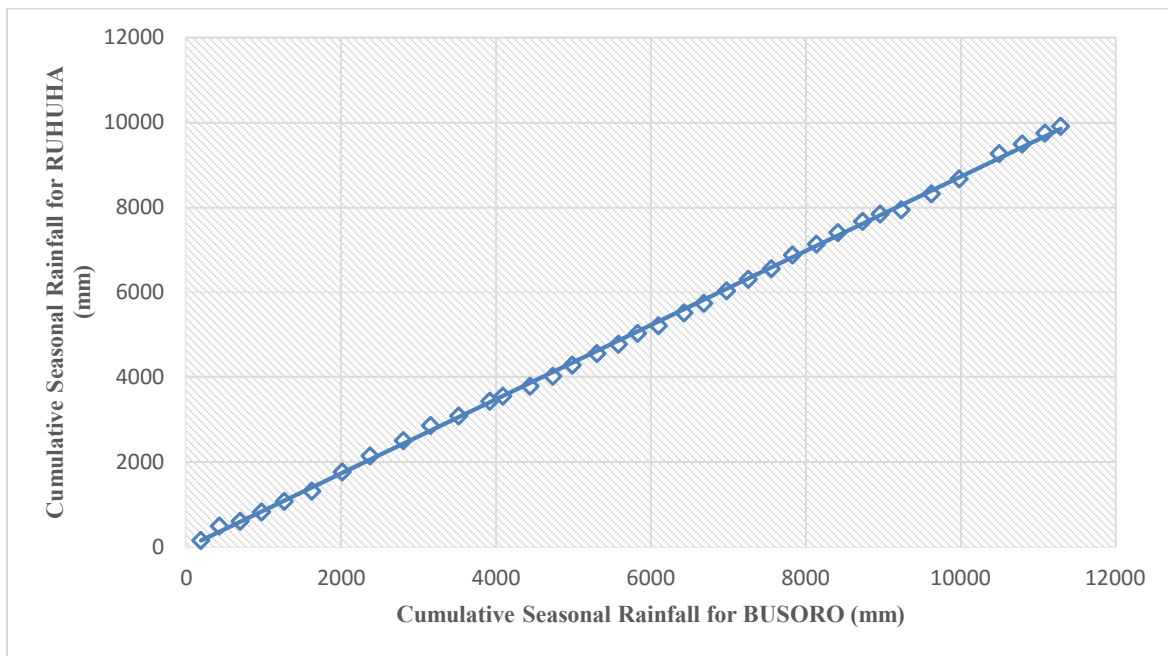


Figure 4: Double Mass curve for Busoro and Ruhuha locations during the Short rains season from 1981 to 2017

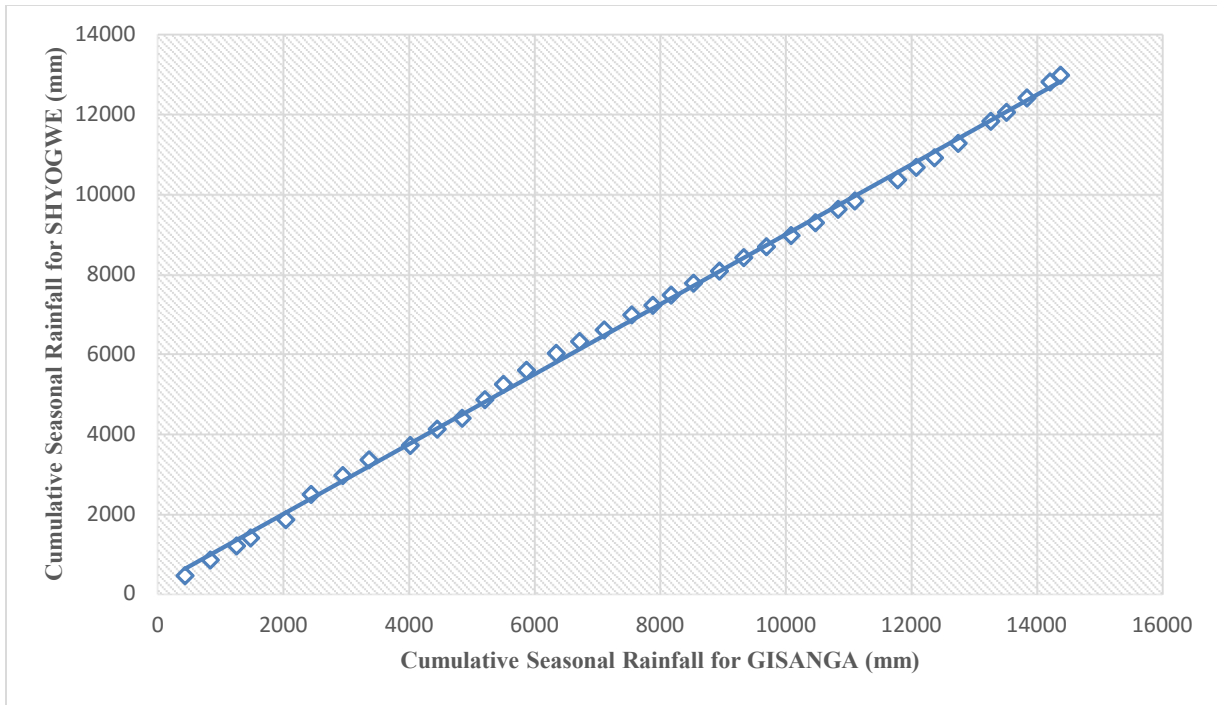


Figure 5: Double Mass curve for Gisanga and Shyogwe during the long rains season from 1981 to 2017

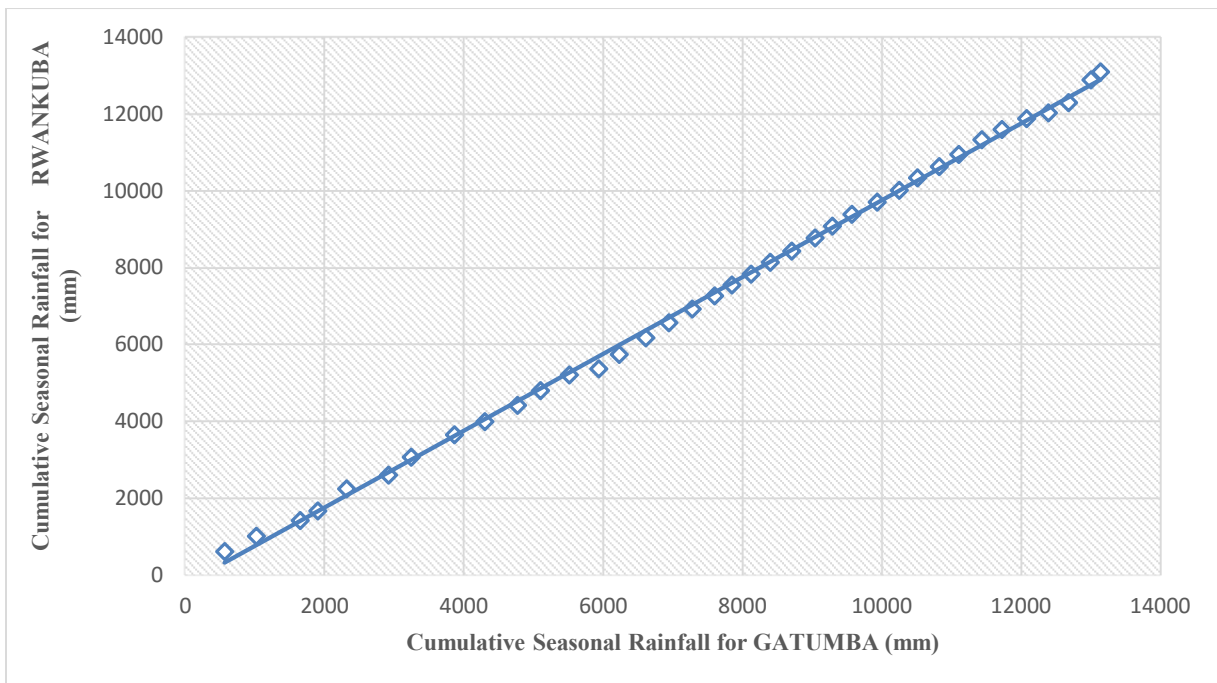


Figure 6: Double Mass curve for Gatumba and Rwankuba during the long rains season from 1981 to 2017

4.1.2 Normality Test

The normality test was preferred in order to show if the seasonal rainfall exhibited a normal distribution around the mean rainfall during the period of study (37) years over identified near homogeneous rainfall zones. Table 2 and Table 3 indicate the results from the normality test of rainfall data from 1981 to 2017 over the representative stations during the short and the long rains seasons respectively.

Table 2: Test of Normality for representative stations during the short rains season from 1981 to 2017 (Lon: Longitude and Lat: Latitude)

Stations Names	Altitude in m	Lon	Lat	Shapiro – Wilk’s statistics	P -- values
Ntendezi	1600	29.05	-2.43	0.95	0.12
Kibuye	1470	29.35	-2.05	0.97	0.38
Tamira	2300	29.35	-1.56	0.97	0.35
Save Paroisse	1725	29.76	-2.55	0.95	0.10
Cyinzuzi	1950	30	-1.76	0.93	0.02
Rugobagoba	1542	29.88	-2.05	0.95	0.09
Rwamagana	1535	30.43	-1.93	0.87	0.0004
Gabiro	1472	30.4	-1.55	0.72	3.91×10^{-7}
Busoro	1478	29.91	-2.28	0.96	0.23
Bukora	1355	30.78	-2.3	0.97	0.48

The stations with a low p-value ($P \leq 0.05$) exhibit a tendency to normal distribution along the means while others exhibit a shift in the distribution towards non-normal distribution that implies some cases of extremes or outliers in the observed rainfall patterns were frequent. As is shown in Table 2, the Bukora station that is situated at a lower altitude in a semi-arid part to the East exhibited a higher p-value. This was linked to the observed higher variability in rainfall characteristics during the short rains season, as there existed a positive correlation between topography and rainfall amount in Rwanda (Ngarukiyimana, 2017). As is shown in Table 3, the Gikonko station that is located in the semi-arid part of the South also exhibited a higher p-value as

a result of higher variability in the long rains seasonal rainfall. Cyinzuzi, Rwamagana and Gabiro stations exhibited a near normally distributed rainfall along the mean rainfall, which means that the low variability existed in these areas from 1981 to 2017 during the short rains season. During the long rains season, Gatumba; Rwankeri; Gisanga; Gatunda and Ntaruka stations exhibited near normally distributed rainfall for the entire period from 1981 to 2017

Table 3: Test of Normality for representative stations during the long rains season from 1981 to 2017 (Lon: Longitude and Lat: Latitude)

Stations Names	Altitude in m	Lon	Lat	Shapiro – Wilk’s statistics	P -- Values
Gatumba	1536	29.61	-1.93	0.88	0.001
Rwankeri	2250	29.51	-1.58	0.91	0.006
Rwamagana	1535	30.43	-1.93	0.97	0.391
Mushubi	2040	29.45	-2.36	0.96	0.275
Gisanga	1550	29.86	-2.13	0.93	0.027
Gikonko	1612	29.86	-2.48	0.98	0.825
Gatunda	1505	30.21	-1.36	0.93	0.026
Butare_Aero	1760	29.71	-2.6	0.97	0.362
Ntaruka	1765	29.75	-1.46	0.94	0.035

4.2 Near-homogeneous Seasonal Rainfall Zones during Short and Long rainfall Seasons over Rwanda

This study used rotated principal component analysis for seasonal rainfall using 215 and 218 gridded rain gauge datasets to zone Rwanda into near homogeneous seasonal rainfall for September to December and March to May seasons, respectively. In order to maximize the variance of the squared loadings of a factor on all variables in a factor matrix, the varimax rotation was used. The varimax rotation is an orthogonal rotation of the factor axes and has the effect of differentiating the original variables by the extracted factor. The results for the 24 significant component rotation is given in Table 4 & 5 for the short and the long rains seasons, respectively.

Table 4: Eigenvalues and Variance explained for the Short rains season from 1981 to 2017 over Rwanda

Component	Eigenvalue	Variance explained	Cumulative variance in %
1.	26.48	12.038	12.038
2.	25.9	11.779	23.817
3.	18.57	8.443	32.26
4.	17.67	8.034	40.294
5.	13.66	6.213	46.507
6.	12.07	5.489	51.996
7.	12.06	5.484	57.48
8.	10.52	4.786	62.266
9.	9.16	4.163	66.429
10.	7.54	3.429	69.858
11.	7.48	3.399	73.257
12.	5.85	2.662	75.919
13.	5.73	2.605	78.524
14.	5.53	2.515	81.039
15.	5.19	2.360	83.399
16.	5.03	2.287	85.686
17.	4.76	2.165	87.851
18.	4.36	1.984	89.835
19.	3.55	1.615	91.45
20.	3.41	1.550	93.000
21.	3.21	1.461	94.461
22.	2.57	1.168	95.629
23.	2.13	0.969	96.598
24.	1.93	0.878	97.476

Table 5: Eigenvalues and Variance explained for the Long rains season from 1981 to 2017 over Rwanda

Component	Eigenvalues	Variance explained	Cumulative variance in %
1.	25.948	11.688	11.688
2.	25.678	11.567	23.255
3.	25.647	11.553	34.808
4.	20.081	9.046	43.854
5.	13.534	6.096	49.95
6.	13.046	5.877	55.827
7.	11.097	4.998	60.825
8.	10.009	4.509	65.334
9.	8.403	3.785	69.119
10.	7.723	3.479	72.598
11.	7.057	3.179	75.777
12.	6.547	2.949	78.726
13.	5.756	2.593	81.319
14.	5.589	2.518	83.837
15.	4.724	2.128	85.965
16.	3.811	1.717	87.682
17.	3.668	1.652	89.334
18.	3.418	1.540	90.874
19.	3.377	1.521	92.395
20.	3.344	1.506	93.901
21.	2.978	1.341	95.242
22.	2.337	1.053	96.295
23.	2.246	1.012	97.307
24.	1.356	0.611	97.918

The principal component analysis indicated 24 significant components for both the short rains season and long rains season over Rwanda that, respectively, accounted for 97.47 % and 97.92 % of the total variance in seasonal rainfall. Clustering of the principal component and simple correlation analysis provided 10 homogeneous rainfall zones for the short rains season and 9 homogeneous rainfall zones for the long rains season. This was due to complex topography that influenced seasonal rainfall through interaction with the synoptic scale patterns respectively. The eigenvalues ranges from 26.48 to 1.93 for the short rains with the cumulative percentage variance of 12% to 97%, respectively and 25.95 to 1.35 for the long rains seasons with the cumulative percentage variance of 11.7% to 98%, respectively. The zoning of Rwanda into near homogeneous rainfall zones using annual rainfall found six near homogeneous rainfall zones (Henninger, 2013).

The study results are not in agreement with previous study by Henninger (2013) because seasonal rainfall amount was considered in zoning the near homogeneous rainfall zones for both the short and the long rains season. The mechanism associated with seasonal rainfall pattern were better represented at seasonal timescales rather than annual timescales and these leads to increased number of near homogeneous rainfall zones for both seasons rather the existing six near homogeneous rainfall zones for the annual patterns.

Figure 7 indicates delineated near-homogeneous rainfall zones for the short rains season as a map where a roman number from one to ten identifies each zone whereas Figure 8 indicates the near-homogeneous rainfall zones for the long rains season. Stars in each graph represent stations that were used in this study.

The grouping of near homogeneous rainfall zones was based on occurrence and amount of seasonal rainfall events. The near homogeneous rainfall zones are represented by roman letters on the **Figure 7** and **Figure 8** respectively as : I, II, III, IV, V, VI, VII, VIII, IX and X for short rains and I, II, III, IV, V, VI, VII, VIII, IX for long rains.

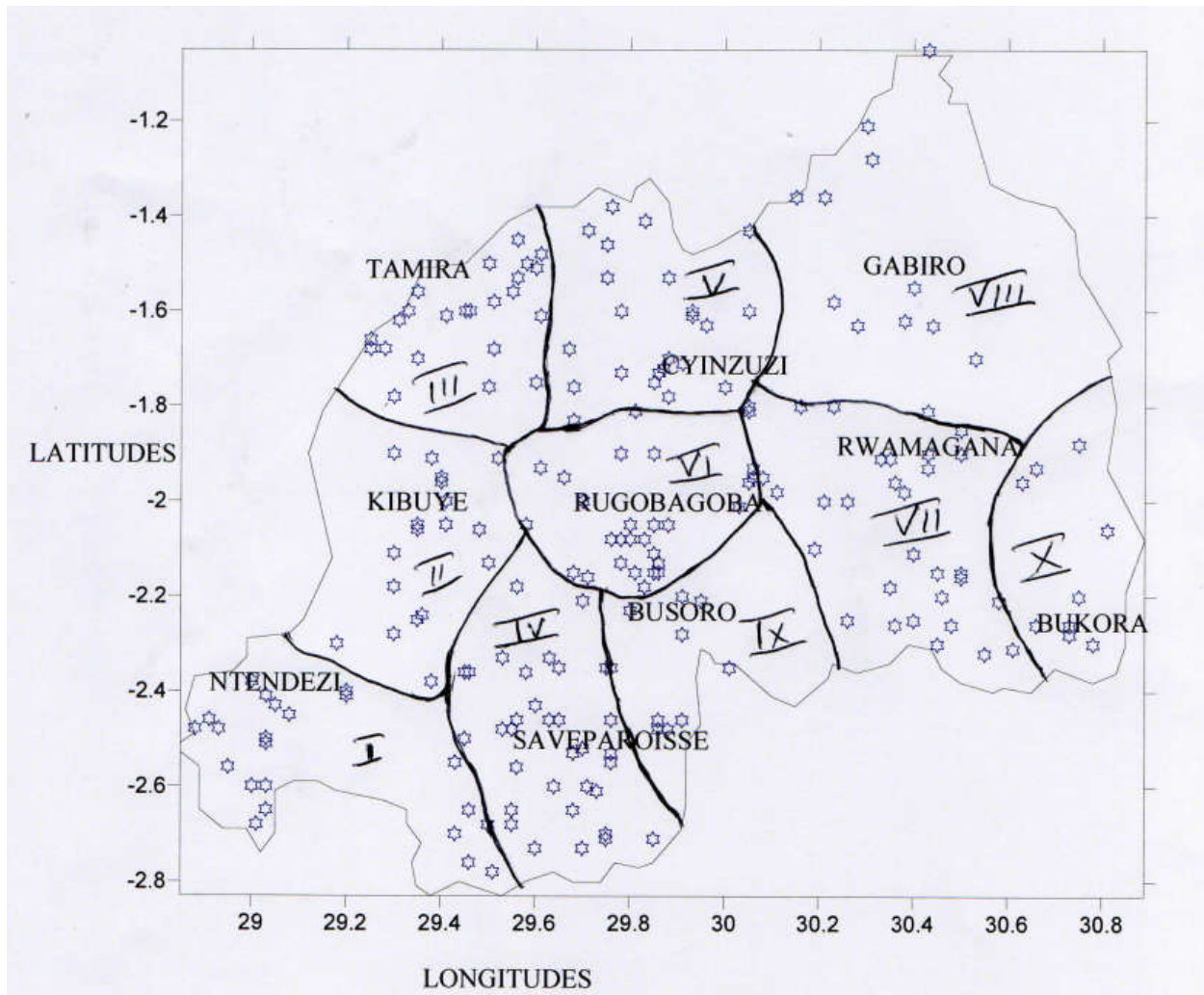


Figure 7: Derived near homogeneous rainfall zones during Short rains season from 1981 to 2017 over Rwanda. Stars represent meteorological stations

During the short rains season, zone I: extends over Southwestern Rwanda including the Nyungwe National Park and its surrounding areas over the Southern province. Zone II extends over the central western parts of Rwanda from the mountain of Crete Congo Nile towards the Lake Kivu and zone III extends over Northwestern of Rwanda. The eastern slope of Crete Congo Nile was subdivided into three near homogenous rainfall zones from the south to north, which are zone IV, V and Zone VI due to the mechanism that generates rainfall. The eastern lowlands combined with a part of the lowlands of southern province and east of Kigali city, known as semi-arid region, was subdivided into four near homogeneous rainfall zones, which are VII, VIII, IX and X to account

for the regional teleconnections; in contrast with Henninger (2013) that considers it as one zone based on annual patterns.

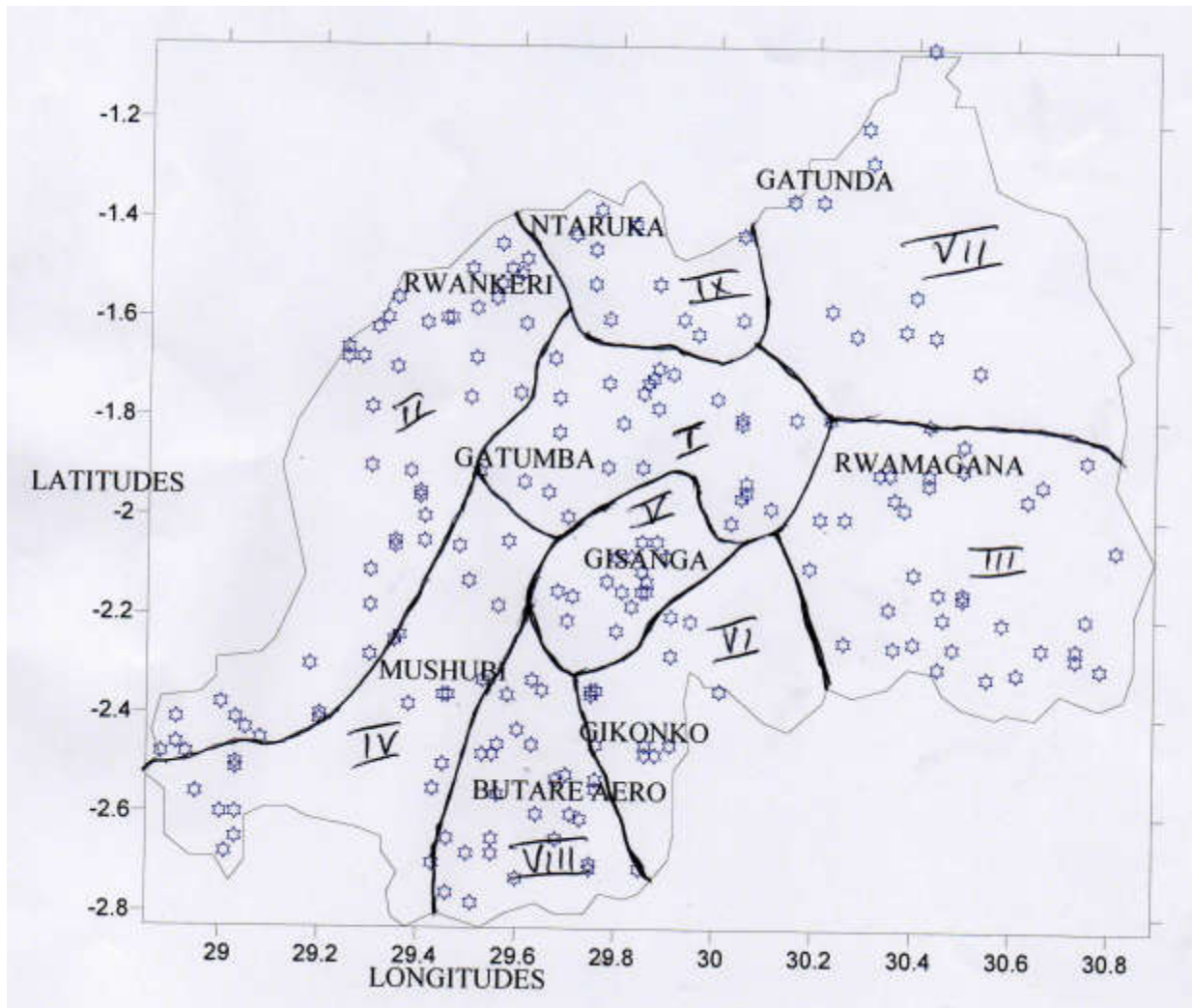


Figure 8: Derived near homogeneous rainfall zones during long rains season from 1981 to 2017 over Rwanda. Stars represent meteorological stations

During the long rain season, the nine near homogeneous rainfall zones delineated for seasonal rainfall are presented on Figure 10 as follows. Zone I extends over northwestern of Kigali city extending to middle highlands of north and reaching the eastern slope of the Crete and englobe the northern highlands of southern province; Zone II extends over the top of the Crete Congo Nile towards the Lake Kivu or the western slope of the Crete Congo Nile. The central part from south to north encompasses more zones that are zone I; zone V; zone VI; zone VIII and zone IX due to

the heterogeneity in topography from the highlands in the north and the edges of the Crete Congo Nile to the central plateau and lowlands of the southern province. Zone IV lies on the southern reach of the eastern slope of the Crete Congo Nile and the Nyungwe National Park. The eastern part of Rwanda exhibits two distinct near homogeneous rainfall zones during long rains season that are zone III and zone VII due to observed shift in rainfall patterns as the ITCZ migrates northward from the south and changes in wind regimes from south easterlies to north easterlies. Furthermore, the homogeneous rainfall zones are characterized in terms of rainfall onset/cessation, rainfall amount and its trend here below.

4.3 Temporal Variability of Onset and Cessation from 1981 to 2017

The onset of rains or the start of rainfall season was defined as the 1st day of a five-day period from 1st of September or 1st March for short and long rains respectively with at least a total rainfall of 20 mm recorded. The rainfall cessation day was defined as any day from the 1st of December or the 1st of May after which there are more than 7 consecutive days of rainfall with amount below 50% of the soil water requirements. Hence, various rainfall onset and cessation were determined for both seasons for the entire period from 1981 – 2017 over 10 zones or locations for short rains seasons and 9 locations for long rains season.

The mean onset dates during the short rains season for the period from 1981 – 2017 indicated that northwestern Rwanda marks its onset early compared to the other locations which is due to the migration of the ITCZ towards the south. The western region marks its onset mid-September with a late mean onset over the central western (Kibuye location). The eastern slope of the Crete Congo Nile and Central Plateau mark their onset during the first, second and third week of October with the late onset over Rwamagana. Eastern Rwanda marks its onset in the fourth week of October with the late onset over Bukora. Hence, there exists a zonal change in onset from west to east. These findings agreed over some locations with the probable sowing dates established by Ilunga *et al* (2008). For example, the mean sowing dates over the Crete Congo Nile and the northern highlands of Rwanda was found to be 26th September, 13th October over Cyeru, 24th October over Zaza and 5th November over Rusumo and it disagrees with the sowing date of 25 September over the central plateau. Table 6 and Table 7 summarise all the mean onset and cessation respectively for the short and long rains seasons over all delineated zones of Rwanda

During the short rains season, the onset in recent years tends to come earlier compared to past years over mainly five locations that are Kibuye, Ntendezi, Rugobagoba, Rwamagana and Gabiro. Late onset in recent years were observed in the northwestern part namely over Cyinzuzi and Tamira locations. This suggested a shift in rainfall onset pattern during short rains over Rwanda. During the short rains, the mean seasonal length duration over the east reduced to one month of November and ten days and more than 3 months over the south western (Ntendezi station) of Rwanda.

Table 6: Mean Onset and Cessation Dates for the short rains season from 1981 to 2017 over all delineated zones (Lon: Longitude and Lat: Latitude)

Zones	Stations Names	Lon	Lat	Mean Onset Dates	Mean Cessation Dates	Rainfall Duration
I	Ntendezi	29.05	-2.43	19 th of Sept	24 th of Dec	97 days
II	Kibuye	29.35	-2.05	2 nd of Oct	7 th of Dec	67 days
III	Tamira	29.35	-1.56	13 th of Sept	5 th of Dec	84 days
IV	Save Paroisse	29.76	-2.55	5 th of Oct	15 th of Dec	72 days
V	Cyinzuzi	30	-1.76	7 th of Oct	10 th of Dec	65 days
VI	Rugobagoba	29.88	-2.05	17 th of Oct	4 th of Dec	49 days
VII	Rwamagana	30.43	-1.93	20 th of Oct	4 th of Dec	46 days
VIII	Gabiro	30.4	-1.55	23 rd of Oct	4 th of Dec	42 days
IX	Busoro	29.91	-2.28	14 th of Oct	4 th of Dec	51 days
X	Bukora	30.78	-2.3	26 th of Oct	3 rd of Dec	39 days

The mean seasonal length during the short rains season reduces to one month of November and few days over the southeast (Bukora) and more than three months over the southwest (Ntendezi) of Rwanda. This zonal gradient in mean seasonal length is attributed to the rainfall generating mechanism interaction with the high mountains of the western Rwanda. The prolonged seasonal duration increases the rainfall amount recorded within a season.

Table 7: Mean Onset and Cessation Dates for the long rains season from 1981 to 2017 over all delineated zones (Lon: Longitude and Lat: Latitude)

Zones	Stations Names	Lon	Lat	Mean Onset Dates	Mean Cessation Dates	Rainfall Duration
I	Gatumba	29.61	-1.93	21 st of Mar	13 th of May	54 days
II	Rwankeri	29.51	-1.58	12 th of Mar	22 nd of May	72 days
III	Rwamagana	30.43	-1.93	24 th of Mar	7 th of May	45 days
IV	Mushubi	29.45	-2.36	9 th of Mar	16 th of May	69 days
V	Gisanga	29.86	-2.13	15 th of Mar	16 th of May	63 days
VI	Gikonko	29.86	-2.48	16 th of Mar	16 th of May	62 days
VII	Gatunda	30.21	-1.36	16 th of Mar	8 th of May	54 days
VIII	Butare_Aero	29.71	-2.6	11 th of Mar	18 th of May	69 days
IX	Ntaruka	29.75	-1.46	12 th of Mar	18 th of May	68 days

During the long rains season, the early onset is observed on the station (Mushubi) located on the eastern slope of the Crete Congo Nile. Stations over or in the surrounding areas of the Crete got early onset in comparison to the other locations. The analysis was again able to reproduce the movement of ITCZ from the south towards the north mostly over the Crete and central plateau of Rwanda. The mean seasonal length reduces to one month of April and two weeks over the east (Rwamagana) and two months and ten days over the north western (Rwankeri) of Rwanda.

The rainfall cessation computation was done based on the water balance requirement of the soil where the less or equal to 50% water balance was considered as the rainfall cessation. Rainfall cessation is highly influenced by the retraction of the ITCZ and its migration southward or northward depending on the period of the year and the findings are in good agreement over the Crete area.

Figure 9 to Figure 27 indicate the temporal variability in rainfall onset for both the short and long rains seasons over ten and 9 near homogeneous rainfall zones using representative stations for each zone.

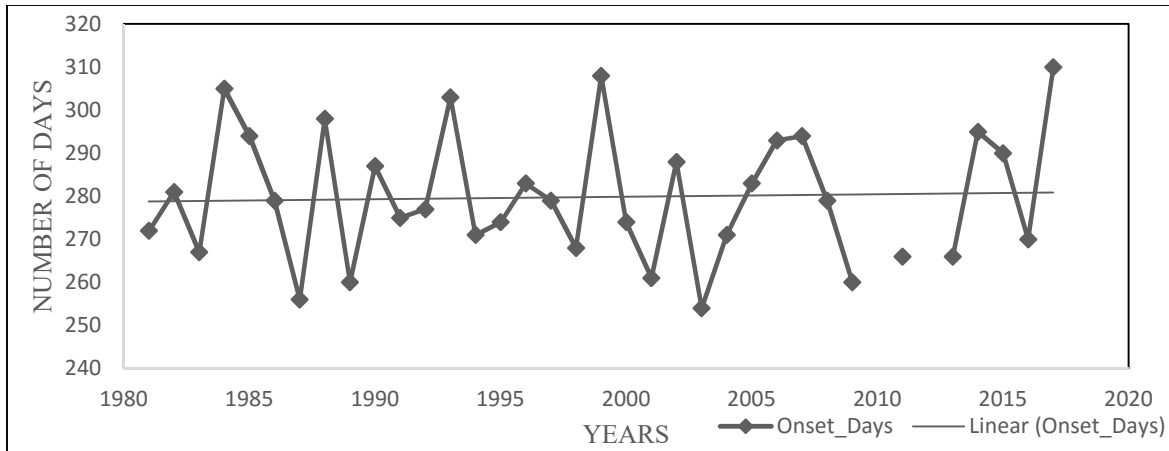


Figure 9: Temporal variability and trend of rainfall Onset days for Save Paroisse location during the short rains season from 1981 to 2017

The rainfall onset over Save Paroisse (Figure 9) tends to come later in recent years. The early onset in last past 37 years was recorded on the 254th day of the year 2003 whereas the later onset was on the 310th day of the year 2017.

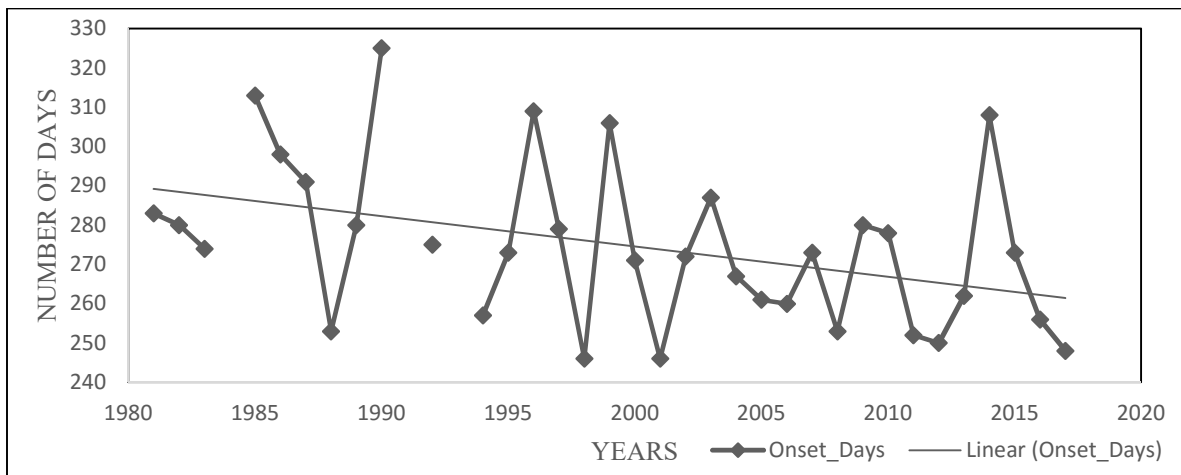


Figure 10: Temporal variability and trend of rainfall Onset days for Kibuye location during the Short rains season from 1981 to 2017

The rainfall onset over Kibuye (Figure 10) tends to come earlier in recent years compared to past years. The earliest onset marked was, on the 246th day of the year 1998 and 2001 whereas the latest onset was marked on the 325th day of the year 1990.

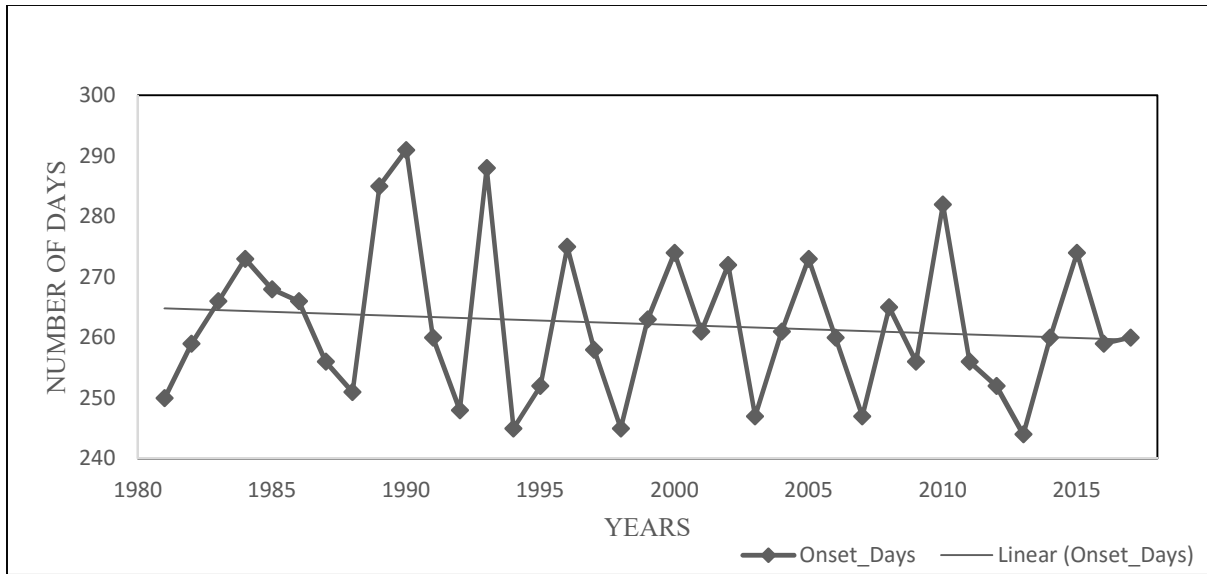


Figure 11: Temporal variability and trend of rainfall Onset days for Ntendezi locations during the short rains season from 1981 to 2017

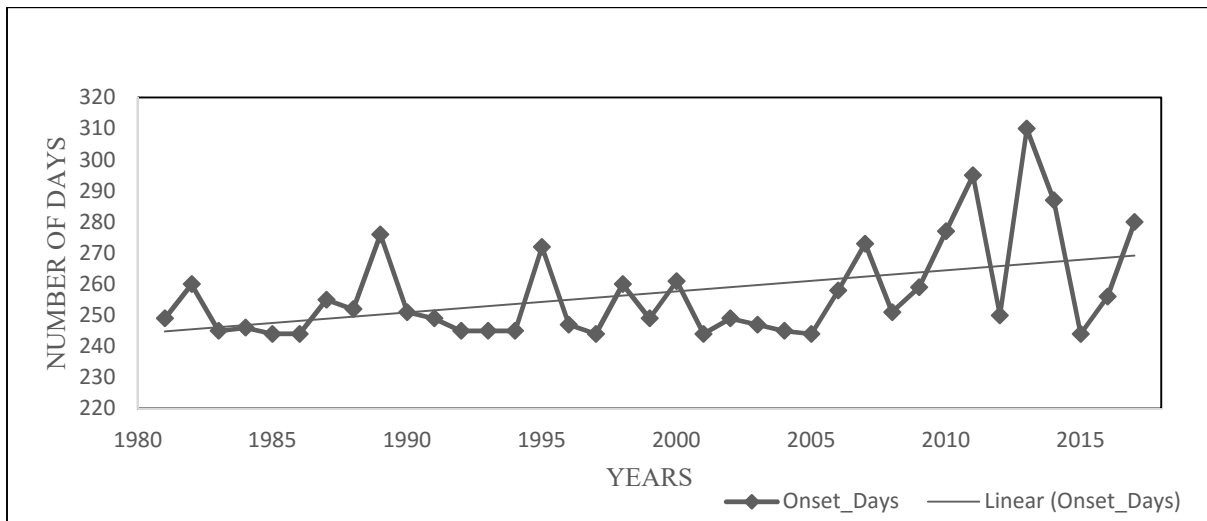


Figure 12: Temporal variability and trend of rainfall Onset days for Tamira location during the Short rains season from 1981 to 2017

There exists a tendency of early onset over Ntendezi (Figure 11) and late onset over Tamira (Figure 12). The earliest onset observed over Ntendezi, was on the 244th day of the year 2013 and on the 244th day in several years like 2015 and 2005 in recent years over Tamira.

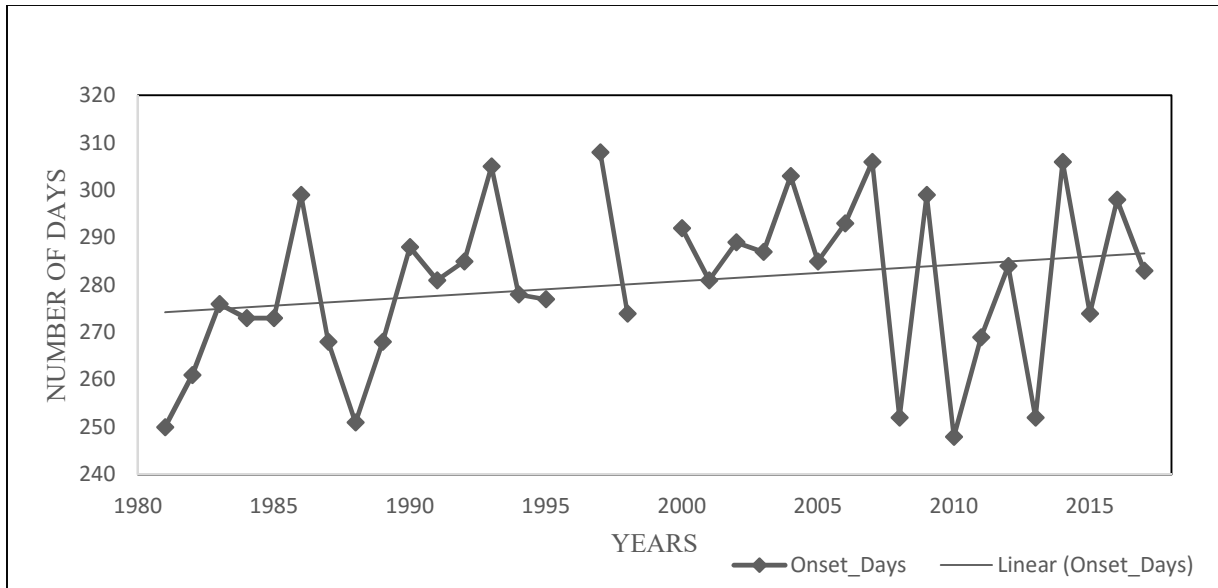


Figure 13: Temporal variability and trend of rainfall Onset days for Cyinzuzi location during the Short rains season from 1981 to 2017

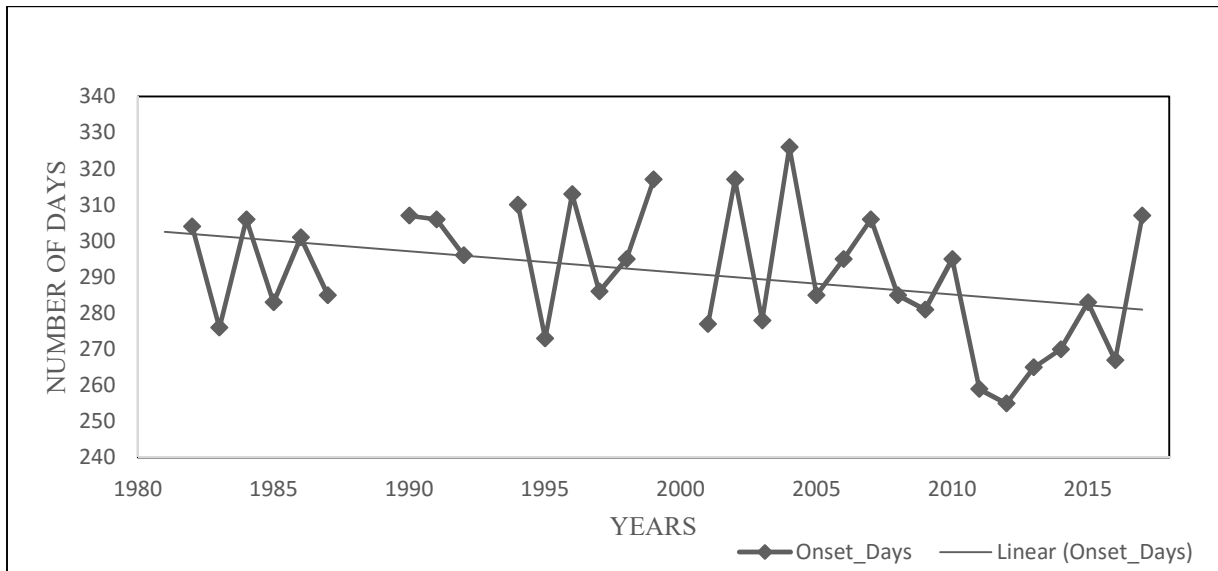


Figure 14: Temporal variability and trend of rainfall Onset days for Rugobagoba location during the short rains season from 1981 to 2017

There is a tendency of rainfall onset to start later in recent years over Cyinzuzi (Figure 13) and to start early over Rugobagoba (Figure 14). The earliest onset recorded over Cyinzuzi was on the 248th day in 2010 and over Rugobagoba, it was on the 255th day in 2012.

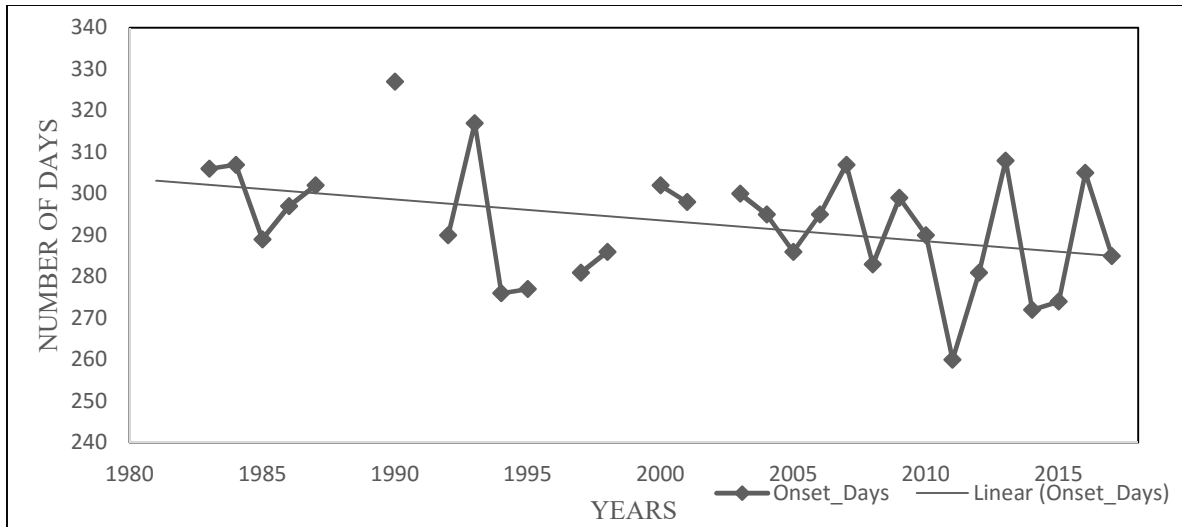


Figure 15: Temporal variability and trend of rainfall Onset days for Rwamagana location during the Short rains season from 1981 to 2017

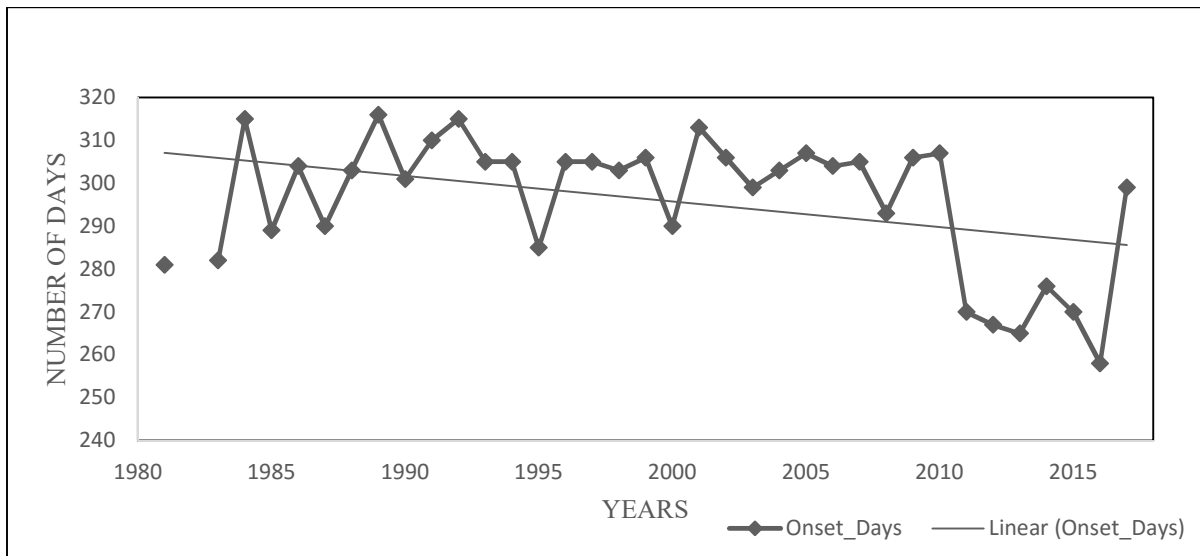


Figure 16: Temporal variability and trend of rainfall Onset days for Gabiro location during the Short rains season from 1981 to 2017

There is a tendency of rainfall onset to start early in recent years over Rwamagana (Figure 15) and Gabiro (Figure 16). The earliest onset recorded over Rwamagana was on the 260th day in 2011 and over Gabiro, it was on the 258th day in 2016.

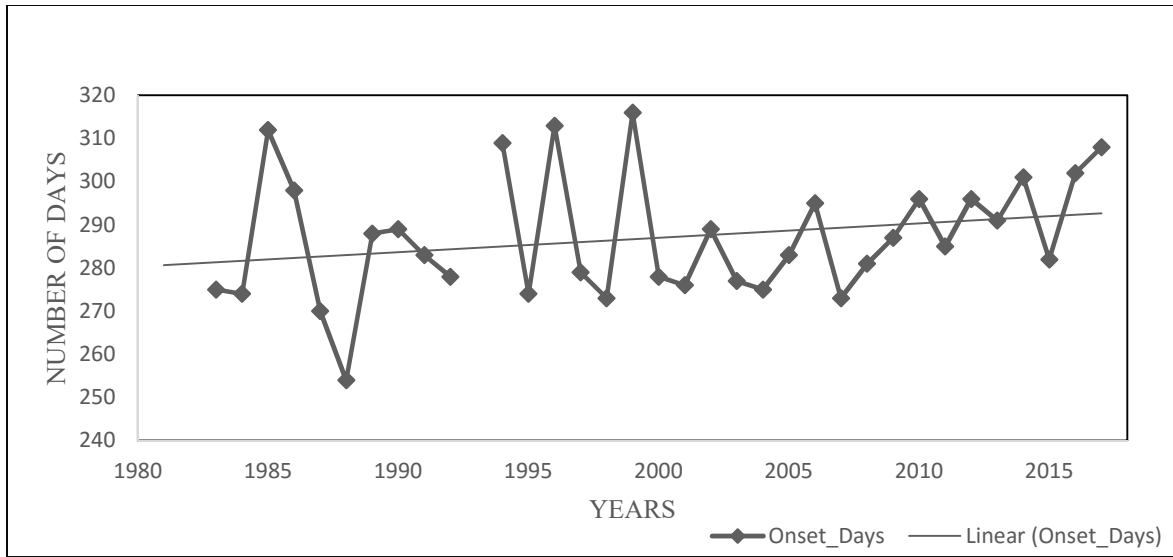


Figure 17: Temporal variability of rainfall Onset days for Busoro location during the Short rains season from 1981 to 2017

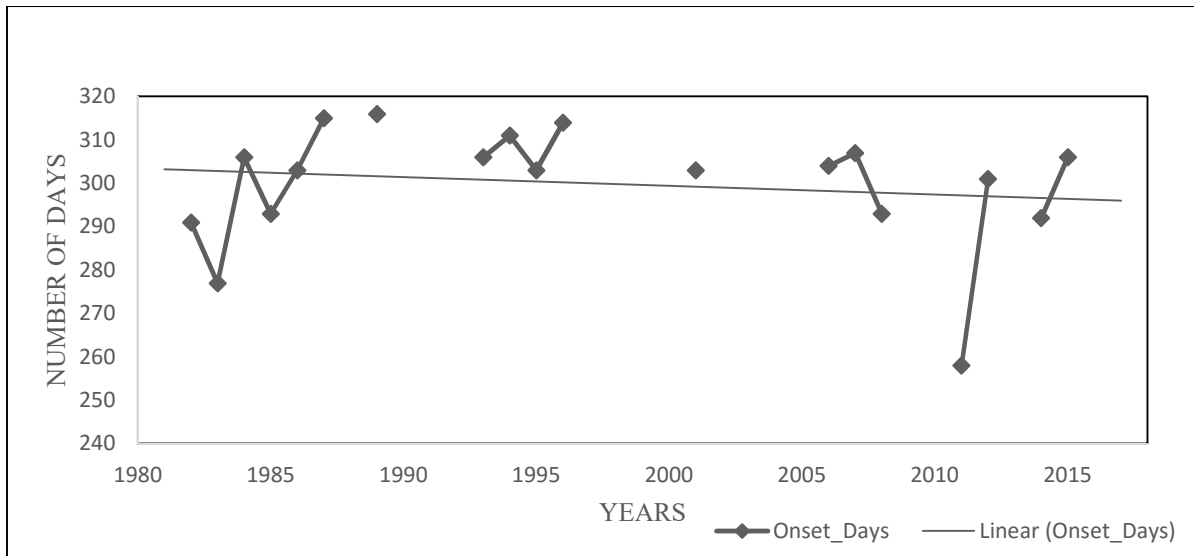


Figure 18: Temporal variability and trend of rainfall Onset days for Bukora location during the Short rains season from 1981 to 2017

There is a tendency of rainfall onset to start later in recent years over Busoro (Figure 17) and to start early over Bukora (Figure 18). The earliest onset recorded over Busoro was on the 254th day in 1988 and over Bukora, it was on the 258th day in 2011.

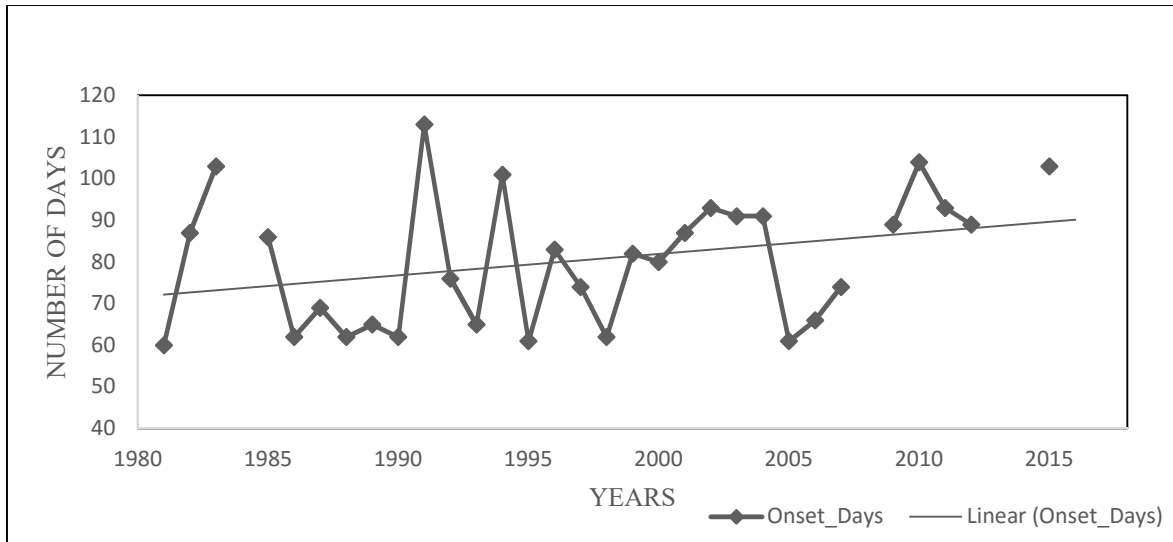


Figure 19: Temporal variability and trend of rainfall Onset days for Gatumba location during the long rains season from 1981 to 2017

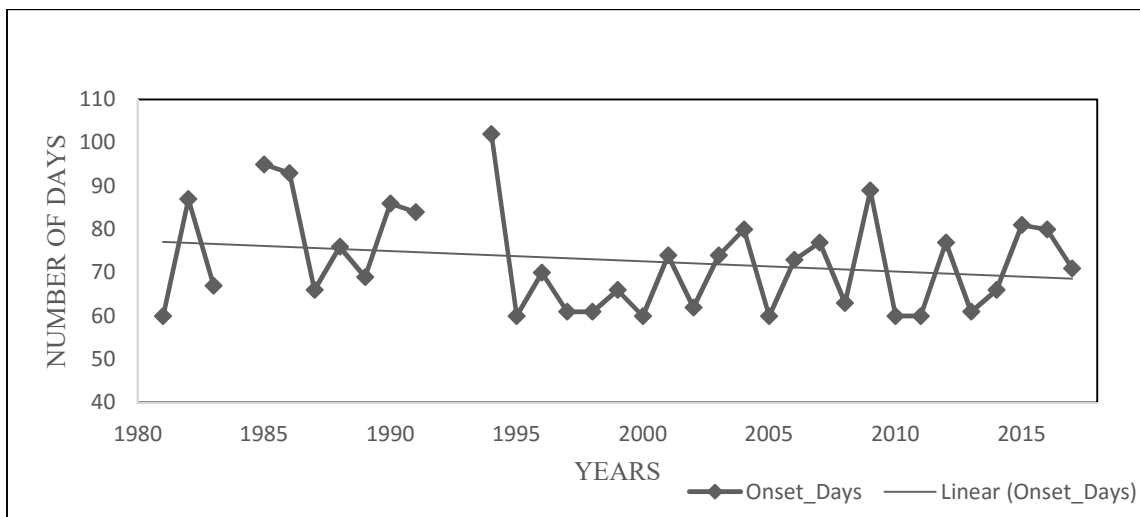


Figure 20: Temporal variability and trend of rainfall Onset days for Rwankeri_Nyabihu location during the long rains season from 1981 to 2017

There is a tendency of rainfall onset to start later in recent years over Gatumba (Figure 19) and to start early over Rwankeri (Figure 20). The earliest onset recorded over Gatumba was on the 60th day of the year 1981 and over Rwankeri, it was on the 60th day in 2011.

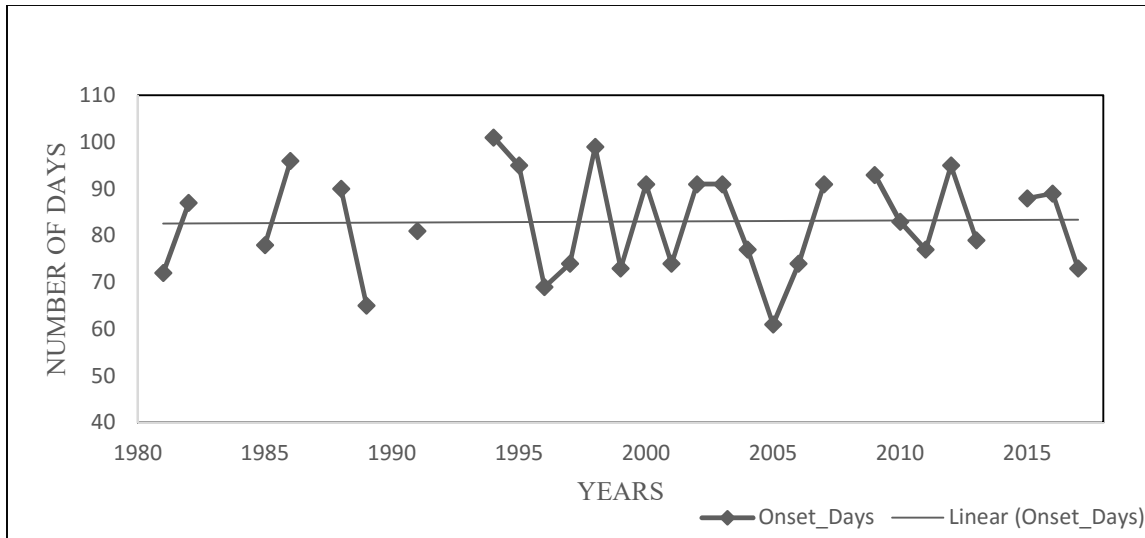


Figure 21: Temporal variability and trend of rainfall Onset days for Rwamagana location during the long rains season from 1981 to 2017

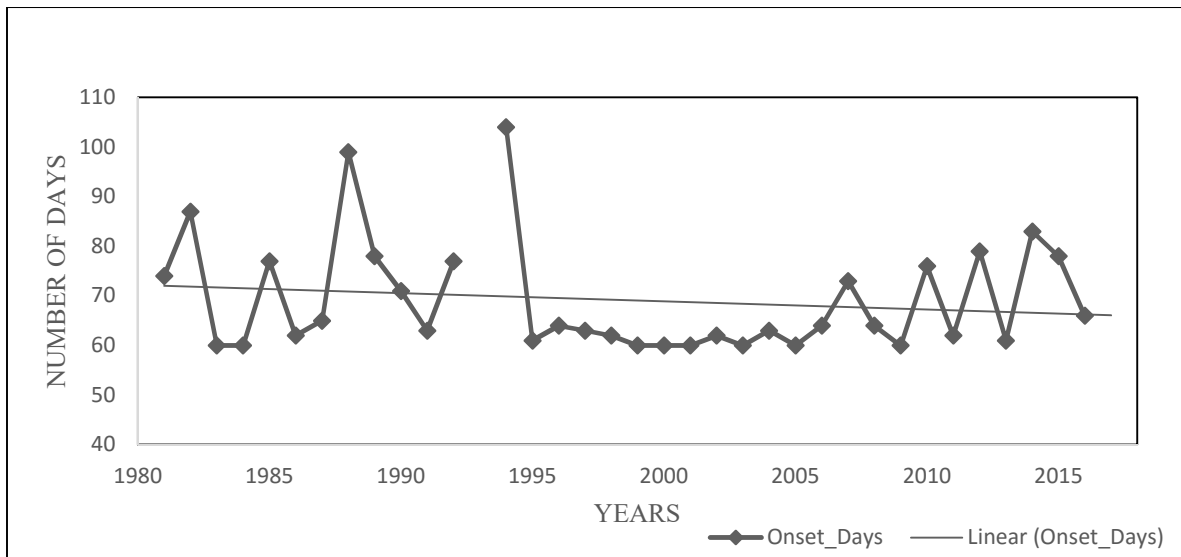


Figure 22: Temporal variability and trend of rainfall Onset days for Mushubi location during the long rains season from 1981 to 2017

There is a tendency of rainfall onset to start slightly later in recent years over Rwamagana (Figure 21) and Mushubi (Figure 22). The earliest onset recorded over Rwamagana was on the 61th day of the year 2005 and over Mushubi, it was on the 61th day in 2013.

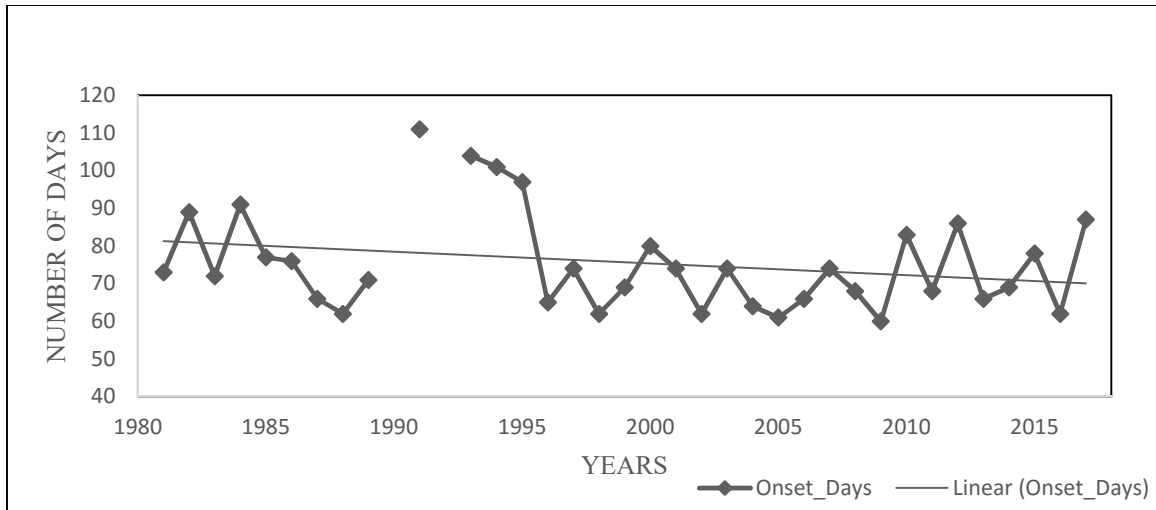


Figure 23: Temporal variability and trend of rainfall Onset days for Gisanga location during the long rains season from 1981 to 2017

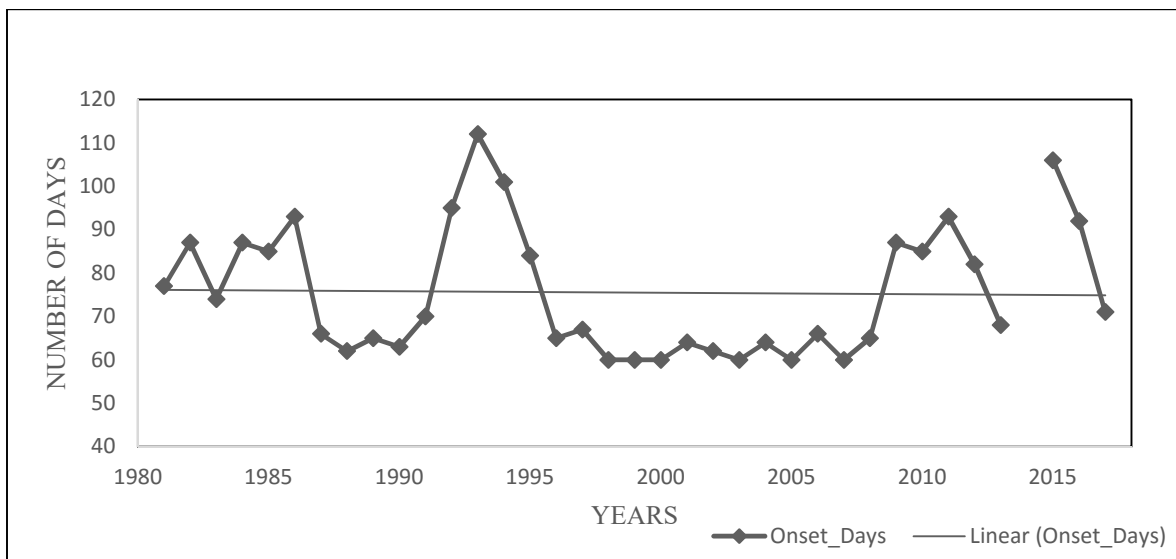


Figure 24: Temporal variability and trend of rainfall Onset days for Gikonko location during the long rains season from 1981 to 2017

There is a tendency of rainfall onset to start early in recent years over Gisanga (Figure 23) and almost a constant trend in onset over Gikonko (Figure 24). The earliest onset recorded over Gisanga was on the 60th day of the year 2009 and over Gikonko, it was on the 60th day in 2007.

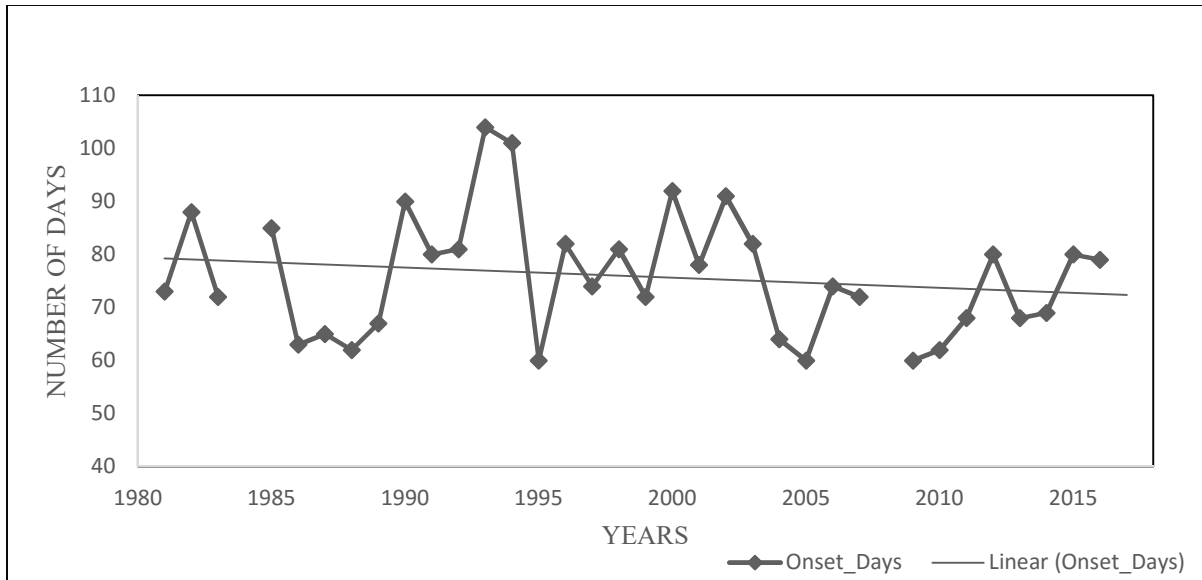


Figure 25: Temporal variability and trend of rainfall Onset days for Gatunda location during the long rains season from 1981 to 2017

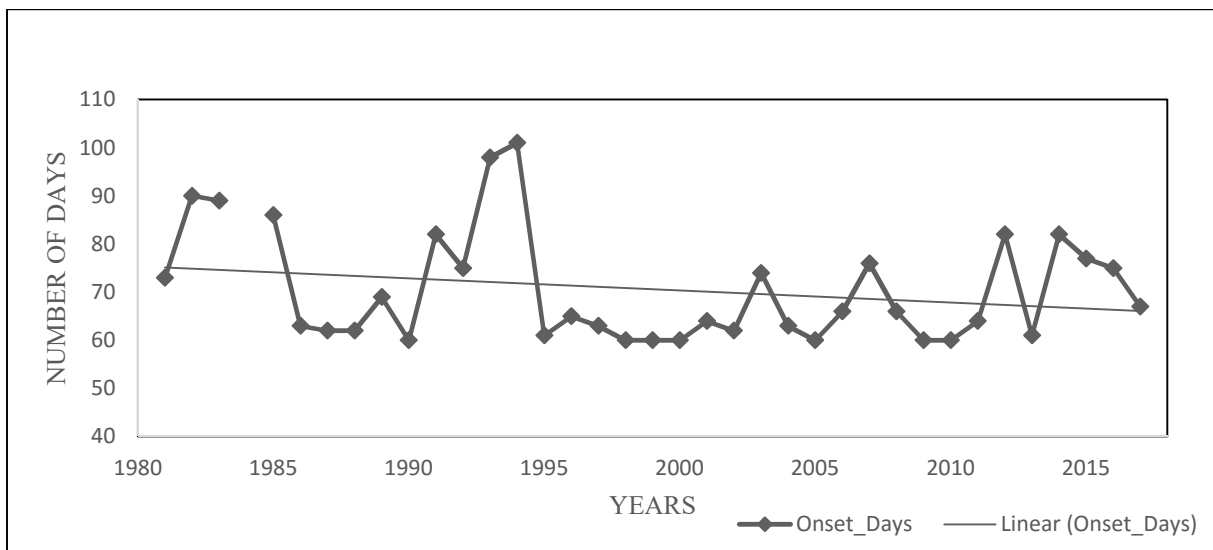


Figure 26: Temporal variability and trend of rainfall Onset days for Butare Aero location during the long rains season from 1981 to 2017

There is a tendency of rainfall onset to start slightly early in recent years over Gatunda (Figure 25) and over Butare Aero (Figure 26). The earliest onset recorded over Gatunda and Butare Aero were on the 60th day of the year 2009 and 2010 respectively.

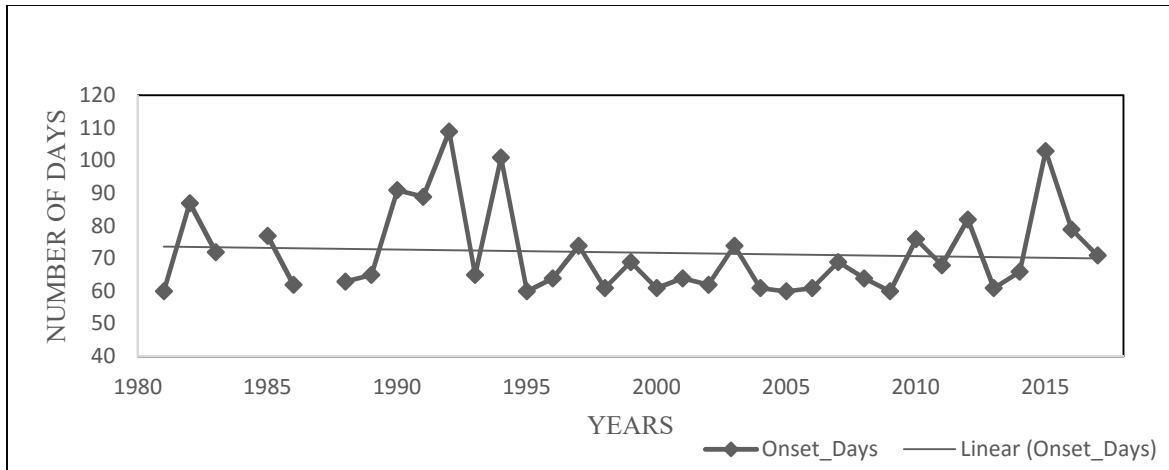


Figure 27: Temporal variability and trend of rainfall Onset days for Ntaruka location during the long rains season from 1981 to 2017

The earliest onset recorded over Ntaruka (Figure 27) in recent years was on the 60th day of the year 2009 and the latest was on the 103th day of the year 2015.

Figure 28 to Figure 46 indicate the rainfall cessation during both the short and the long rains seasons from 1981 to 2017 over each delineated zone of Rwanda.

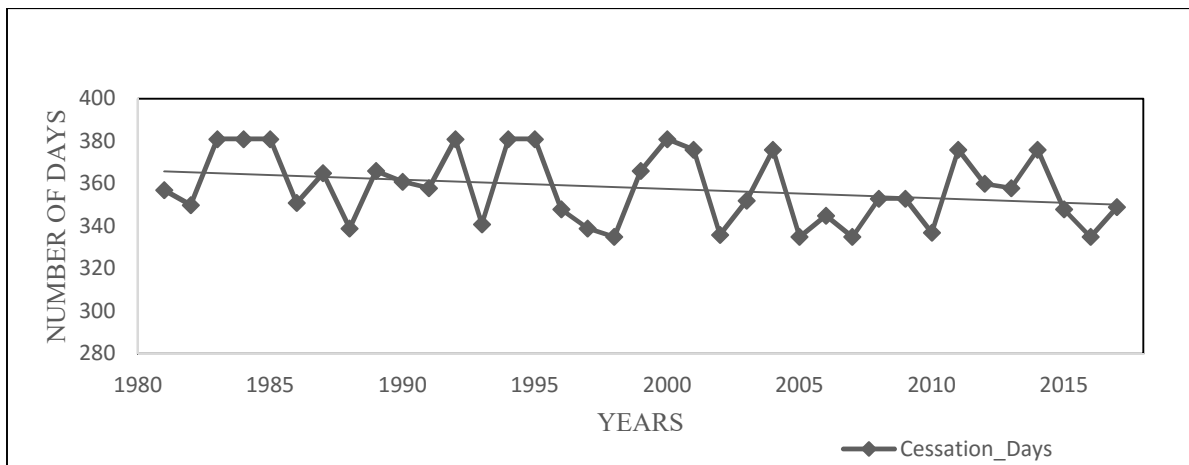


Figure 28: Temporal variability and trend of rainfall Cessation days for Ntendezi location during the Short rains season from 1981 to 2017

The earliest rainfall cessation recorded over Ntendezi (Figure 28) in recent years was on the 335th day of the year 2015 and the latest extends in January of the next year.

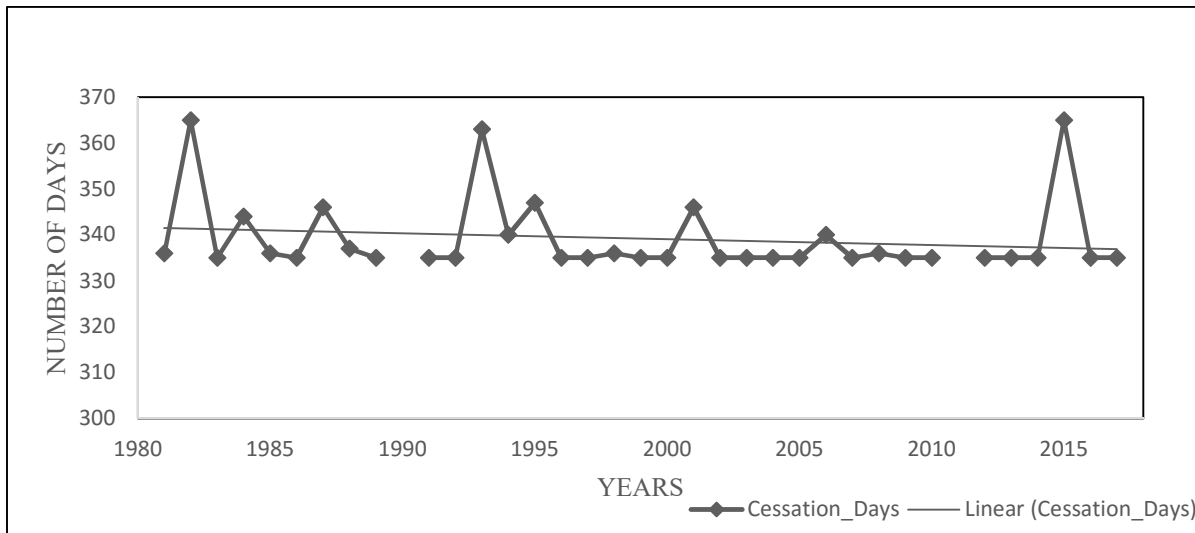


Figure 29: Temporal variability and trend of rainfall Cessation days for Kibuye location during the Short rains season from 1981 to 2017

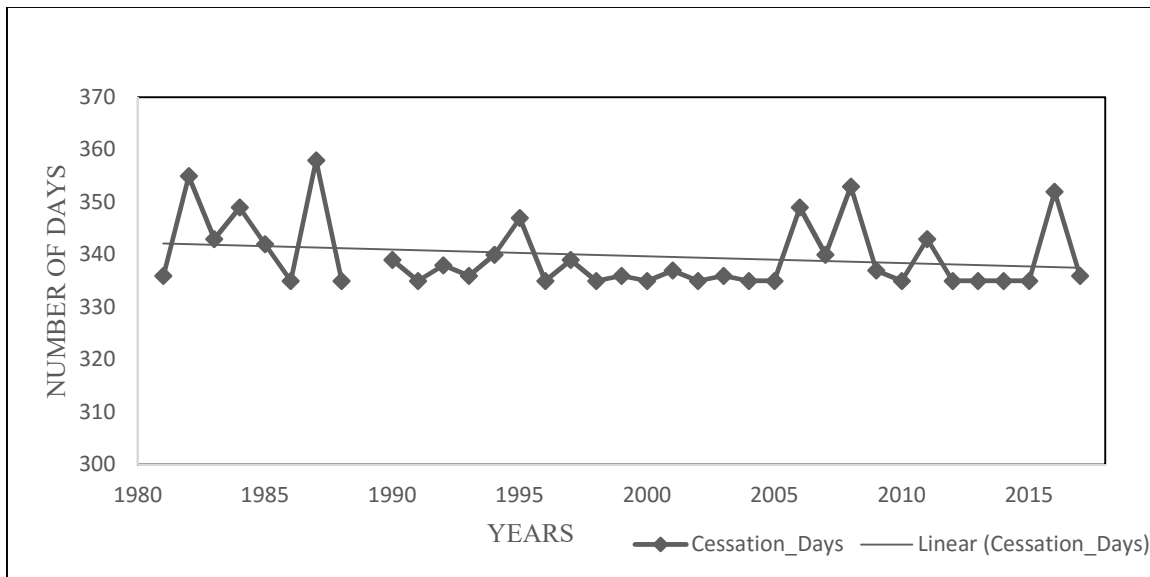


Figure 30: Temporal variability and trend of rainfall Cessation days for Tamira location during the Short rains season from 1981 to 2017

There is a tendency of rainfall cessation to end slightly early in recent years over Kibuye (Figure 29) and over Tamira (Figure 30). The earliest cessation recorded over Kibuye and Tamira was on the 335th day of the year 2017 and 2015 respectively.

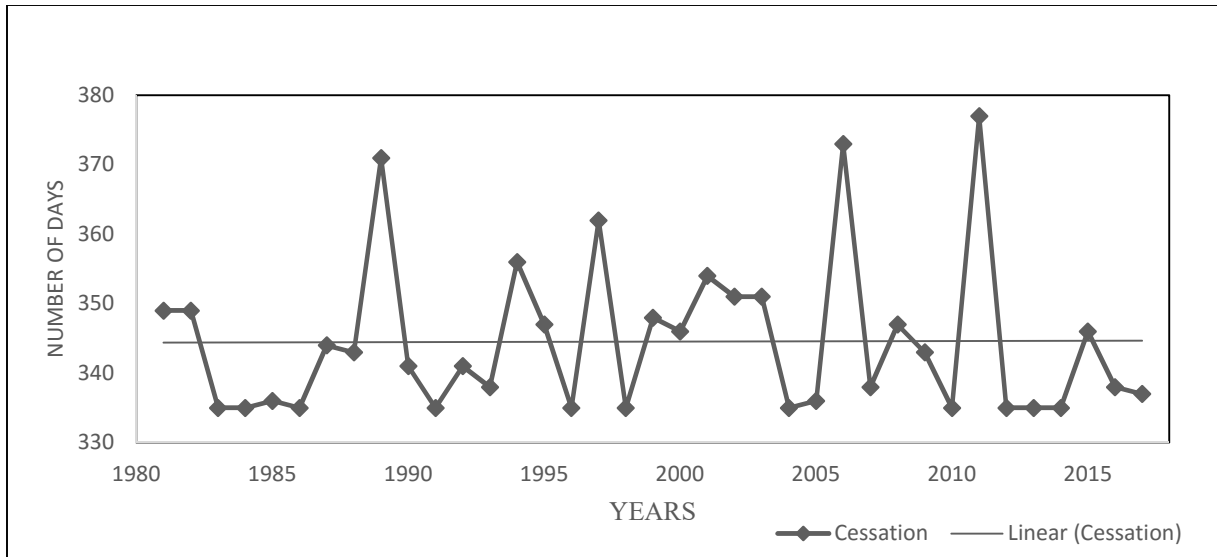


Figure 31: Temporal variability and trend of rainfall Cessation days for Save Paroisse location during the Short rains season from 1981 to 2017

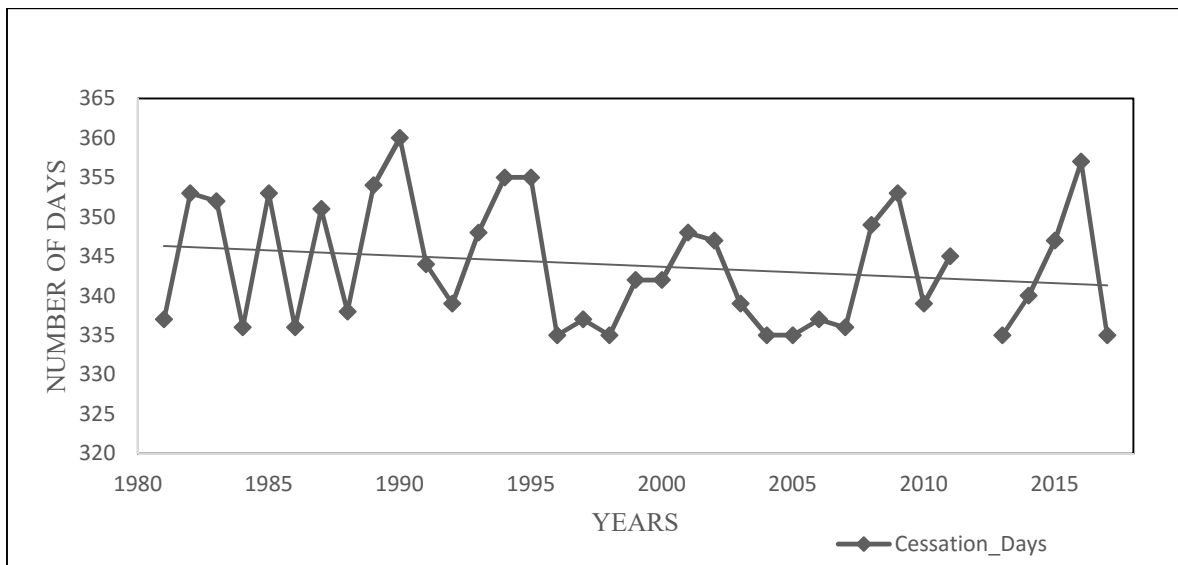


Figure 32: Temporal variability and trend of rainfall Cessation days for Cyinzuzi location during the Short rains season from 1981 to 2017

There is a tendency of rainfall cessation to end early in recent years over Save Paroisse (Figure 31) where the earliest cessation recorded was on the 335th day of the year 2014.

The latest rainfall cessation recorded over Cyinzuzi (Figure 32) in recent years was on the 357th day of the year 2016.

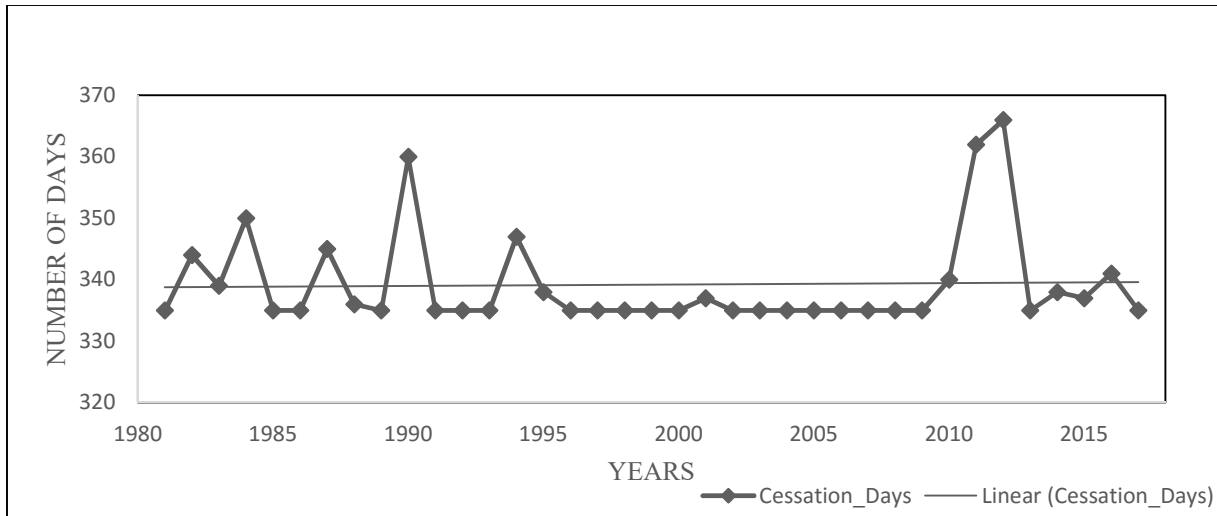


Figure 33: Temporal variability and trend of rainfall Cessation days for Rugobagoba location during the Short rains season from 1981 to 2017

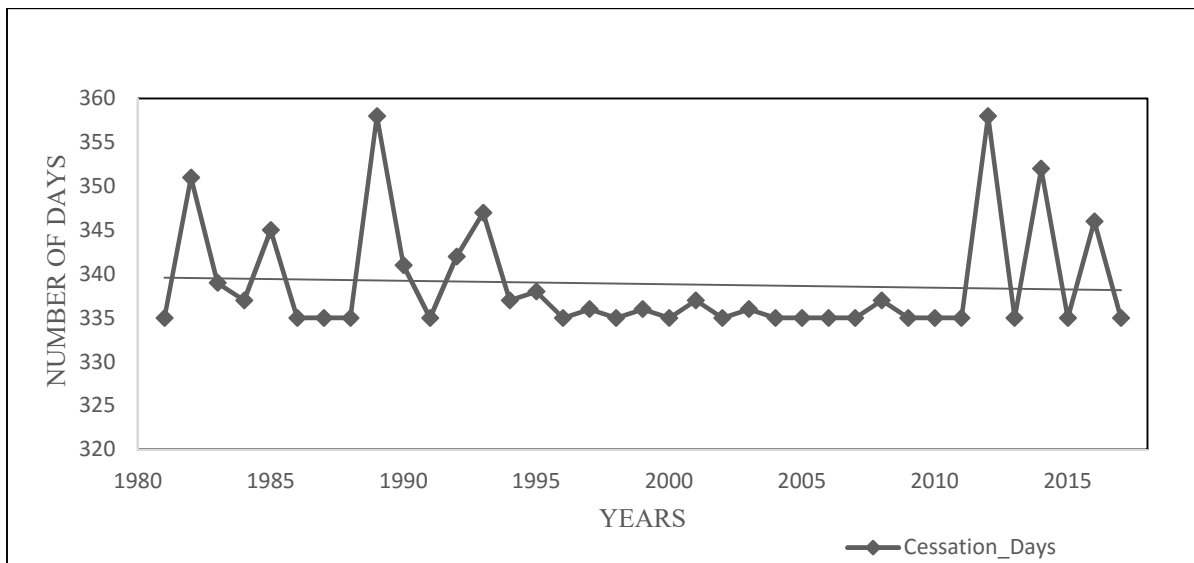


Figure 34: Temporal variability and trend of rainfall Cessation days for Rwamagana location during the Short rains season from 1981 to 2017

There was a constant trend in rainfall cessation over Rugobagoba (Figure 33) and Rwamagana (Figure 34). There was a remarkable period from 1995 to 2010 with nearly constant rainfall cessation. That may have been due to the smoothing in the ENACTs rainfall dataset. Hence, further investigation is required. The earliest cessation recorded was on the 335th day of the year 2017 for both locations.

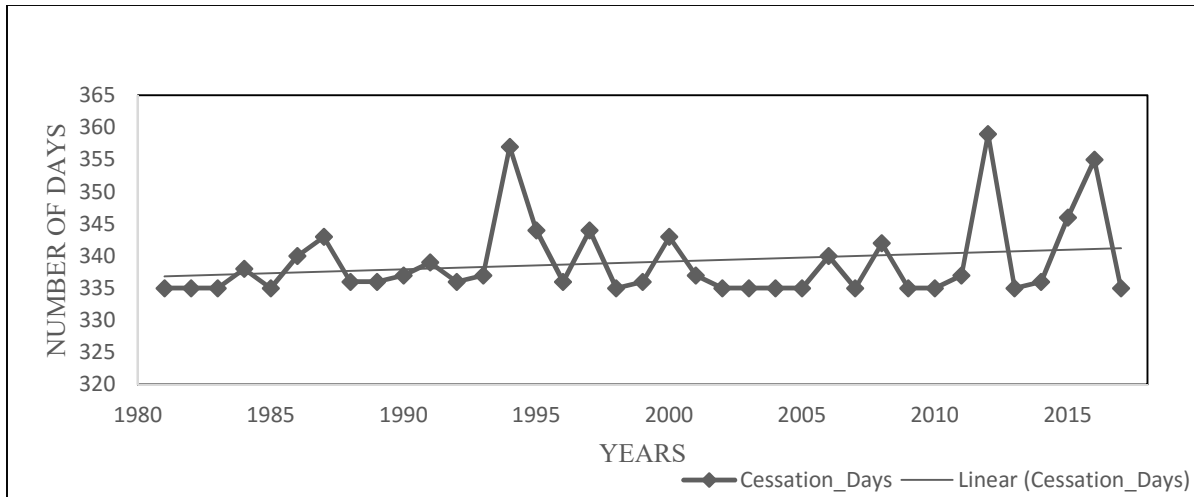


Figure 35: Temporal variability and trend of rainfall Cessation days for Gabiro location during the Short rains season from 1981 to 2017

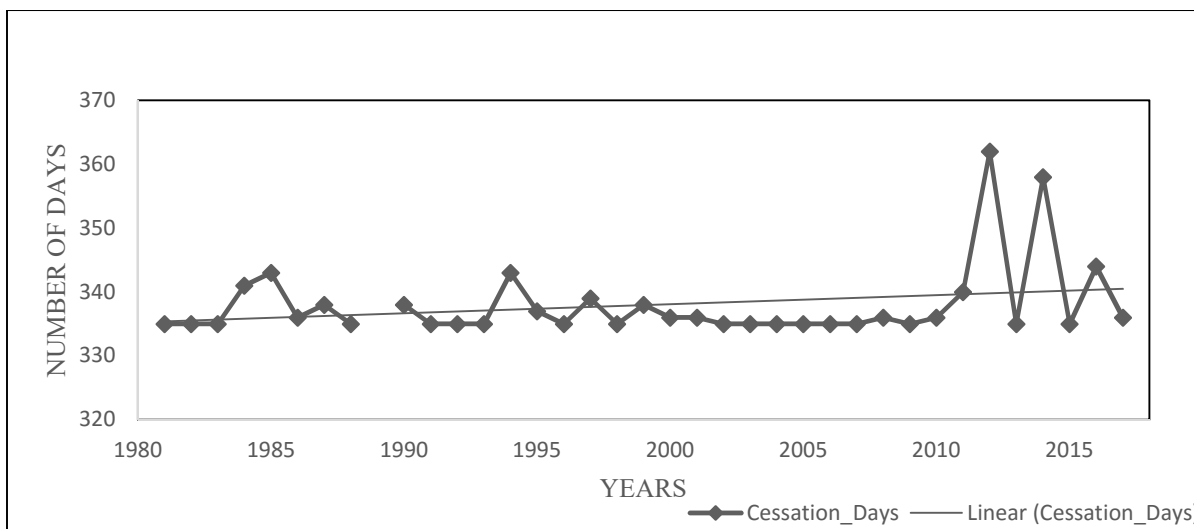


Figure 36: Temporal variability and trend of rainfall Cessation days for Busoro location during the Short rains season from 1981 to 2017

There is a tendency of rainfall cessation to end late in recent years over Gabiro (Figure 35) where the latest cessation recorded was on the 359th day of the year 2012.

The latest rainfall cessation recorded over Busoro (Figure 36) in recent years was on the 362th day of the year 2012.

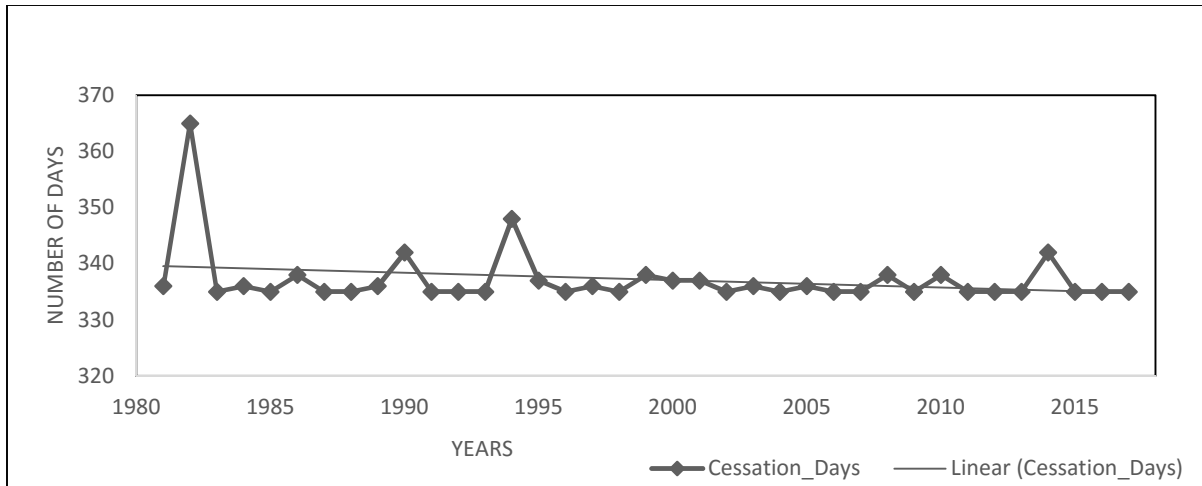


Figure 37: Temporal variability and trend of rainfall Cessation days for Bukora location during the Short rains season from 1981 to 2017

The latest rainfall cessation recorded over Bukora (Figure 37) in recent years was on the 342th day of the year 2014. Generally, the rainfall cessation occurred on the 335th day of the years.

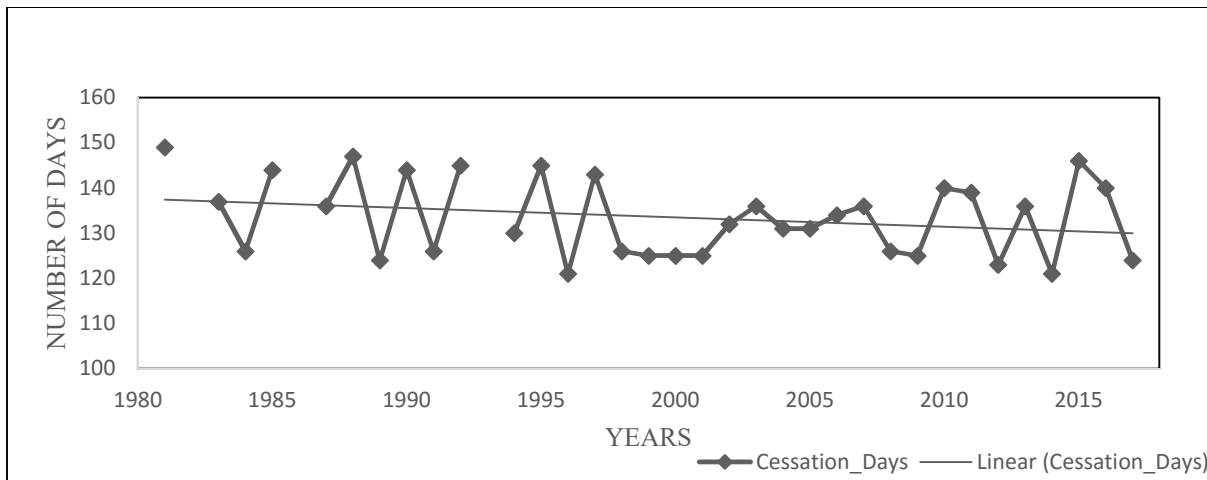


Figure 38: Temporal variability and trend of rainfall Cessation days for Gatumba location during the Long rains season from 1981 to 2017

There is a tendency of rainfall cessation to end slightly early in recent years over Gatumba (Figure 38) where the earliest cessation recorded was on the 121th day of the year 2014.

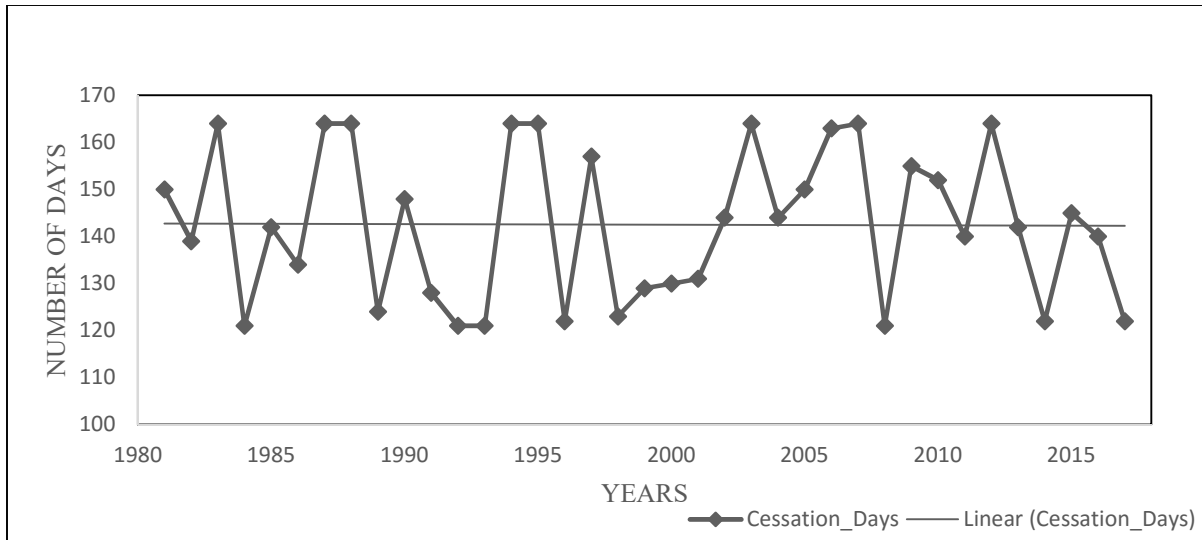


Figure 39: Temporal variability and trend of rainfall Cessation days for Rwankeri location during long rains season from 1981 to 2017

There is a tendency of rainfall cessation to end early in recent years over Rwankeri (Figure 39) where the earliest cessation recorded was on the 122th day of the year 2017.

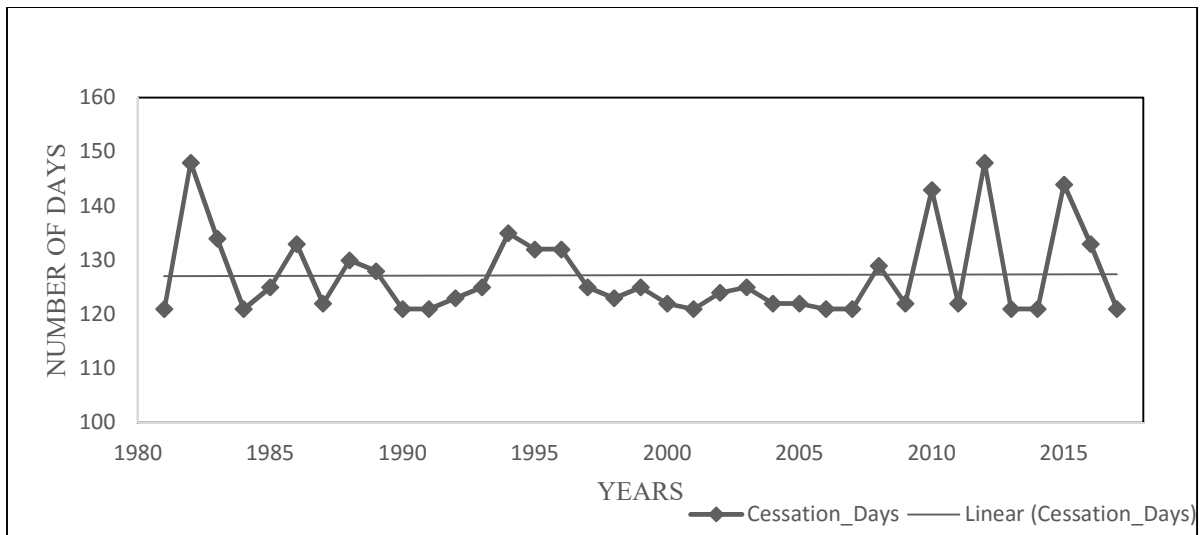


Figure 40: Temporal variability and trend of rainfall Cessation days for Rwamagana location during long rains season from 1981 to 2017

There is a tendency of rainfall cessation to end late in recent years over Rwamagana (Figure 40) where the latest cessation recorded was on the 148th day of the year 2012.

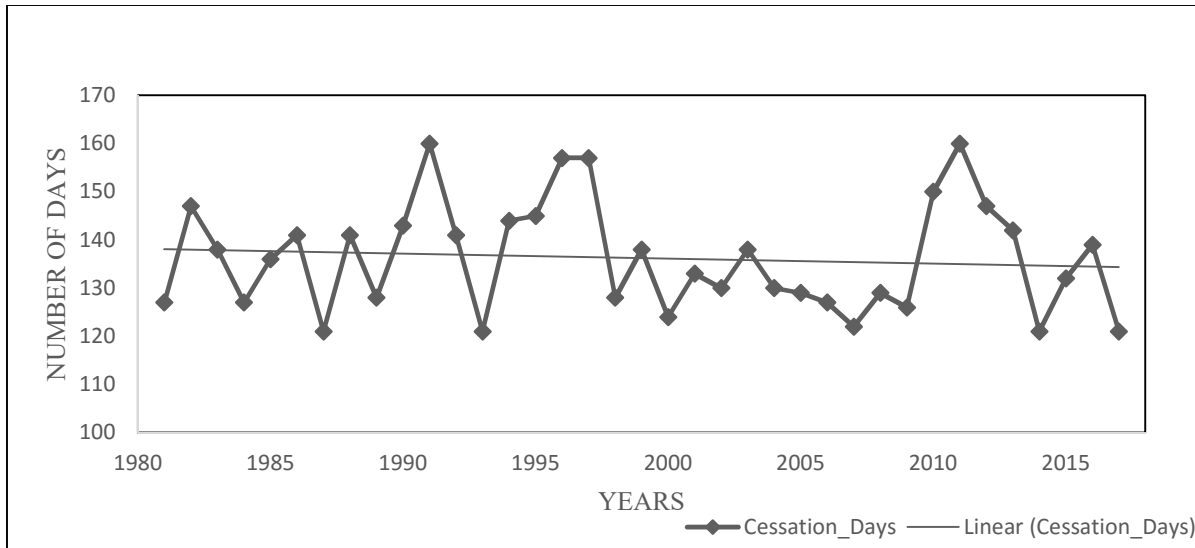


Figure 41: Temporal variability and trend of rainfall Cessation Days for Mushubi location during long rains season from 1981 to 2017

There is a tendency of rainfall cessation to end slightly early in recent years over Mushubi (Figure 41) where the earliest cessation recorded was on the 121th day of the year 2017 and the latest on the 160th day in 2011.

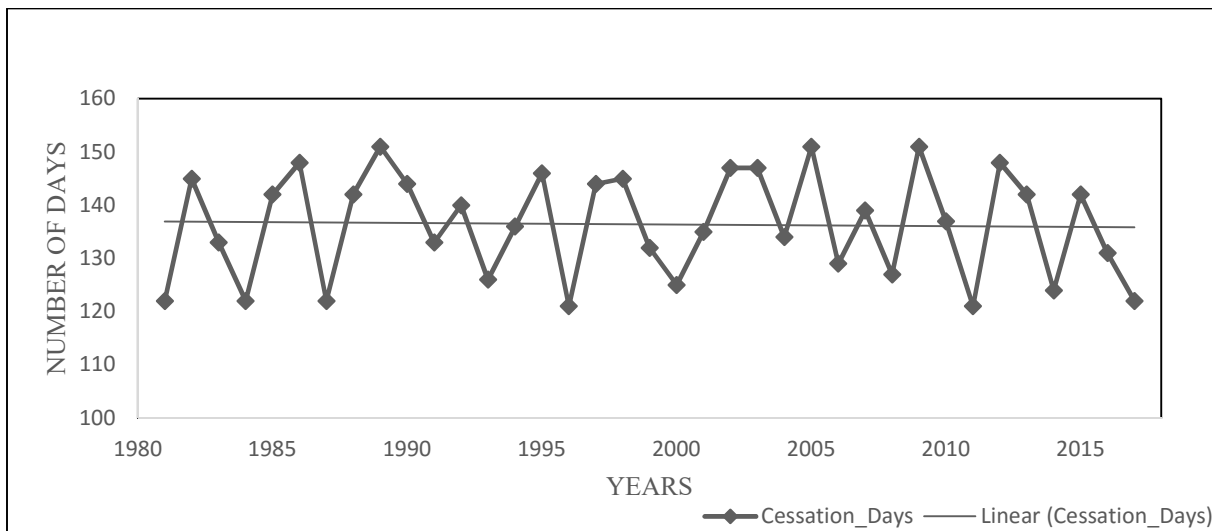


Figure 42: Temporal variability and trend of rainfall Cessation days for Gisanga location during long rains season from 1981 to 2017

There is a tendency of rainfall cessation to end slightly early in recent years over Gisanga (Figure 42) where the earliest cessation recorded was on the 121th day of the year 2011.

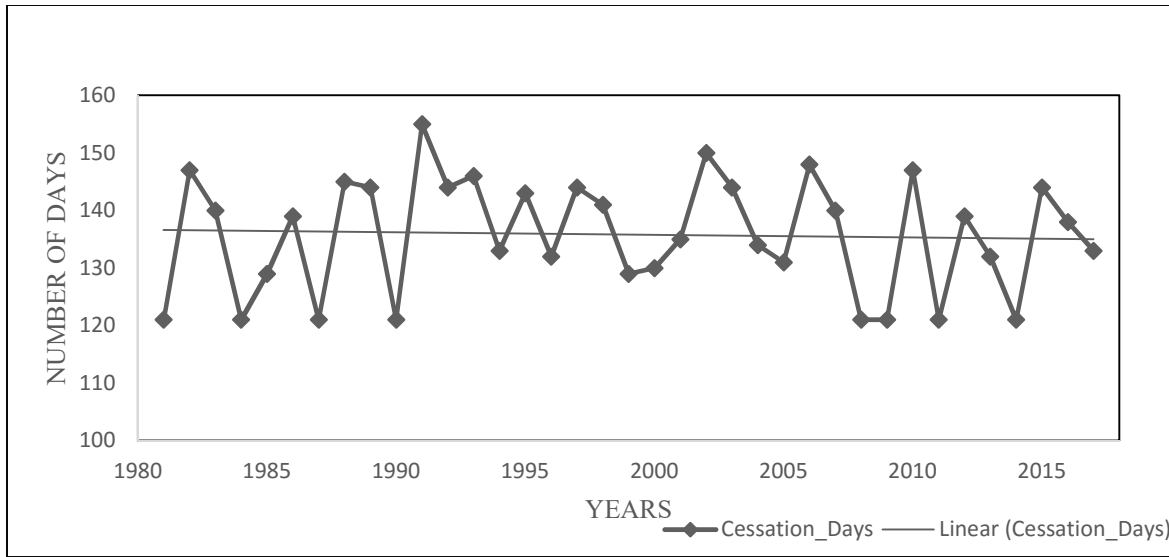


Figure 43: Temporal variability and trend of rainfall Cessation days for Gikonko location during long rains season from 1981 to 2017

There is a tendency of rainfall cessation to end slightly early in recent years over Gikonko (Figure 43) where the earliest cessation recorded was on the 121th day of the year 2014.

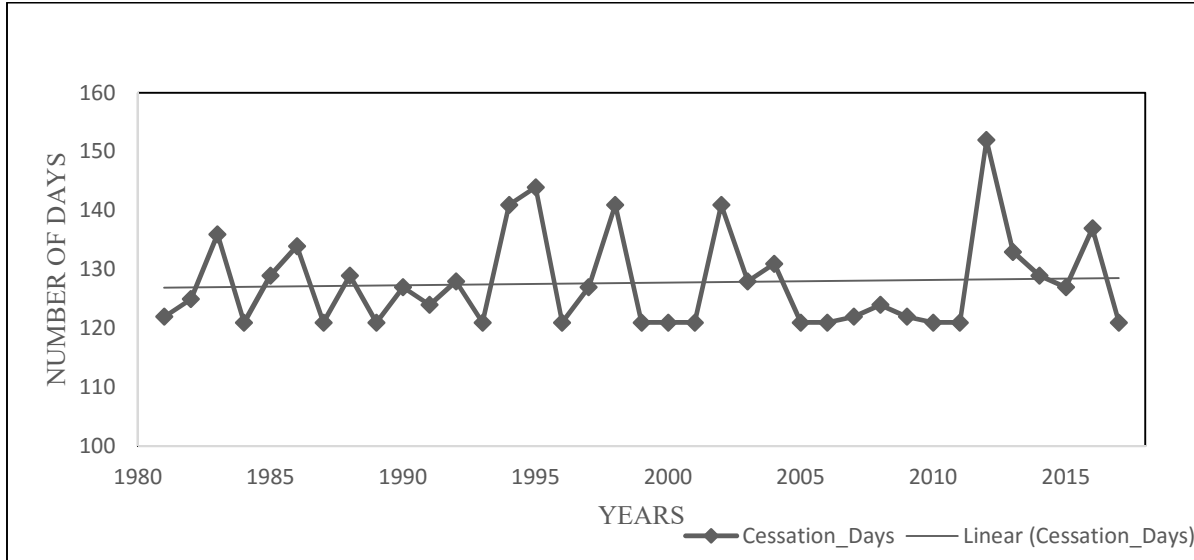


Figure 44: Temporal variability and trend of rainfall Cessation days for Gatunda location during long rains season from 1981 to 2017

There is a tendency of rainfall cessation to end late in recent years over Gatunda (Figure 44) where the latest cessation recorded was on the 152th day of the year 2012.

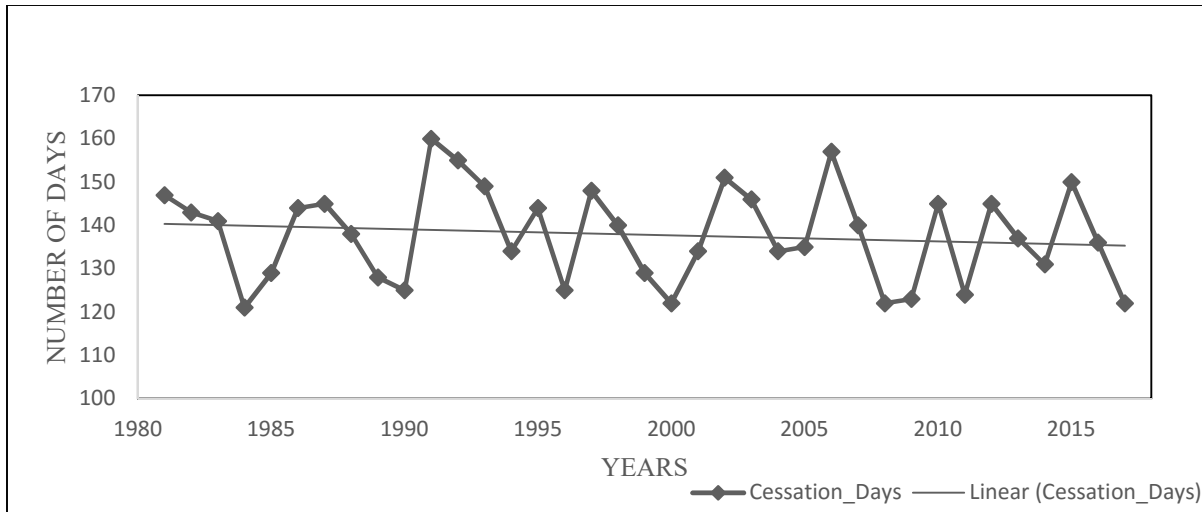


Figure 45: Temporal variability and trend of rainfall Cessation days for Butare Aero location during long rains season from 1981 to 2017

There is a tendency of rainfall cessation to end early in recent years over Butare Aero (Figure 45) where the earliest cessation recorded was on the 122th day of the year 2017.

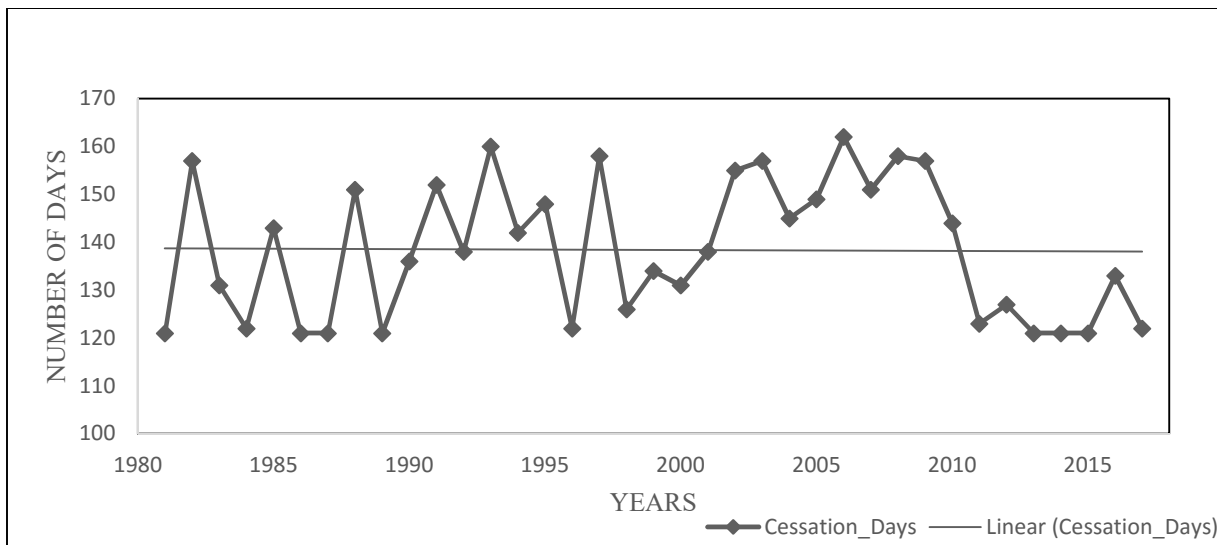


Figure 46: Temporal variability and trend of rainfall Cessation days for Ntaruka location during long rains season from 1981 to 2017

There is a tendency of rainfall cessation to end early in recent years over Ntaruka (Figure 46) where the earliest cessation recorded was on the 121th day of the year 2015. The rainfall cessation was below the mean cessation from 2011.

4.4 Rainfall Amount and Frequency

The standardized precipitation index (SPI) was computed for every month in the season (SPI-1) and seasonal value (SPI-3) in order to comprehend the distribution of rainfall amount within the season. The season was then classified into frequency based on the SPI Values. Here, three month SPI averages based on the identified near homogeneous rainfall zones and seasons are presented. Three-month SPI values are indicative of the short and medium moisture conditions that can be related to the growth of crops while one-month SPI value was used to understand the level of stress on the crop.

Figure 47 to Figure 65 indicate the temporal variability of seasonal rainfall amounts from 1981 to 2017 expressed in terms of Standardized Precipitation Index (SPI) over each delineated zone for both the long and the short rains seasons. How did the seasonal rainfall amounts vary with time from 1981 to 2017 over each location? Some locations exhibited a decreasing trend whereas others exhibited an increasing trend, for instance Gatumba and Rwankeri_Nyabihu.

Location by location comparison reveals a variability in rainfall amount expressed by SPI values and each station behaviour can be understood in terms of climate modes of variability like ENSO episodes and its locations with respect to the meridional arm of the ITCZ. In terms of strong El Niño episodes of 1987/1988 and 1991/1992 or very strong episode of 1982/1983; 1997/1998 and 2015/2016. For example, Gatumba (Figure 47) was extremely wet during 1982/1983 long rains season in contrast with Rwankeri_Nyabihu (Figure 48) location, which was extremely wet during 2015/2016 long rains season for El Niño episodes. There is for example an opposite behaviour on two locations of eastern Rwanda namely Gabiro (Figure 63) and Bukora (Figure 65) during 2016 September – December season characterized by extremely wet and extremely dry conditions respectively. The years 2016/2017 were dry during long rains season with extremely severe effects over the whole country. There exists an observable declining trend of rainfall amounts over some locations like Gatumba (Figure 47) and Mushubi (Figure 50) during the long rains season. There has been a transition from wet to dry seasons due to the fact that most of the years before 2000 have a positive index whereas most of the years after have a negative index over these two areas. An exceptionally dry year before 2000 occurred in 1984 and after 2000 were 2014 in some locations and 2017 during the long rains season.

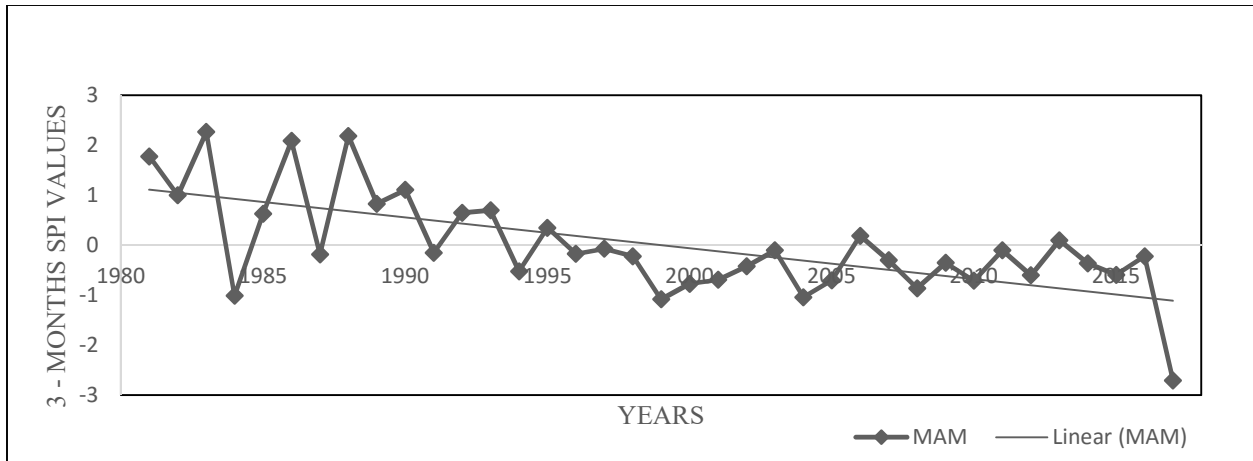


Figure 47: Temporal variability and trend of SPI for Gatumba location during long rains season from 1981 to 2017

There is a declining trend of seasonal rainfall amount over Gatumba (Figure 47) marked with an extremely dry year of 2017 whereas the extremely wet conditions occurred in 1983 in the period from 1981 to 2017.

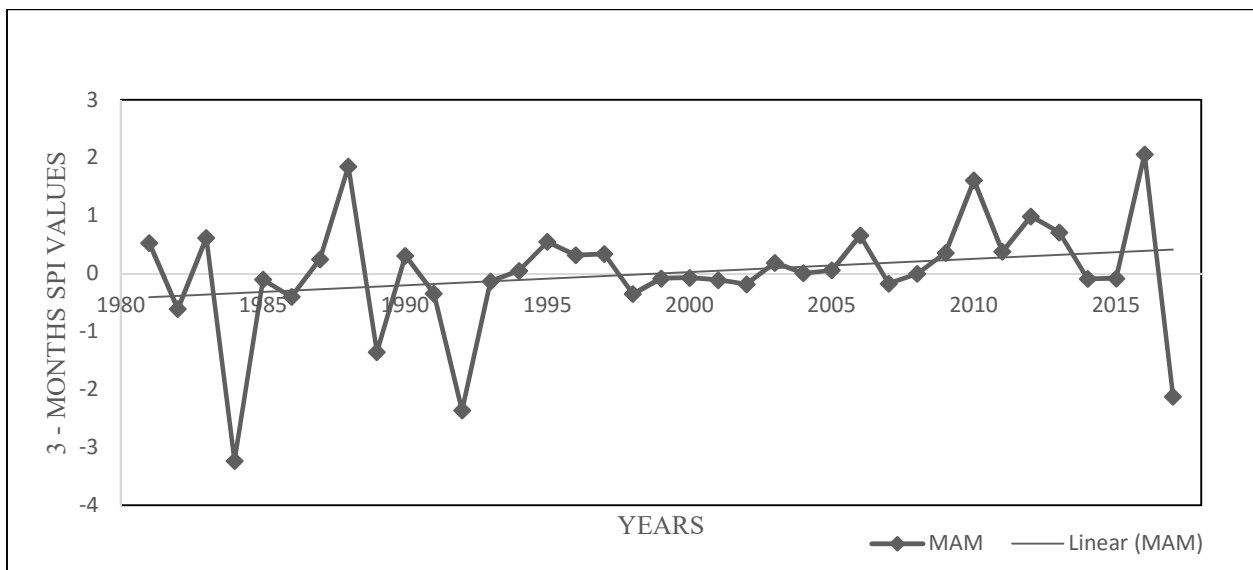


Figure 48: Temporal variability and trend of SPI for Rwankeri_Nyabihu location during long rains season from 1981 to 2017

There is an increasing trend of seasonal rainfall amount over Rwankeri (Figure 48) marked with the extremely dry year of 1984 whereas the extremely wet year occurred in 2016 in the period from 1981 to 2017.

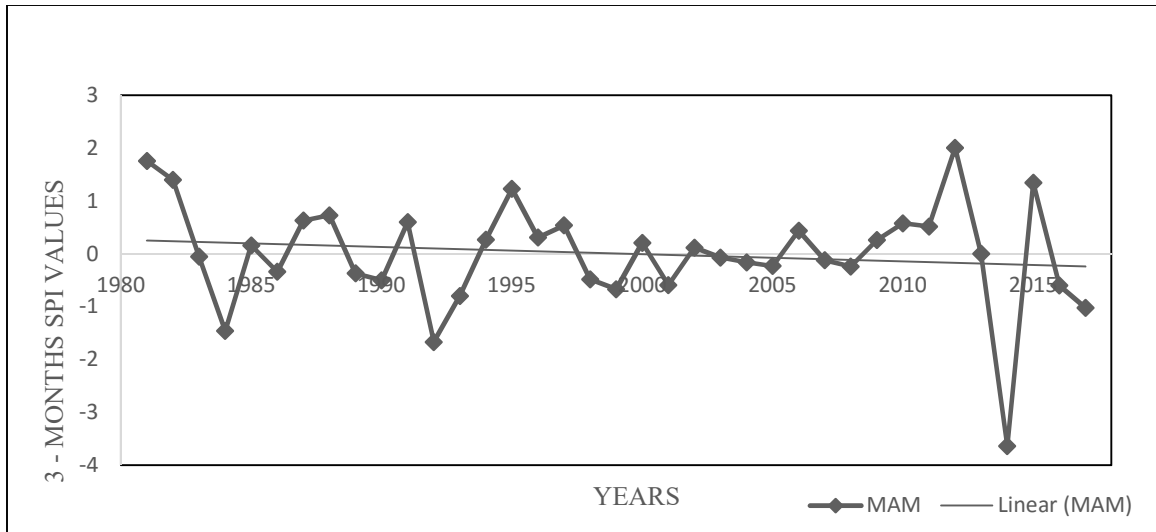


Figure 49: Temporal variability and trend of SPI for Rwamagana location during the long rains season from 1981 to 2017

There is slightly declining trend of seasonal rainfall amount over Rwamagana (Figure 49) marked with the extremely dry year of 2014 whereas the extremely wet year occurred in 2012 in the period from 1981 to 2017.

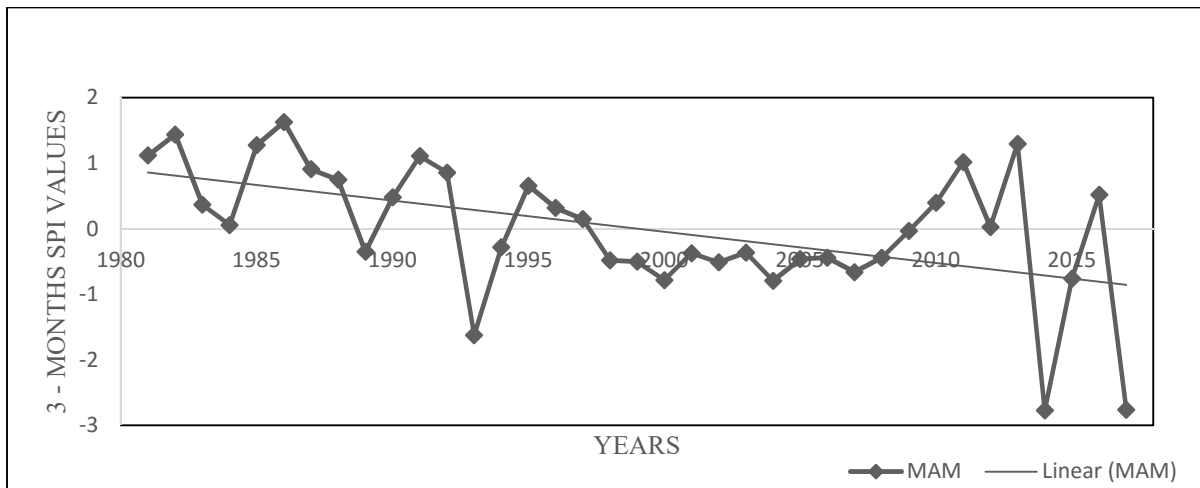


Figure 50: Temporal variability and trend of SPI for Mushubi location during the long rains season from 1981 to 2017

There is declining trend of seasonal rainfall amount over Mushubi (Figure 50) marked with two extremely dry year of 2014 and 2017 whereas the severely wet year occurred in 1986 in the period from 1981 to 2017.

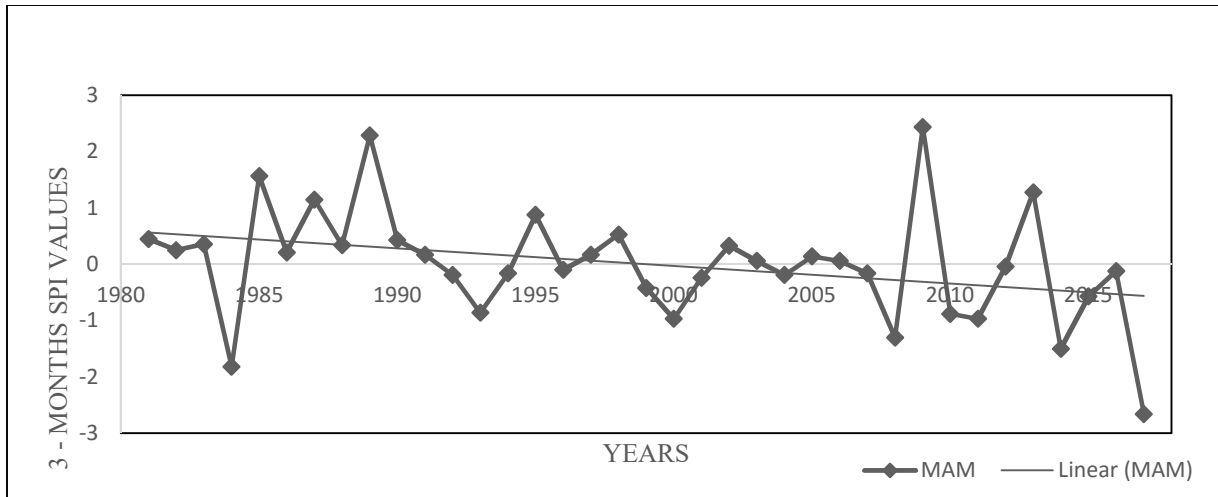


Figure 51: Temporal variability and trend of SPI for Gisanga location during the long rains season from 1981 to 2017

There is declining trend of seasonal rainfall amount over Gisanga (Figure 51) marked with the extremely dry year of 2017 whereas the extremely wet years occurred in 1989 and 2009 in the period from 1981 to 2017.

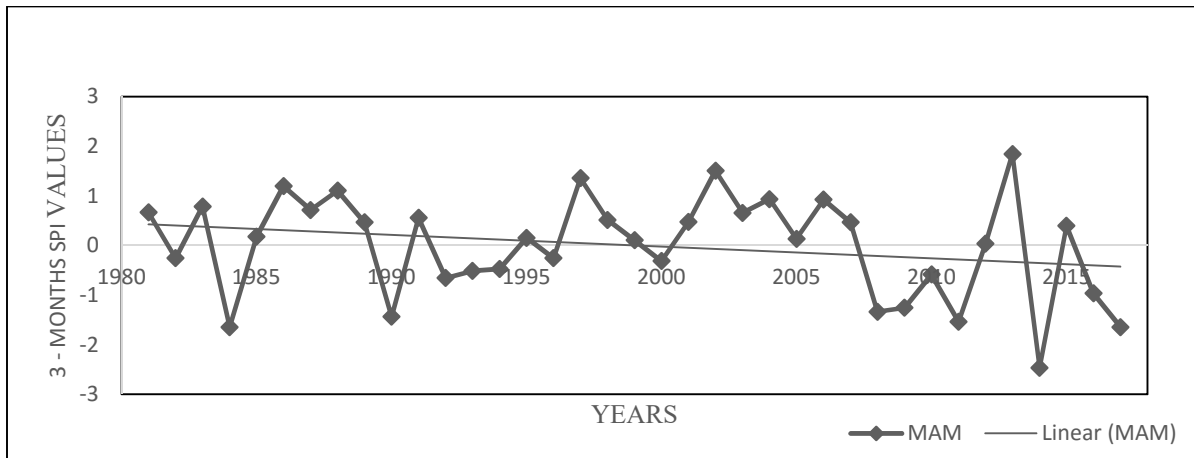


Figure 52: Temporal variability and trend of SPI for Gikonko location during the long rains season from 1981 to 2017

There is declining trend of seasonal rainfall amount over Gikonko (Figure 52) marked with the extremely dry year of 2014 whereas the severely wet year occurred in 2013 in the period from 1981 to 2017.

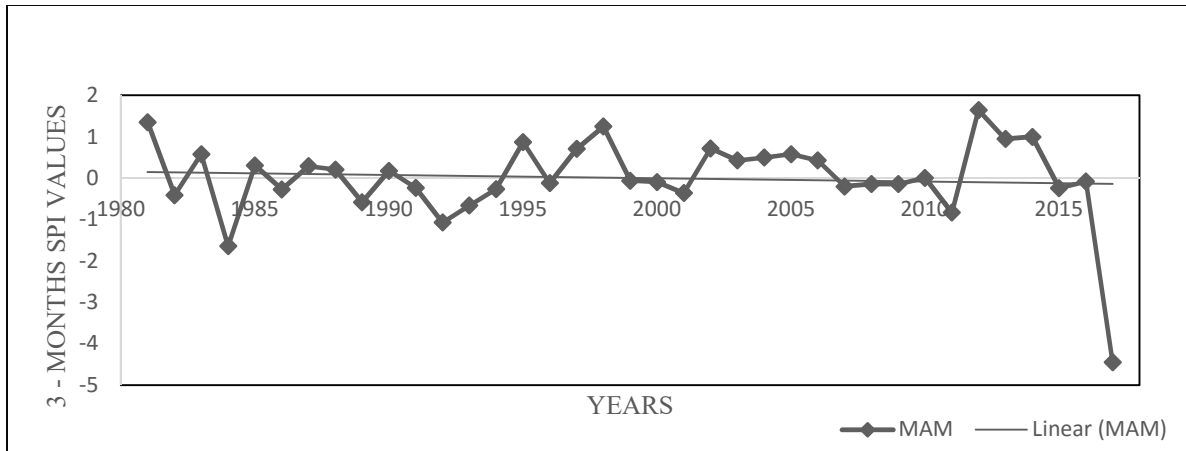


Figure 53: Temporal variability and trend of SPI for Gatunda location during the long rains season from 1981 to 2017

There is slightly decreasing trend of seasonal rainfall amount over Gatunda (Figure 53) marked with the extremely dry year of 2017 whereas the severely wet year occurred in 2012 in the period from 1981 to 2017.

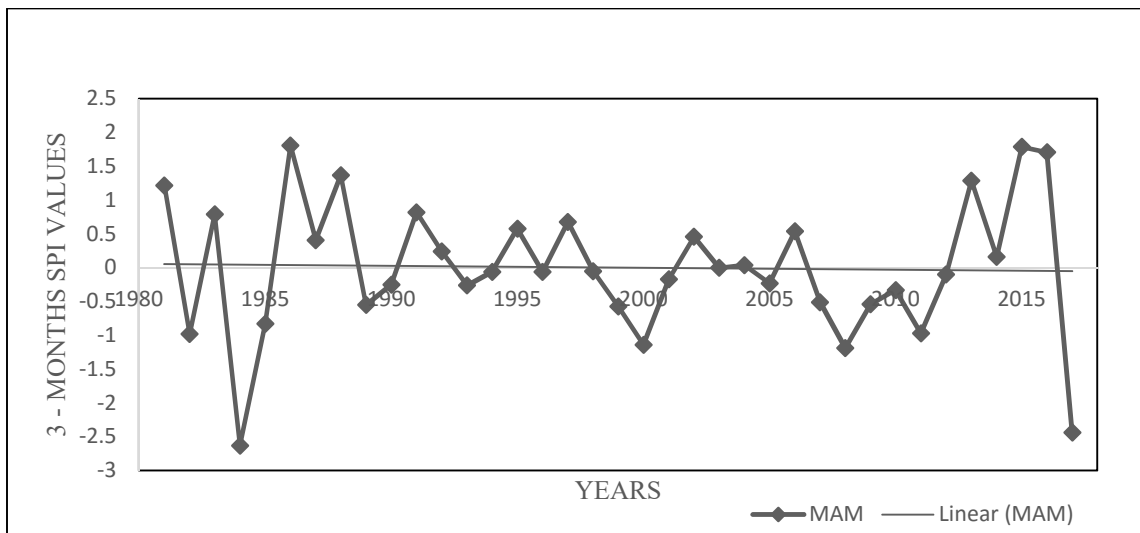


Figure 54: Temporal variability and trend of SPI for Butare Aero location during the long rains season from 1981 to 2017

There is almost a constant trend of seasonal rainfall amount over Butare Aero (Figure 54) marked with an extremely dry year of 2017 whereas the extremely wet year occurred in 1984 in the period from 1981 to 2017.

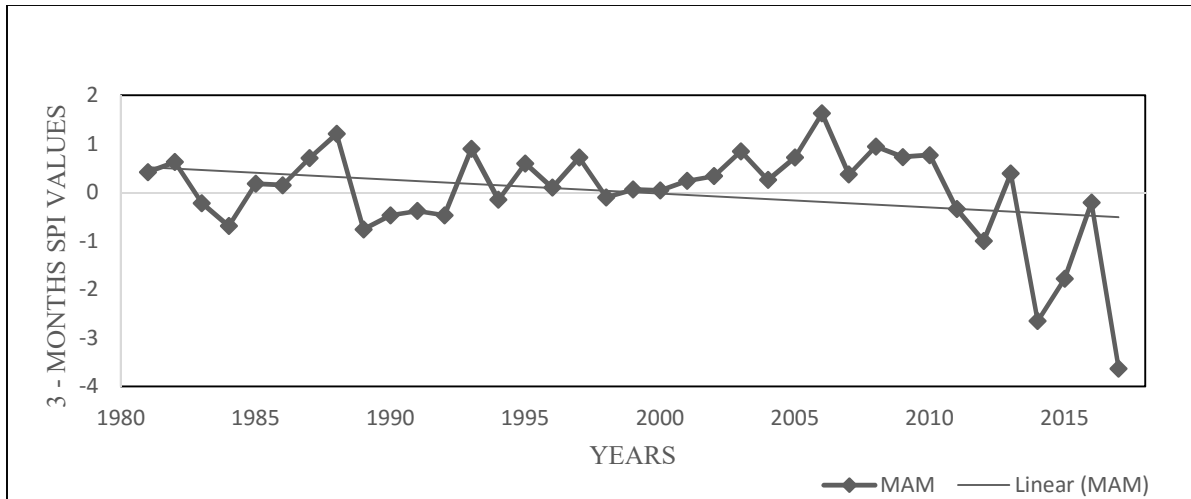


Figure 55: Temporal variability and trend of SPI for Ntaruka location during the long rains season from 1981 to 2017

There is declining trend of seasonal rainfall amount over Ntaruka (Figure 55) marked with the extremely dry year of 2017 whereas the severely wet year occurred in 2006 in the period from 1981 to 2017.

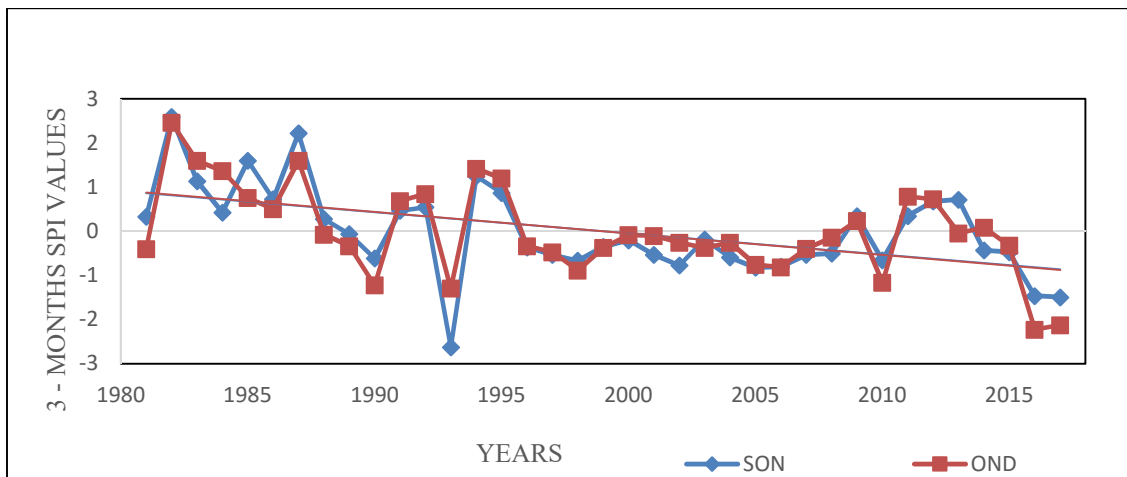


Figure 56: Temporal variability and trend of SPI for Ntendezi during the Short rains season from 1981 to 2017

There is declining trend of seasonal rainfall amount over Ntendezi (Figure 56) marked with the extremely dry SON and OND of 1993 and 2016 & 2017 respectively whereas the severely wet year occurred in 1982 in the period from 1981 to 2017.

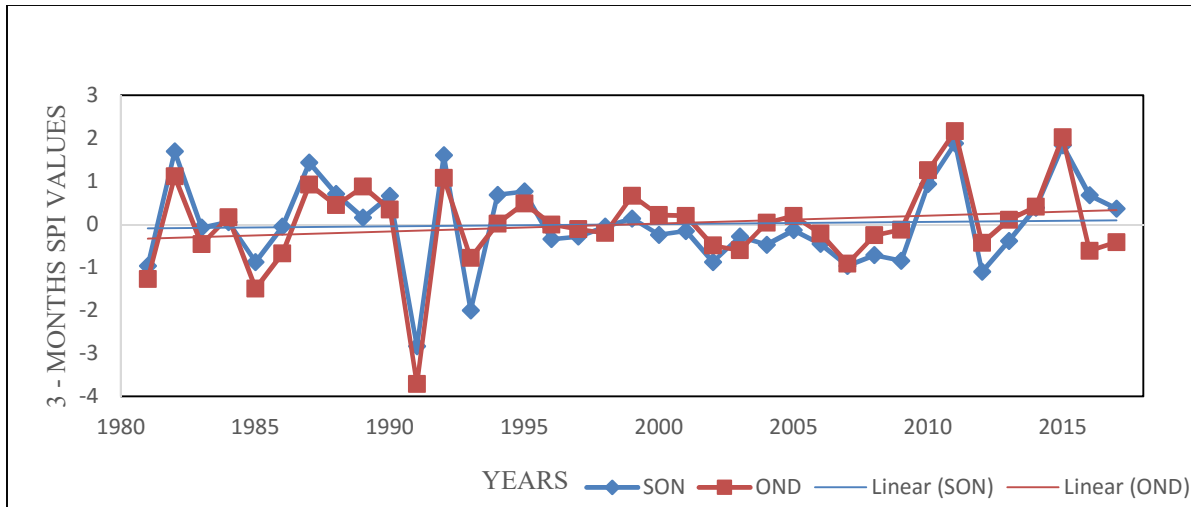


Figure 57: Temporal variability and trend of SPI for Kibuye location during the Short rains season from 1981 to 2017

There is slightly an increasing trend of seasonal rainfall amount over Kibuye (Figure 57) marked for example with the extremely dry OND of 1991 whereas the extremely wet OND occurred in 2011 and 2015 in the period from 1981 to 2017.

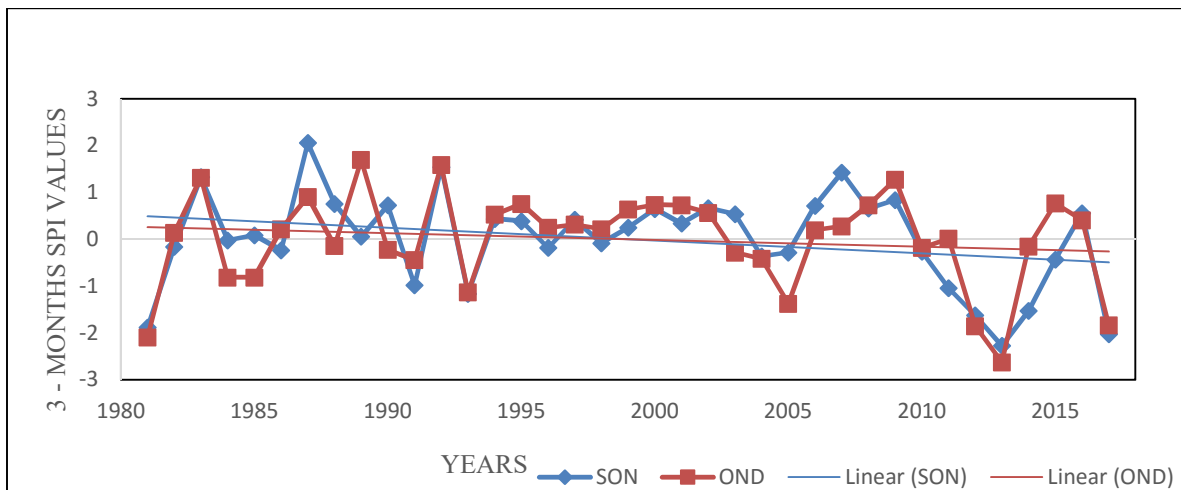


Figure 58: Temporal variability and trend of SPI for Tamira location during the Short rains season from 1981 to 2017

There is a slightly decreasing trend of seasonal rainfall amount over Tamira (Figure 58) marked for example with the extremely dry OND of 1981 and 2013 whereas the severely wet OND occurred in 1989 in the period from 1981 to 2017. The year 2013 was the driest over this location.

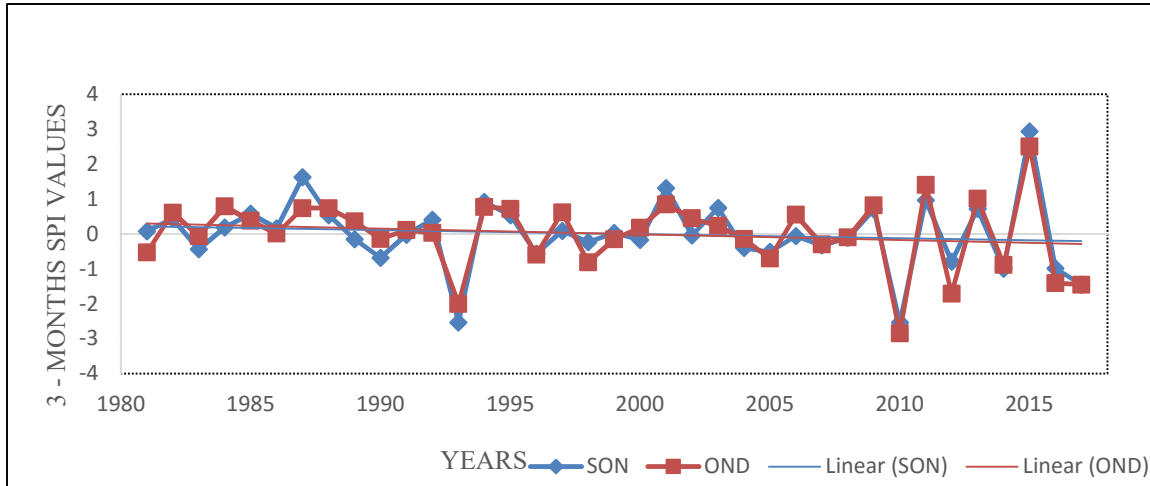


Figure 59: Temporal variability and trend of SPI for Save Paroisse location during the Short rains season from 1981 to 2017

There is a slightly decreasing trend of seasonal rainfall amount over Save Paroisse (Figure 59) marked for example with the extremely dry OND of 2010 and extremely dry SON of 1993 whereas the extremely wet SON occurred in 2015 in the period from 1981 to 2017. The year of 2015 was wettest over this location.

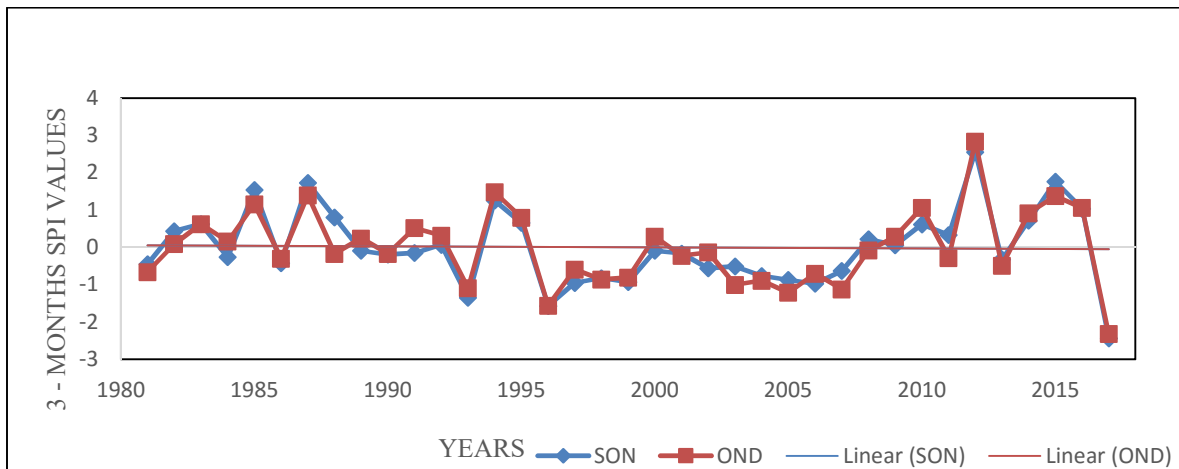


Figure 60: Temporal variability and trend of SPI for Cyinzuzi location during the Short rains season from 1981 to 2017

There is a constant trend in seasonal rainfall amount over Cyinzuzi (Figure 60). The extremely wet SON and OND occurred in 2012 whereas the extremely dry SON and OND was in 2017.

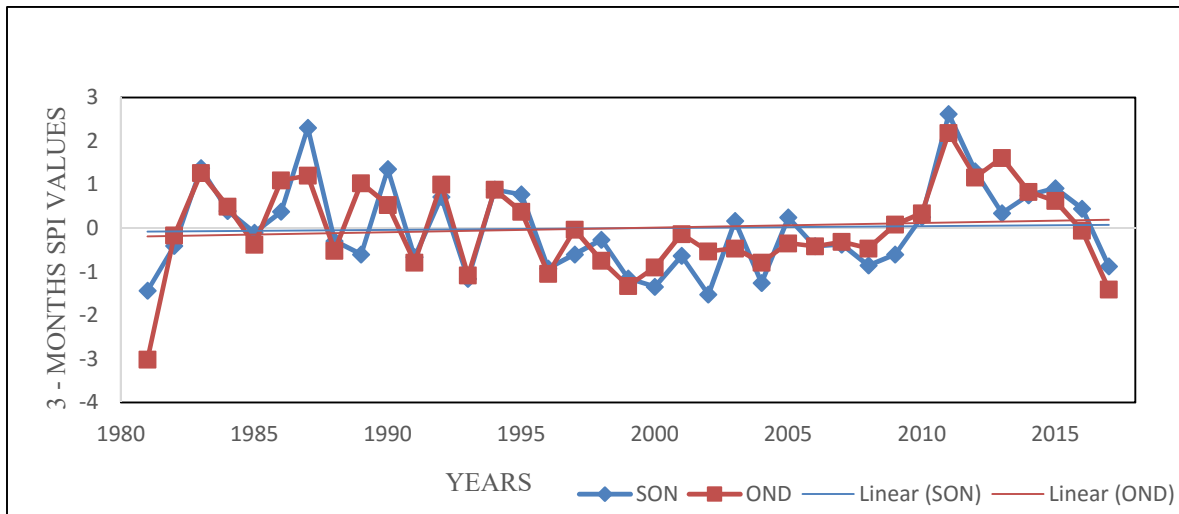


Figure 61: Temporal variability and trend of SPI for Rugobagoba location during the Short rains season from 1981 to 2017

There is slightly Increasing trend of seasonal rainfall amount over Rugobagoba (Figure 61) marked for example with the extremely dry OND of 1981 whereas the extremely wet SON occurred in 1987 and 2011 in the period from 1981 to 2017. The year 2011 was the wettest over this location.

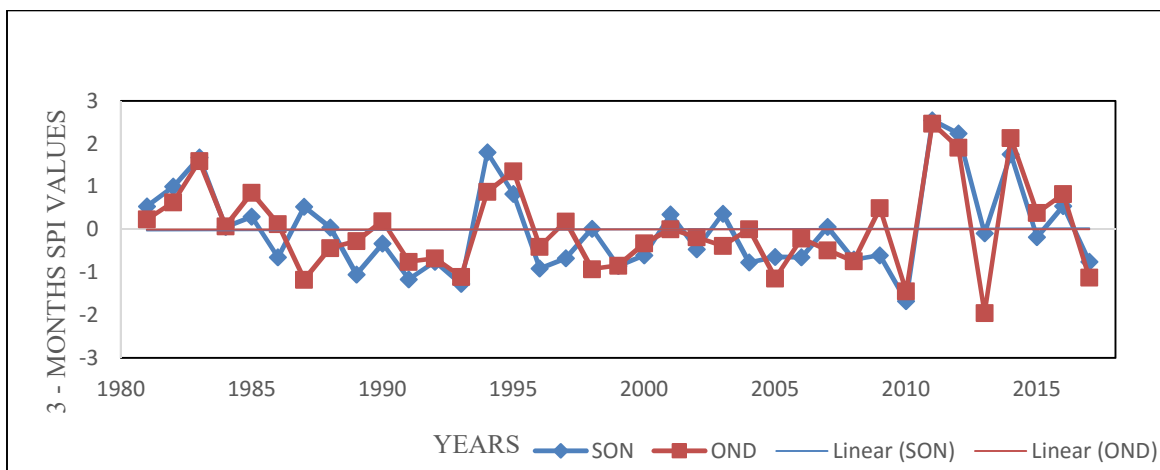


Figure 62: Temporal variability and trend of SPI for Rwamagana location during the Short rains season from 1981 to 2017

There is a constant trend of seasonal rainfall amount over Rwamagana (Figure 62) marked for example with the severely dry OND of 2013 whereas the extremely wet SON and OND occurred in 2011 in the period from 1981 to 2017. The year 2011 was the wettest over this location.

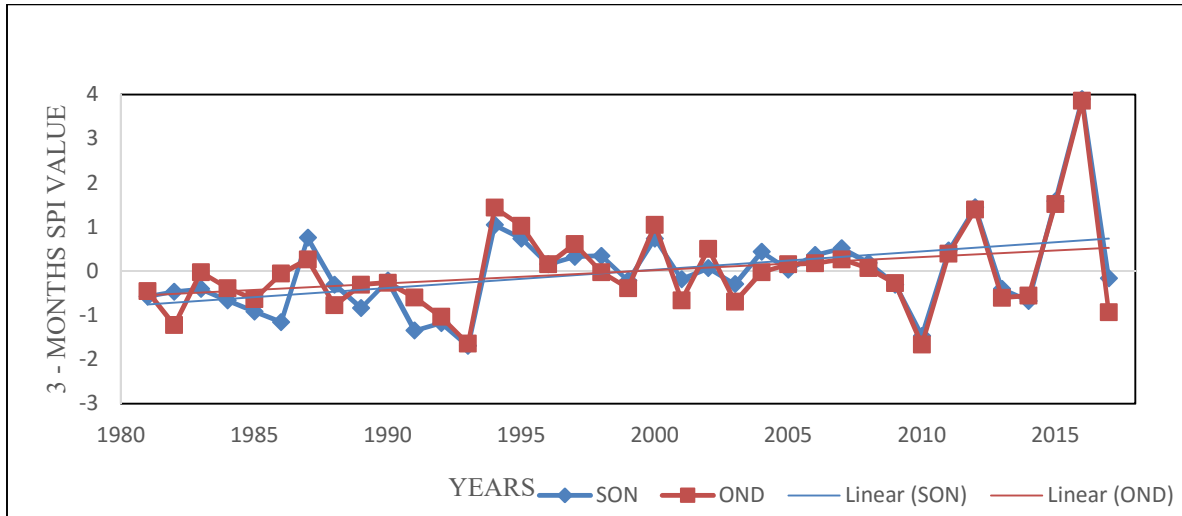


Figure 63: Temporal variability and trend of SPI for Gabiro location during the Short rains season from 1981 to 2017

There is an increasing trend of seasonal rainfall amount over Gabiro (Figure 63) marked for example with the severely dry OND of 2010 whereas the extremely wet SON and OND occurred in 2016 in the period from 1981 to 2017. The year 2016 was the wettest over this location.

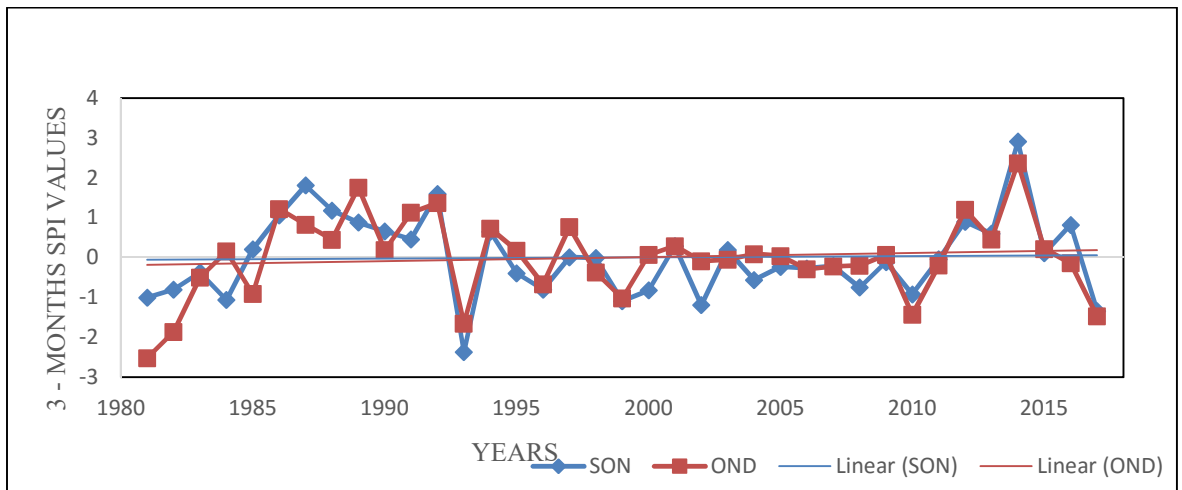


Figure 64: Temporal variability and trend of SPI for Busoro location during the Short rains season from 1981 to 2017

There is almost a constant trend of seasonal rainfall amount over Busoro (Figure 64) marked for example with the extremely dry OND and SON of 1981 and 1993 respectively whereas the extremely wet SON and OND occurred in 2014 in the period from 1981 to 2017. The year 2014 was the wettest over this location.

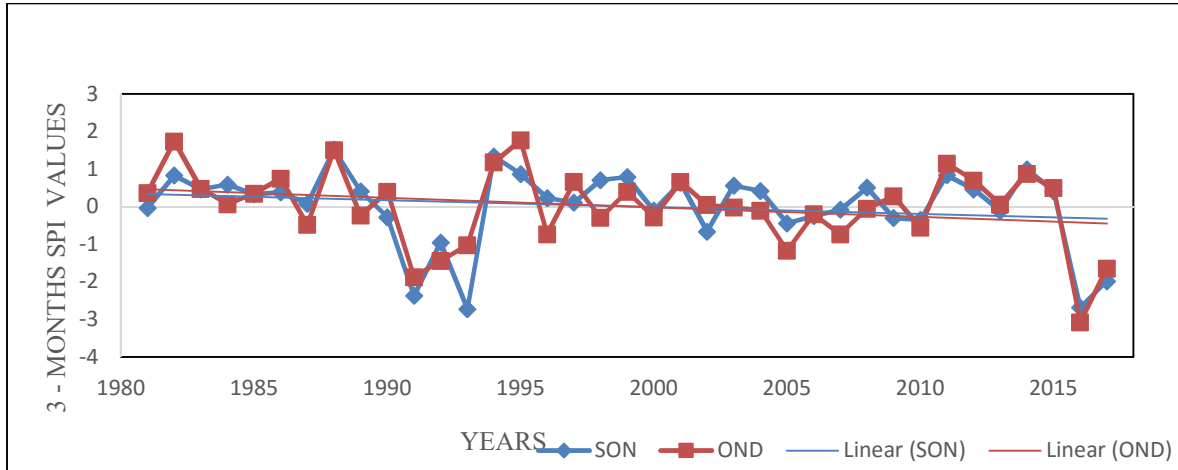


Figure 65: Temporal variability and trend of SPI for Bukora location during the Short rains season from 1981 to 2017

There is a slightly decreasing trend of seasonal rainfall amount over Bukora (Figure 65) marked for example with the extremely dry OND and SON of 2017 in the period from 1981 to 2017. The year 2017 was the driest over this location. The SON was often extremely dry than OND.

The results for rainfall frequency and trends analysis is detailed below as part of the seasonal rainfall variability characterization. In order to comprehend the seasonal rainfall amount distribution across years, the seasons were classified in frequencies based on the Standardized precipitation index (SPI) classification. The analysis of frequency of rainfall amount for 37 years during both the short and the long rains seasons was done in order to determine the percentage frequency within each delineated zone. Tables 8 & 9 indicate the percentage frequency in 7 categories of SPI values from 1981 to 2017 for the short and long seasons on the representative station for each delineated zone respectively.

Table 8: The Percentage Frequency for the Short rains season from 1981 to 2017 based on SPI classifications over the representative stations over Rwanda

Station Names	Period	Extremely Wet	Very Wet	Moderately Wet	Near Normal	Moderately dry	Severely dry	Extremely dry
Ntendezi	SON	5.4	2.7	5.4	78.4	5.4	0	2.7
	OND	2.7	5.4	8.1	70.3	8.1	0	5.4
Kibuye	SON	0	10.8	2.7	78.4	2.7	0	5.4
	OND	5.4	0	8.1	78.4	5.4	0	2.7
Tamira	SON	2.7	2.7	5.4	70.3	5.4	8.1	5.4
	OND	0	5.4	5.4	72.9	5.4	5.4	5.4
Save Paroisse	SON	2.7	2.7	2.7	78.4	8.1	0	5.4
	OND	2.7	0	5.4	78.4	5.4	2.7	5.4
Cyzuzuzi	SON	2.7	8.1	5.4	75.6	2.7	2.7	2.7
	OND	2.7	0	16.2	64.8	10.8	2.7	2.7
Rugobagoba	SON	5.4	0	8.1	70.3	13.5	2.7	0
	OND	2.7	2.7	16.2	64.8	10.8	0	2.7
Rwamagana	SON	5.4	8.1	2.7	72.9	8.1	2.7	0
	OND	5.4	5.4	2.7	70.3	13.5	2.7	0
Gabiro	SON	2.7	2.7	5.4	75.6	10.8	2.7	0
	OND	2.7	2.7	10.8	72.9	5.4	5.4	0
Busoro	SON	2.7	5.4	5.4	70.3	13.5	0	2.7
	OND	2.7	2.7	10.8	67.5	8.1	5.4	2.7
Bukora	SON	0	2.7	5.4	81	0	2.7	8.1
	OND	0	8.1	5.4	70.3	8.1	5.4	2.7

The low percentage of near normal years in Table 8 is 64.8 during OND for both Rugobagoba, which is in the central plateau of Rwanda and Cyinzuzi that lies on the central axis towards northern Rwanda followed by Busoro with 67.5. The three months of September to November have more near normal frequency than October to December season. This suggested that more

years had more near normal seasonal rainfall from September to November than October to December. Hence, growing crops in SON may be advantageous than OND in a near normal season.

Table 9: The Percentage Frequency for the long rains season from 1981 to 2017 based on SPI classifications over the representative stations over Rwanda

Stations Names	Extremely Wet	Very Wet	Moderately Wet	Near Normal	Moderately dry	Severely dry	Extremely dry
Gatumba	8.1	2.7	5.4	72.9	8.1	0	2.7
Rwankeri	2.7	5.4	0	81	2.7	0	8.1
Rwamagana	2.7	2.7	8.1	75.6	5.4	2.7	2.7
Mushubi	0	2.7	16.2	72.9	0	2.7	5.4
Gisanga	5.4	2.7	5.4	75.6	2.7	5.4	2.7
Gikonko	0	5.4	8.1	67.5	8.1	8.1	2.7
Gatunda	0	2.7	8.1	81	2.7	2.7	2.7
Butare Aero	0	8.1	8.1	72.9	5.4	0	5.4
Ntaruka	0	2.7	2.7	83.7	2.7	2.7	5.4

The low percentage of near normal rainfall years (67.5) in Table 9 was recorded over Gikonko station location during long rains season. This indicated that the station had a higher number of non-normal years, which were expressed in cases of dry years. Hence, this is an indicator of the shift in the mean rainfall patterns towards below rainfall for several cases than any other station. The abnormality behaviours exhibited by Gikonko may be related to high frequency of extremes or outliers in a normal distribution.

The next section presents the analysis of the trend of seasonal rainfall amount over each delineated zone during both the short and the long rains season.

4.5 Mann Kendall and Sen's Slope Statistics

The Mann-Kendall (MK) trend test suggests that the null hypothesis of no trend is rejected for $|Z_s| > 1.96$ at the 5% significance level. MK was used to know the direction of the trend. The Sen's slope estimator provided the magnitude of the trend. In this study, the knowledge about the rainfall trend and its magnitudes provides a baseline of understanding the effects of reduced or enhanced

rainfall on crop yields. Table 10 and Table 11 indicate the sign of the trend and the steepness of the trend of seasonal rainfall amount for the representative stations for each delineated near homogeneous rainfall zone for the short and the long rains season during the last 37 years from 1981 to 2017.

Table 10: Mann - Kendall trend Test and Sen's slope estimates over Rwanda for the Short rains season from 1981 to 2017 over the representative stations. Qmin is the smallest and Qmax is the largest rank of the slope respectively.

Station Names	Period	Mann – Kendall trend test (Zs)	Sen's slope estimates (at 95%)		
			Sen's slope	Qmin	Qmax
Ntendezi	SON	-3.07	-0.048	-0.067	-0.020
	OND	-2.45	-0.047	-0.082	-0.006
Kibuye	SON	-0.27	-0.004	-0.036	0.032
	OND	0.13	0.002	-0.026	0.037
Tamira	SON	-1.35	-0.017	-0.057	0.016
	OND	-0.52	-0.010	-0.045	0.022
Save Paroisse	SON	-1.43	-0.021	-0.042	0.010
	OND	-0.95	-0.014	-0.050	0.014
Cyzuzuzi	SON	0.52	0.004	-0.010	0.019
	OND	0.56	0.006	-0.016	0.024
Rugobagoba	SON	0.21	0.002	-0.033	0.040
	OND	0.20	0.003	-0.034	0.042
Rwamagana	SON	-0.30	-0.004	-0.038	0.024
	OND	-0.60	-0.012	-0.044	0.027
Gabiro	SON	2.34	0.032	0.005	0.059
	OND	1.53	0.020	-0.007	0.049
Busoro	SON	-0.10	-0.002	-0.035	0.037
	OND	-0.03	-0.001	-0.032	0.035
Bukora	SON	-1.22	-0.017	-0.039	0.009
	OND	-1.07	-0.018	-0.054	0.013

The Qmedian gives the Sen's slope estimates and its interval of variation ranges between Qmin and Qmax provided in Table 10 for the short rains season. The low steepness indicated a weak trend in rainfall amount with time while high steepness indicated sharp changes. For example, Ntendezi (Table 10) had a significant declining trend in seasonal rainfall amount for both the SON (-3.07) and OND (-2.45) with negative steepness of -0.048 and -0.047 respectively. Hence, the researcher is 95% confident that there was a declining trend of seasonal rainfall amount over Ntendezi.

Table 11: Mann - Kendall trend test and Sen's slope estimates for rainfall during the long rains season from 1981 to 2017 over Rwanda. Qmin is the smallest and Qmax is the largest rank of the slope respectively.

Stations Names	Mann – Kendall trend test (Zs)	Sen's slope estimates (at 95%)		
		Sen's slope	Qmin	Qmax
Gatumba	-3.68	-0.054	-0.084	-0.027
Rwankeri	1.75	0.016	-0.003	0.041
Rwamagana	-0.72	-0.010	-0.042	0.021
Mushubi	-3.06	-0.046	-0.076	-0.016
Gisanga	-2.83	-0.033	-0.059	-0.010
Gikonko	-1.49	-0.021	-0.056	0.012
Gatunda	0.44	0.006	-0.020	0.027
Butare Aero	-0.39	-0.008	-0.044	0.025
Ntaruka	-0.17	-0.005	-0.035	0.023

During the short rains season both Ntendezi and Gabiro stations locations exhibited significant trends in the rainfall where there was a considerable decline and an increase in rainfall respectively. During the long rains season, stations of Gatumba, and Gisanga in the central plateau and Mushubi over the windward of the Crete Congo Nile of Rwanda exhibited a considerable decline in rainfall, which may cause low crop yields if there are no strategies to undertake irrigation farming in the near future. In terms of the Sen's slope estimates, there was mostly negative steepness that suggest a decrease in rainfall amount. These results agreed with the findings of Henninger (2013) that revealed a drying trend. For example, Gatumba (Table 11) had a significant declining trend in

seasonal rainfall amount for the long rains season (-3.68) with a negative steepness of -0.054. Hence, the researcher is 95% confident that there was a declining trend of seasonal rainfall amount over Gatumba.

4.6 Analysis of Rainfall and Crop Yields for Maize and Beans

This section presents the analysis on the available 12-year data on crop yields for maize and 9-year data on beans' yields and how they are influenced by seasonal rainfall, using correlation and multiple linear regression techniques. Firstly, the analysis of the temporal variability of maize and beans' yields. Later, there is seasonal rainfall amount, rainfall intensity, rainfall frequency and seasonal length correlation with crop yields. Monthly rainfall is a powerful determinant of crop production (Alam *et al*, 2011). Hence, the monthly rainfall contribution on seasonal yields was analyzed using a regression model. Figure 66 to Figure 69 indicate the temporal variability of maize and beans' yields over six zones during both the short rains and long rains season for the 2006 to 2017 period.

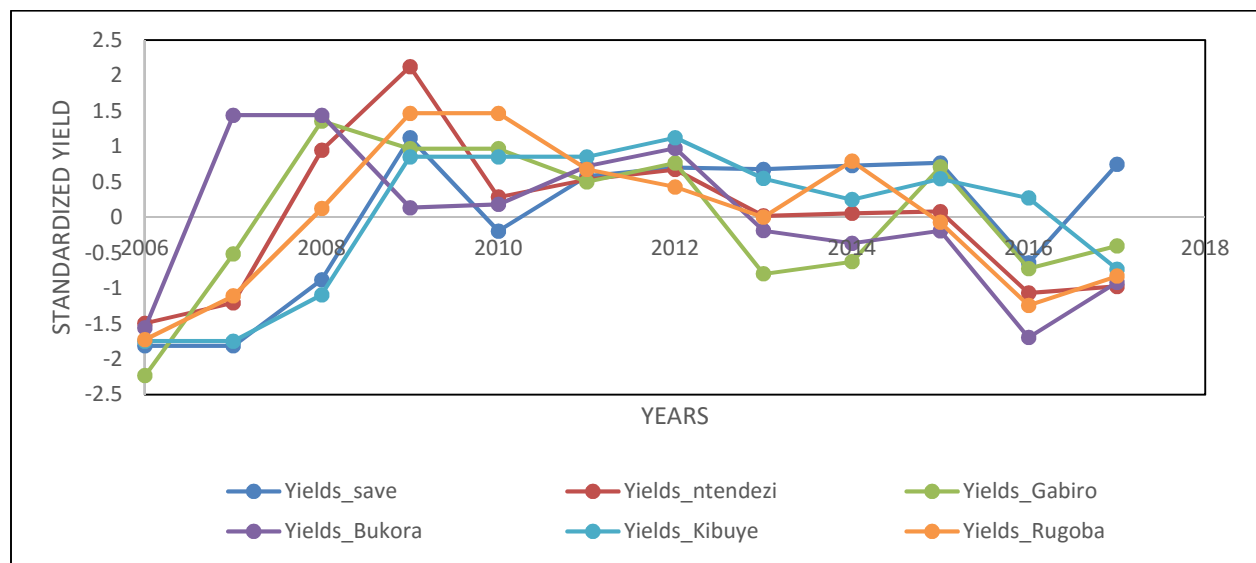


Figure 66: Temporal variability of Maize yields during the Short rains season (Season A for Agriculture) from 2006 to 2017

The years 2016 and 2017 were marked with below average crop yields of maize as shown in Figure 66 in five out of six locations during the short rains season. The period from 2006 to 2017 was marked with variability in maize yield from one season to another and from one location to another. Generally, above average crop yield of maize all over was realised during the period 2009-2012.

A below average crop yield meant a shortage in the supply of maize that may lead to hunger and other associated effects in families.

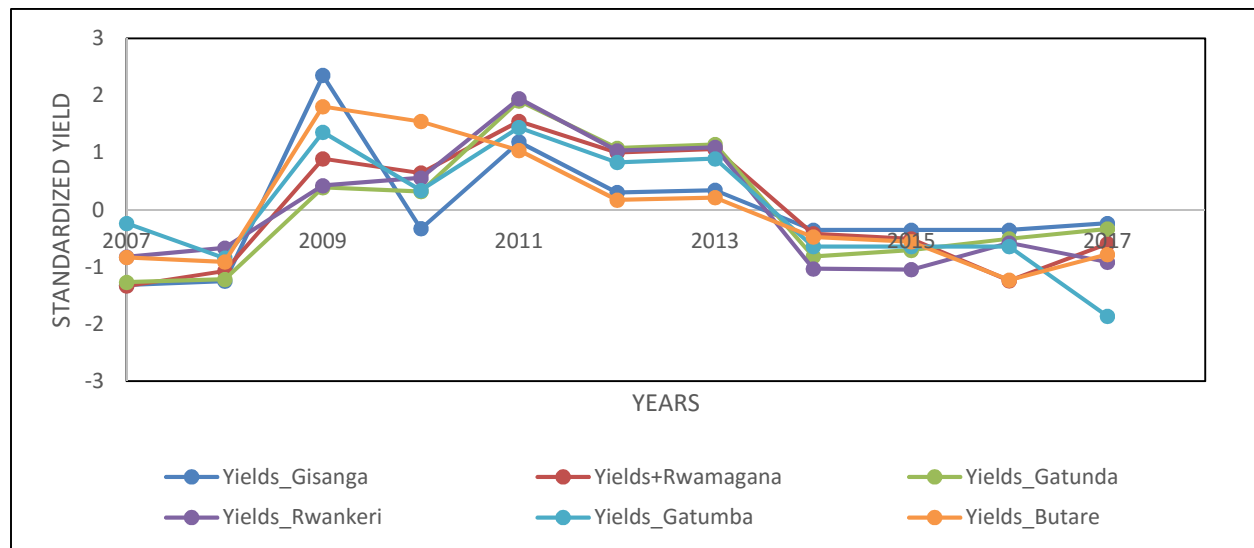


Figure 67: Temporal variability of Maize yields during the Long rains season (Season B for Agriculture) from 2007 to 2017

The years 2014 to 2017 were marked with below average crop yields of maize as shown in Figure 67 in all the six locations during the long rains season. The period from 2007 to 2017 was marked with variability in maize yield from one season to another and from one location to another. Generally, above average maize yield all over was realised during the period 2009-2013. A below average crop yield meant a shortage in the supply of maize that may lead to hunger and other associated effects in families.

The years 2013 to 2017 were marked with below average yields in beans as shown in Figure 68 below in all the six locations during the short rains season. The period from 2009 to 2017 was marked with variability in beans' yield from one season to another and from one location to another. Generally, above average beans' yield all over was realised during the years 2011 and 2012. In Rwanda, beans are mixed with vegetables and consumed with for example, rice or sweet and Irish potatoes. A below average crop yield meant a shortage in the supply of beans that may lead to hunger and other associated effects in families.

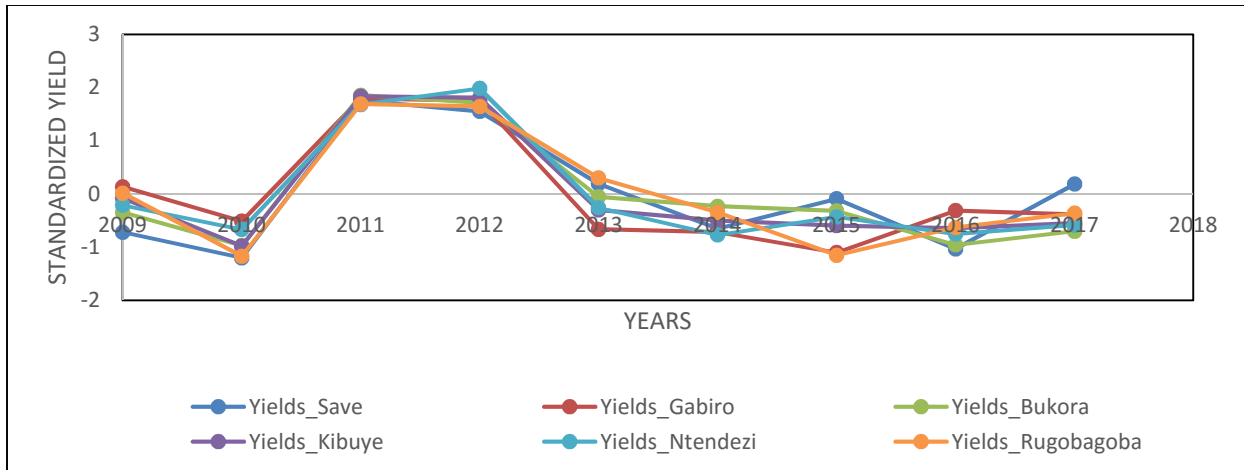


Figure 68: Temporal variability of Beans yields during the Short rains season (Season A for Agriculture) from 2009 to 2017

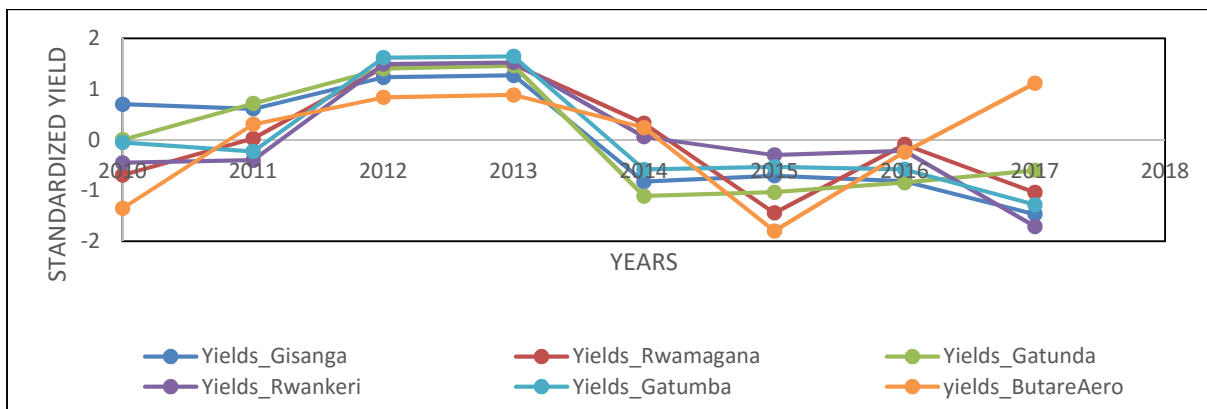


Figure 69: Temporal variability of Beans yields during the Long rains season (Season B for Agriculture) from 2010 to 2017

The years 2014 to 2017 were marked with below average yields in beans as shown in Figure 69 above in almost all the six locations during the long rains season. The period from 2010 to 2017 was marked with variability in beans' yield from one season to another and from one location to another. Generally, above average beans' yield all over was realised during the years 2012 and 2013. A below average crop yield meant a shortage in the supply of beans that may lead to hunger and other associated effects in families like malnutrition. The temporal variability of crop yields indicated mostly a shortage in maize and beans yields from 2014 to 2017 almost countrywide and season-wide with enhanced shortage during 2016 and 2017. This result agreed with local observations.

The Table 12 to Table 23 were used to summarize the results from correlation and multiple linear regression analysis of crop yields and rainfall. Table 12 presents the analysis of monthly contribution on maize and beans yields during the short rains season. The strong correlation between monthly rainfall and maize yields was found over Rugobagoba location with 66.7% variability in maize explained by monthly rainfall variability. In addition, beans yields moderately correlate with monthly rainfall over Save Paroisse location with 55.4% of variance in beans explained by monthly rains variability during the short rains.

Table 12: Monthly (September, October, November, December) Rainfall Contribution on Maize and Beans Yields during the short rains from 2006 – 2017 over Rwanda

Station Name	Regression Equation					Pearson correlation	R-squared
Maize							
	Constant	Sept	Oct	Nov	Dec		
Save Paroisse	-0.052	0.655	0.26	-0.287	-0.189	0.703	0.494
Ntendezi	0.318	0.316	0.804	-0.028	0.029	0.678	0.459
Gabiro	0.198	-0.054	-0.468	0.117	0.519	0.412	0.169
Bukora	0.203	0.262	0.610	0.476	-0.676	0.714	0.510
Kibuye	-0.371	0.296	0.203	0.050	0.488	0.578	0.335
Rugobagoba	-0.259	-3.122	1.559	2.271	0.624	0.817	0.667
Beans							
Save Paroisse	-0.259	0.791	-0.728	0.142	0.295	0.745	0.554
Ntendezi	0.234	0.208	0.655	-0.022	0.100	0.675	0.456
Gabiro	-0.108	0.387	-0.567	0.151	0.620	0.539	0.290
Bukora	-0.236	-0.187	0.234	-0.179	0.967	0.722	0.521
Kibuye	-0.096	-0.174	-0.214	0.088	0.422	0.424	0.180
Rugobagoba	-0.505	-0.582	0.177	1.181	0.204	0.706	0.498

During the short rains season for example, the September rainfall contributed negatively on the maize yields over Rugobagoba. This implies that suitable months for growing maize over there

start with October rainfall. The test of significance of the level of association between the crop yields and monthly rainfall was done to confirm or reject the level of significance of the relationship. Table 13 summarizes the results from the test of significance of the relationship between monthly rainfall and crop yields from 2006 to 2017 for maize and from 2009 to 2017 for beans. Test of significance of the correlations between monthly rainfall and crop yields for the short rains season indicated that there exists a significant relationship between monthly rainfall and crop yields over central (Rugobagoba & Save Paroisse), southwestern (Ntendezi) and southeastern (Bukora) Rwanda. The researcher is confident at 95% significance level that a significant relationship exists simultaneously between monthly rainfall, maize and beans yields over these locations.

Table 13: Test of significance of the monthly (September, October, November and December) rainfall contribution on Maize and Beans yields during the short rains from 2006 to 2017

Station Name	Pearson correlation	T calculated	T tabulated	Significance at 5% level
Maize				
Save Paroisse	0.703	3.125	2.228	Significant
Ntendezi	0.678	2.916	2.228	Significant
Gabiro	0.412	1.429	2.228	Not Significant
Bukora	0.714	3.224	2.228	Significant
Kibuye	0.578	2.239	2.228	Significant
Rugobagoba	0.817	6.038	2.228	Significant
Beans				
Save Paroisse	0.745	2.955	2.365	Significant
Ntendezi	0.675	2.420	2.365	Significant
Gabiro	0.539	1.693	2.365	Not significant
Bukora	0.722	2.761	2.365	Significant
Kibuye	0.424	1.238	2.365	Not significant
Rugobagoba	0.706	2.637	2.365	Significant

Table 14 below presents the analysis of monthly contribution on maize and beans' yields during the long rains season. The strong correlation between monthly rainfall and maize yields was found over Gisanga location with 62.7% variability in maize explained by monthly rainfall variability. In addition, beans yields moderately correlate with monthly rainfall over Gisanga location with 73.8% of variance in beans explained by monthly rains variability during the long rains.

Table 14: Monthly (March, April, May) Rainfall contribution on Maize and Beans yields during the long rains from 2007 – 2017 over Rwanda

Station Name	Regression Equation				Pearson correlation	R-Squared
Maize						
	Constant	March	April	May		
Gisanga	0.141	0.671	-0.303	0.368	0.792	0.627
Rwamagana	0.181	0.477	-0.095	0.371	0.619	0.384
Gatunda	0.025	0.197	-0.245	0.449	0.415	0.172
Rwankeri	-0.185	0.356	-0.399	0.939	0.759	0.577
Gatumba	0.625	0.522	0.459	0.565	0.748	0.560
Butare Aero	0.093	0.138	-0.273	0.977	0.673	0.453
Beans						
Gisanga	0.641	0.476	0.182	0.694	0.859	0.738
Rwamagana	0.075	0.131	-0.006	-0.023	0.148	0.022
Gatunda	0.132	0.142	-0.169	0.586	0.546	0.298
Rwankeri	-0.088	0.149	-0.118	0.647	0.603	0.364
Gatumba	0.696	0.277	0.819	-0.426	0.716	0.513
Butare Aero	-0.039	0.166	-0.447	-0.380	0.652	0.425

During the long rains season, the month of April contributed negatively to the maize yields over five out of six locations.

Table 15 summarizes the results from the test of significance of the relationship between monthly rainfall and crop yields from 2007 to 2017 for maize and from 2009 to 2017 for beans during the

long rains season. Test of significance of the correlations between monthly rainfall and crop yields for the long rains season indicated that there exist significant relationship between monthly rainfall and crop yields over central (Gisanga & Gatumba) Rwanda. The researcher is confident at 95% significance level that a significant relationship exists simultaneously between monthly rainfall, maize and beans yields over these locations.

Table 15: Test of significance of the monthly (March, April, May) rainfall contribution on Maize and Beans yields during the long rains from 2007 to 2017

Station Name	Pearson correlation	T calculated	T tabulated	Significance at 5% level
Maize				
Gisanga	0.792	3.892	2.262	Significant
Rwamagana	0.619	2.364	2.262	Significant
Gatunda	0.415	1.368	2.262	Not significant
Rwankeri	0.759	3.497	2.262	Significant
Gatumba	0.748	3.381	2.262	Significant
Butare Aero	0.673	2.729	2.262	Significant
Beans				
Gisanga	0.859	4.108	2.447	Significant
Rwamagana	0.148	0.366	2.447	Not significant
Gatunda	0.546	1.596	2.447	Not significant
Rwankeri	0.603	1.851	2.447	Not significant
Gatumba	0.716	2.512	2.447	Significant
Butare Aero	0.652	2.106*	2.447	Not significant

*: Significant correlation between monthly rainfall and crop yields at 10% significance level

Table 16 indicates the results from seasonal rainfall amount correlation with maize for the period from 2006 to 2017 and with beans from 2009 to 2017 during the short rains season. There is a significant relationship at 5% significance level between seasonal rainfall amount and maize yields over the southwest (Ntendezi) areas of Rwanda. Again, the test of significance was conducted at 10% significance level. This revealed that the level of association between seasonal rainfall

amount and maize yields was significant over Kibuye and Bukora during the short rains season. Rugobagoba, Bukora and Ntendezi stations seasonal rainfall amount relationship with beans yields was also significant at 10%. Hence, the researcher is confident at 90% that seasonal rainfall amount and crop yields are correlated over Rugobagoba, Ntendezi, Bukora and Kibuye representative stations during the short rains season.

Table 16: Significance of the Pearson’s Correlation of the relationship between seasonal rainfall amount and crop yields during the short rains season from 2006 to 2017 over Rwanda

Station Name	Correlation coefficient between Seasonal rainfall & Crop yield	T calculated	T tabulated	Significance at 5% level
Maize				
Save Paroisse	0.240	0.782	2.228	Not significant
Ntendezi	0.609	2.427	2.228	Significant
Gabiro	-0.108	-0.343	2.228	Not significant
Bukora	0.557	2.121*	2.228	Not significant
Kibuye	0.546	2.061*	2.228	Not significant
Rugobagoba	0.412	1.429	2.228	Not significant
Beans				
Save Paroisse	0.365	1.036	2.365	Not significant
Ntendezi	0.635	2.175*	2.365	Not significant
Gabiro	0.166	0.445	2.365	Not significant
Bukora	0.628	2.134*	2.365	Not significant
Kibuye	0.066	0.175	2.365	Not significant
Rugobagoba	0.614	2.057*	2.365	Not significant

*: significant correlation between seasonal rainfall and crop yields at 10% significance level

Table 17 indicates the results from seasonal rainfall amount correlation with maize for the period from 2007 to 2017 and with beans from 2010 to 2017 during the long rains season. There is a significant relationship at 5% significance level between seasonal rainfall amount and maize yields

over the central (Gatumba) areas of Rwanda. Again, the test of significance was conducted at 10% significance level. This revealed that the level of association between seasonal rainfall amount and maize yields was significant over the central (Gisanga) areas. Beans yields relationship with seasonal rainfall amount was also significant at that location. Hence, the researcher is confident at 90% that seasonal rainfall amount and crop yields are correlated over Gisanga in the central area of Rwanda during the long rains season as summarized in Table 17 below.

Table 17: Significance of the Pearson’s Correlation of the relationship between seasonal rainfall amount and crop yields during the long rains from 2007 to 2017 over Rwanda

Station Name	Correlation coefficient between Seasonal rainfall & Crop yields	T calculated	T tabulated	Significance at 5% level
Maize				
Gisanga	0.593	2.209*	2.262	Not significant
Rwamagana	0.395	1.289	2.262	Not significant
Gatunda	0.154	0.467	2.262	Not significant
Rwankeri	0.407	1.337	2.262	Not Significant
Gatumba	0.676	2.752	2.262	Significant
Butare Aero	-0.148	-0.449	2.262	Not significant
Beans				
Gisanga	0.696	2.374*	2.447	Not significant
Rwamagana	0.035	0.086	2.447	Not significant
Gatunda	0.355	0.929	2.447	Not significant
Rwankeri	0.508	1.444	2.447	Not significant
Gatumba	0.514	1.467	2.447	Not significant
Butare Aero	-0.472	-1.311	2.447	Not significant

*: significant correlation between seasonal rainfall and crop yields at 10% significance level

Table 18 indicates the results from seasonal rainfall intensity correlation with maize for the period from 2006 to 2017 and with beans from 2009 to 2017 during the short rains season. There is a significant relationship at 5% significance level between seasonal rainfall intensity and maize

yields over the southwestern (Ntendezi) areas of Rwanda. The significant correlation between rainfall intensity and beans yields exists over Rugobagoba in the central and Bukora in the south east of Rwanda.

Table 18: Significance of the Pearson’s Correlation of the relationship between rainfall Intensity and crop yields during the short rains season from 2006 to 2017 over Rwanda

Station Name	Correlation coefficient between Rainfall intensity & Crop yield	T calculated	T tabulated	Significance at 5% level
Maize				
Save Paroisse	0.288	0.951	2.228	Not significant
Ntendezi	0.607	2.415	2.228	Significant
Gabiro	-0.114	-0.362	2.228	Not significant
Bukora	0.517	1.909*	2.228	Not significant
Kibuye	0.531	1.982*	2.228	Not significant
Rugobagoba	0.394	1.355	2.228	Not significant
Beans				
Save Paroisse	0.308	0.856	2.365	Not significant
Ntendezi	0.656	2.299*	2.365	Not significant
Gabiro	0.096	0.255	2.365	Not significant
Bukora	0.684	2.481	2.365	Significant
Kibuye	0.496	1.511	2.365	Not significant
Rugobagoba	0.668	2.375	2.365	Significant

*: significant correlation between rainfall intensity and crop yields at 10% significance level

Again, the test of significance was conducted at 10% significance level. This revealed that the level of association between seasonal rainfall intensity and maize yields was again significant over the central western (Kibuye) and southeast (Bukora) areas of Rwanda. At this level, Beans yields relationship with seasonal rainfall intensity was also significant over Ntendezi location. Hence, the researcher is confident at 90% that seasonal rainfall intensity and crop yields are correlated over these stations during the short rains season as summarized in the Table 18 above.

Table 19 indicates the results from seasonal rainfall intensity correlation with maize for the period from 2007 to 2017 and with beans from 2010 to 2017 during the long rains season. There is a significant relationship at 5% significance level between seasonal rainfall intensity and maize yields over the central (Gisanga and Gatumba stations) areas of Rwanda.

Table 19: Significance of the Pearson's Correlation of the relationship between rainfall intensity and crop yields during the long rains season from 2007 to 2017 over Rwanda

Station Name	Correlation coefficient between Rainfall Intensity & Crop yield	T calculated	T tabulated	Significance at 5% level
Maize				
Gisanga	0.653	2.586	2.262	Significant
Rwamagana	0.438	1.462	2.262	Not significant
Gatunda	0.185	0.565	2.262	Not significant
Rwankeri	0.372	1.202	2.262	Not significant
Gatumba	0.683	2.805	2.262	Significant
Butare Aero	-0.205	-0.628	2.262	Not significant
Beans				
Gisanga	0.680	2.272*	2.447	Not significant
Rwamagana	0.094	0.231	2.447	Not significant
Gatunda	0.405	1.085	2.447	Not significant
Rwankeri	0.435	1.183	2.447	Not significant
Gatumba	0.518	1.483	2.447	Not significant
Butare Aero	-0.468	-1.297	2.447	Not significant

*: significant correlation between rainfall intensity and crop yields at 10% significance level

Again, the test of significance was conducted at 10% significance level. At this level, Beans yields relationship with seasonal rainfall intensity was significant over Gisanga location. Hence, the researcher is confident at 90% that seasonal rainfall intensity and crop yields are correlated over the central (Gisanga and Gatumba) areas during the long rains season as summarized in the Table 19 above.

Table 20 indicates the results from the rainfall frequency correlation with maize for the period from 2006 to 2017 and with beans from 2009 to 2017 during the short rains season. The number of days for example, with rainfall amount greater than 30 mm correlate with maize yield over Kibuye with a correlation coefficient of 0.507.

Table 20: Pearson's Correlation between rainfall frequency and crop yields during the short rains season from 2006 to 2017 in Rwanda

Station Names	Pearson correlation coefficient for days with rainfall of indicated amounts				
	≤ 1mm	> 1mm & 5mm	> 5mm & 15mm	> 15mm & 30mm	more than 30mm
Maize					
Save Paroisse	0.118	-0.452	-0.191	0.415	0.326
Ntendezi	-0.415	-0.211	0.369	0.355	-0.005
Gabiro	-0.027	-0.007	0.198	-0.186	-0.295
Bukora	-0.203	0.035	-0.011	0.601	0.455
Kibuye	-0.381	-0.349	0.519	0.217	0.507
Rugobagoba	-0.075	-0.314	0.292	0.302	0.439
Beans					
Save Paroisse	-0.311	-0.203	0.535	0.188	0.002
Ntendezi	-0.644	0.363	0.693	0.295	-0.206
Gabiro	-0.486	0.525	0.267	0.022	-0.176
Bukora	-0.676	0.482	0.751	0.015	0.843
Kibuye	-0.210	-0.298	0.582	0.009	-0.277
Rugobagoba	-0.789	0.597	0.435	0.375	0.069

The highest correlation coefficient (0.601) was achieved for the maize yield and the number of days with rainfall amount between 15mm and 30mm over Bukora during the short rains season. Again, the number of days with rainfall greater than 30 mm had a strong correlation (0.843) with beans yields over Bukora as summarized in the Table 20 above.

Table 21 indicates the results from the rainfall frequency correlation with maize for the period from 2006 to 2017 and with beans from 2009 to 2017 during the long rains season. The number of days for example, with rainfall amount between the 5mm and 15 mm correlate with maize yield over Rwankeri with a correlation coefficient of 0.587. The highest correlation coefficient (0.711) was achieved for the maize yield and the number of days with rainfall amount between 15mm and 30mm over Gisanga during the long rains season

Table 21: Pearson’s Correlation between rainfall frequency and Crop yields during the long rains season from 2007 to 2017 in Rwanda

Station Names	Pearson correlation coefficient for days with rainfall of indicated amounts				
	≤ 1mm	> 1mm & 5mm	> 5mm & 15mm	> 15mm & 30mm	more than 30mm
Maize					
Gisanga	-0.305	-0.581	0.223	0.711	0.405
Rwamagana	-0.407	0.024	0.368	0.215	0.462
Gatunda	-0.079	0.064	-0.147	0.277	0.347
Rwankeri	-0.382	-0.227	0.587	-0.094	0.317
Gatumba	-0.350	-0.042	0.515	0.207	0.385
Butare Aero	0.077	0.364	-0.288	-0.199	0.359
Beans					
Gisanga	-0.751	-0.206	0.703	0.575	-0.271
Rwamagana	0.125	-0.503	-0.057	0.488	0.054
Gatunda	-0.388	0.123	0.176	0.448	0.459
Rwankeri	-0.026	-0.661	0.613	-0.028	0.309
Gatumba	-0.257	-0.407	0.458	0.318	0.195
Butare Aero	0.314	-0.112	0.061	-0.585	0.143

Again, the number of days with rainfall between the 5mm and 15 mm had a strong correlation (0.703) with beans yields over Gisanga as summarized in the Table 21 above.

Table 22 indicates the results from seasonal length correlation with maize for the period from 2006 to 2017 and with beans from 2009 to 2017 during the short rains season. There is a non-significant

relationship at 5% and 10% significance level between seasonal length and maize yields over all the studied locations. The beans yields relationship with seasonal length was significant at the 5% significance level over Rugobagoba location.

Table 22: Significance of the Pearson’s Correlation of the relationship between season length and crop yields during the short rains season from 2006 to 2017 over Rwanda

Station Name	Correlation coefficient between Season length & Crop yield	T calculated	T tabulated	Significance at 5% level
Maize				
Save Paroisse	0.062	0.196	2.228	Not significant
Ntendezi	0.257	0.841	2.228	Not significant
Gabiro	0.025	0.079	2.228	Not significant
Bukora	0.157	0.503	2.228	Not significant
Kibuye	-0.153	-0.489	2.228	Not significant
Rugobagoba	0.343	1.155	2.228	Not significant
Beans				
Save Paroisse	-0.406	-1.175	2.365	Not significant
Ntendezi	0.524	1.627	2.365	Not significant
Gabiro	0.248	0.677	2.365	Not significant
Bukora	0.477	1.436	2.365	Not significant
Kibuye	0.244	0.665	2.365	Not significant
Rugobagoba	0.817	3.749	2.365	Significant

Again, the test of significance was conducted at 10% significance level. Hence, the researcher is confident at 95% that seasonal length and beans yields are correlated over the central (Rugobagoba) areas during the short rains season as summarized in the Table 22 above.

Table 23 indicates the results from seasonal length correlation with maize for the period from 2007 to 2017 and with beans from 2010 to 2017 during the long rains season. There is a significant relationship at 5% significance level between seasonal length and maize yields over the western

(Rwankeri) areas of Rwanda. Again, the test of significance was conducted at 10% significance level. Hence, the researcher is confident at 95% level that seasonal length and maize yields are correlated over the western (Rwankeri) areas during the long rains season as summarized in the Table 23 below.

Table 23: Significance of the Pearson’s Correlation of the relationship between season length and crop yields during the long rains season from 2007 to 2017 over Rwanda

Station Name	Seasonal length & Crop yield coefficient	T calculated	T tabulated	Significance at 5% level
Maize				
Gisanga	0.471	1.602	2.262	Not significant
Rwamagana	0.148	0.448	2.262	Not significant
Gatunda	0.472	1.606	2.262	Not significant
Rwankeri	0.638	2.485	2.262	Significant
Gatumba	-0.561	-2.033*	2.262	Not significant
Butare Aero	0.454	1.528	2.262	Not significant
Beans				
Gisanga	0.484	1.354	2.447	Not significant
Rwamagana	-0.448	-1.227	2.447	Not significant
Gatunda	0.641	2.045*	2.447	Not significant
Rwankeri	0.552	1.621	2.447	Not significant
Gatumba	-0.848	-3.918	2.447	Significant
Butare Aero	-0.551	-1.617	2.447	Not significant

*: significant correlation between seasonal length and crop yields at 10% significance level

CHAPTER FIVE

5.0 CONCLUSIONS AND RECOMMENDATIONS

5.1 Conclusions

In order to achieve the set objectives, Rwanda was delineated into near homogeneous rainfall zones for both the short and long rains seasons using rainfall patterns for the last 37 years. Later on, the rainfall onset and cessation; rainfall amount; rainfall frequency and intensity; rainfall trends and its magnitude and the effects of rainfall amount on crop yields for maize and beans were analyzed. The EOF analysis indicated that there exists ten and nine near homogeneous rainfall zones over Rwanda during the short and long rains, respectively. Each zone is distinct in rainfall characteristics like rainfall onset and cessation based on its location and with respect to various climate modes of variability. In terms of the onset/cessation, during the short rains season, the early onset was found in the northwestern (Tamira station) areas whereas the late onset was found in the southeastern (Bukora station) areas.

The early cessation was observed over southeastern (Bukora station) whereas the late cessation was observed over southwestern, (Ntendezi station). This is in agreement with the southward migration of Inter tropical convergence zone. During the long rains season, the early onset was recorded over the eastern slope of Crete Congo Nile at Mushubi station whereas the late one was recorded over Rwamagana station in eastern Rwanda. The early cessation was found to be over Rwamagana station again in the eastern part while the late cessation was observed over Rwankeri station in the western areas of Rwanda. This is in agreement with the northward migration of the Inter tropical convergence zone. During the short rains season, two hotspot areas were identified to have a significant trend in seasonal rainfall amount, namely, Ntendezi (southwestern) and Gabiro (northeastern). During the long rains season, three hotspot areas namely Gatumba, Mushubi and Gisanga were identified to have a significant trend in seasonal rainfall amount. There is a need to enhance strategies to maintain water for crops available.

During the short rains seasons, the analysis of monthly rainfall amount effects on crop yields, indicated that there exists a strong linear association between monthly rainfall amount and crop yields over Rugobagoba (0.817) for maize and Save Paroisse (0.745) for beans. During the long

rains, a strong linear association between monthly rainfall and crop yields exist over Gisanga locations in the central plateau with a coefficient of 0.792 for maize and of 0.859 for beans. These findings are in agreement with Muhire *et al* (2014), who identified the central plateau to be the most suitable for growing crops up to 2050 using stochastic weather generators. The poor linear association between monthly rainfall and crop yields was found mainly in eastern Rwanda. However, there exists a weak linear association between monthly rainfall and yield of beans over the central western (Kibuye) with a coefficient of 0.424 during the short rains season. The analysis of the temporal variability of crop yields revealed that the yield shortage in recent years from 2014 to 2017 was recorded. Among other rainfall characteristics, the variability in the monthly rainfall amount was able to explain 66.7% of the maize variability over Rugobagoba location and 55.4 % of the variability in beans yields over Save Paroisse during the short rains. During the long rains season, the monthly rainfall variability was able to explain 62.7% of the variability in maize yields and 73.8% of beans yields variability over Gisanga in the central plateau of Rwanda. Hence, the seasonal rainfall variability strongly affects the variability in crop yields. In order to achieve food security, prior knowledge about the anticipated seasonal rainfall characteristics is crucial.

5.2 Recommendations

The recommendations from this research targets various users like weather and climate scientists, policy makers in agriculture and finally, farmers.

5.2.1 Recommendations for Weather and Climate Scientists

The ENACTs rainfall data exhibited a slightly smoothed pattern over some locations that can be investigated further during the years from 1995 to 2005. The research findings can be used to validate the near homogeneous seasonal rainfall zones and use them in seasonal weather forecasting. In order to understand deeply the effects of rainfall amount on crop yields, there is a need to assess water availability in each delineated zones because in some zones like Gabiro, there are irrigation schemes that are independent of rainfall influences. In addition, other factors like seed variety and fertilizers need to be understood for better estimation of the crop yields and rainfall relationship.

5.2.2 Recommendations for Policy Makers

Identified hotspots need more attention in terms of policy and environmental practices in order to reduce the effects of the drying trend on water resources and food production. Information on

seasonal rainfall characteristics needs to be mainstreamed into policy and plans for agriculture in order to improve crop yields.

5.2.3 Recommendations for End users

The Bukora station with a very short seasonal length need more strategies including irrigation in terms of the growing period. Due to the observed high variability in seasonal rainfall amount over Gikonko location, there is a need to implement a scheme for crop irrigation during drier seasons.

REFERENCES

- Adelekan, I.O., & Adegebo, B.O., 2014: Variation in onset and cessation of the rainy season in Ibadan, Nigeria. *Journal of Science Research* **13**: 13 -21.
- Ahmad, I., Tang, D., Wang, T., Wang, M., & Wagan, B., 2014: Precipitation Trends over Time Using Mann-Kendall and Spearman's rho Tests in Swat River Basin, Pakistan, *Hindawi Publishing Corporation Advances in Meteorology* **2015**, Article ID 431860, 15 pages <http://dx.doi.org/10.1155/2015/431860>
- Albrecht, R. I., Goodman, J.S., Buechler, E. D., Blakeslee, J. R., Hugh, J. C., 2016: where are the lightning hotspots on Earth, *Bulletin of American Meteorological Society*, DOI: 10.1175/BAMS-D-14-00193.1
- Basalirwa C.P.K, 1995: Delineation of Uganda into Climatological rainfall zones using the method of principal component analysis, *International Journal of Climatology*, **15**, 1161-1 177 (1995)
- Basalirwa C.P.K, Odiyo J.O, Mngodo R.J, & Mpetta E.J., 1999: The Climatological regions of Tanzania based on the rainfall characteristics, *International Journal of Climatology*. **19**: 69–80 (1999)
- Blain, C.G., & Meschiatti, C.M., 2015: Inadequacy of the gamma distribution to calculate the Standardized Precipitation Index. *R. Bras. Eng. Agric. Ambiental* **19**(12), p.1129-1135. Doi: <http://dx.doi.org/10.1590/1807-1929/agriambi.v19n12p1129-1135>
- Camberlin, P., Moron, V., Okoola, R., Philippon, N., Gitau, W., 2009: Components of rainy seasons variability in Equatorial East Africa: onset, cessation, rainfall frequency and intensity, *Theoretical and Applied Climatology*
- Centre for GIS and Remote Sensing, University of Rwanda (2015, December 5th) *Rwanda Elevation Map*. Retrieved from: <http://cgis.ur.ac.rw/content/rwanda-elevation-map>
- Dinku, T., Block, P., Sharoff, J., Hailemariam, K., Osgood, D., Del Corral, J., Cousin, R., Thomson, C.M., 2014: Bridging critical gaps in climate services and applications in Africa, *Earth Perspectives*, 1:15

- Dinku, T., Cousin, R., Del Corral, J., Ceccato, P., Thomson, M., Faniriantsoa, R., Khomyakov, I., & Vadillo, A., 2016: The ENACTS approach transforming climate services in Africa one country at a time. *A World Policy Paper*
- Diro G. T., Grimes D.I.F, & Black E., 2011: Large Scale Features Affecting Ethiopian Rainfall. In “African Climate and Climate Change, Physical, Social and Political Perspectives“, Eds: Charles J. R. Williams, Dominic R. Kniveton, Springer Wien, 13-50, ISBN: 978-90-481-3841-8 (Print)
- Eliakim, M.E., 2002: Impacts of Congo convection on tropical Africa’s circulation, rainfall and resources, *MSc Thesis*, Zululand University
- Food and Agriculture Organization of the United Nations, 2010: The state of food insecurity in the world addressing the food insecurity in protracted crises
- Gachene, C.K.K., Karuma, A.N., Baaru, M.W., 2015: Climate change and crop yield in Sub – Saharan Africa. In “sustainable intensification to advance food security and Enhance Climate resilience in Africa“, Eds: Rattan Lal, Bal Ram Singh, Dismas L. Mwaseba, David Kraybil, David O. Hansen, Lars Olav Eik, *Springer International Publishing Switzerland*, ISBN 978-3-319-09359-8 (Print) DOI 10.1007/978-3-319-09360-4
- Goddard, L. and Graham, N.E., 1999: Importance of the Indian Ocean for simulating Rainfall anomalies over eastern and Southern Africa, *Journal of Geophysical Research*, **104**, NO. D16, 19,099–19,116
- Gonzalez – Rouco, J.F., Jimenez,J.L., Quesada, V., Valero, F., 2000: Quality Control and Homogeneity of Precipitation Data in the Southwest of Europe, *Journal of Climate* **14**
- Hannachi, A; Jolliffe, I.T.; Stephenson, D.B.; 2007: Empirical orthogonal function and related techniques in atmospheric science: A review. *International Journal of Climatology*, **27**: 1119-1152. Doi: 10.1002/joc.1499
- Henninger, M.S., 2013: Does the global warming modify the local Rwandan climate, *Natural science* **5**, No.1A, 124-129 (2013) <http://dx.doi.org/10.4236/ns.2013.51A019>

- Ilunga, I., & Muhire, I., 2010: comparison of the Rwandan annual mean rainfall fluctuations with the el Niño/la nina events and sunspots. *Geo-Eco-Trop.***34**:75-86
- Ilunga, I., Muhire, I., & Mbaragijimana, C., 2004: Pluviometric seasons and rainfall origin in Rwanda. *Geo-Eco-Trop.***28**, 1-2:61-68
- Ilunga, I., Mukingambeho, D., Mugwaneza, A., Mugiraneza, A., Maguru, M., Uwimana, J., Muhire, I., 2008: Probable sowing time in Rwanda. *Geo-Eco-Trop.***32**:29-36
- Indeje, M., Semazzi, F.H.M., & Ogallo, J. L., 2000: Enso signals in East African rainfall seasons, *International Journal of Climatology.* **20**: 19–46 (2000)
- Jolliffe, I.T., 2002: Principal component Analysis, second edition. Springer series in statistics. ISBN: 0-387-95442-2
- Kumar, M.N., Murthy, C.S., Sessa Sai, M.V.R., & Roy, P.S., 2009: on the use of Standardized Precipitation Index (SPI) for drought intensity assessment, *Meteorological Applications Meteorol. Appl.* **16**: 381–389 DOI: 10.1002/met.136
- Mbululo, Y., & Nyihirani, F., 2012: Climate Characteristics over Southern Highlands Tanzania, *Atmospheric and Climate Sciences*, 2012, 2, 454-463 <http://dx.doi.org/10.4236/acs.2012.24039> Published Online October 2012 (<http://www.SciRP.org/journal/acs>)
- McKee, T.B., Doesken, N.J., & Kleist, J., 1993: The relationship of drought frequency and duration of time scales. In Eighth Conference on Applied Climatology, *American Meteorological Society*, Anaheim, CA, 17–23 January 1993, 179–186.
- Mensah, C., Amekudzi, K. L., Kluste, B.A.N., & Aryee A.N.J, 2016: comparison of rainy season onset, cessation and duration for Ghana from RegCM4 and GMet Datasets. *Atmospheric and Climate Sciences* **6**, 300 – 309
- MIDIMAR, 2016: April-June 2016 Report on Disaster by Disaster Management Unit under Ministry of Disaster Management and Refugee Affairs of Rwanda: <http://www.midimar.gov.rw/index.php?id=107>

- Mugume, I., Mesquita, M.D.S., Basalirwa, C., Bamutaze, Y., Reuder, J., Nimusiima, A., Waiswa, D., Mujuni, G., Tao, S., & Ngailo, T.J., 2016: Patterns of Dekadal Rainfall Variation Over a Selected Region in Lake Victoria Basin, Uganda, *Atmosphere* 2016, *11*, 150; doi:10.3390/atmos7110150
- Muhire, I., Ahmed, F., & Abutaleb, K., 2014: Relationships between Rwandan seasonal rainfall anomalies and ENSO events, *Theoretical and Applied Climatology*. DOI 10.1007/s00704-014-1299-4
- Muhire, I., Ahmed, F., Abutaleb, K., & Kabera, G., 2015: Impacts of projected changes and variability in climatic data on major food crop yields in Rwanda. *International Journal of Plant Production*. **9** (3):347 – 372. ISSN: 1735-6814 (Print), 1735-8043 (Online)
- National Institute of Statistics of Rwanda (NISR), *GDP National Accounts*, 2017 Quarter 1 Edition, June 2017
- National Institute of Statistics of Rwanda (NISR), *Seasonal Agriculture Survey 2016 (SAS2016) report*, December 2016
- National Institute of Statistics of Rwanda (NISR), *The Statistical Yearbook*, 2014 Edition, November 2014
- Ndabarasa J.F, 2015: Characteristics of extreme rainfall events over Rwanda, *PGD thesis*, University of Nairobi
- Ngabitsinze, J.C., 2014: Analysis of economic efficiency of maize production in huye district in Rwanda. *International Journal of Agriculture Innovations and Research* **3**(3). ISSN (online) 2319-1473.
- Ngarukiyimana, J.P., Fu, Y., Yang, Y., Ogwang, B.A., Ongoma, V., & Ntwali, D., 2017: Dominant atmospheric circulations associated with abnormal rainfall events over Rwanda, East Africa. *International Journal of Climatology*. **38**:187-202. Doi:10.1002/joc.5169
- Nile Basin Water Initiative, 2008: *Efficient water use for Agriculture Production project*

- Nsubuga, F.N.W., Olwoch, J.M., Rautenbach deW.C.J., & Botai, O.J., 2014: Analysis of mid-twentieth century rainfall trends and variability over southwestern Uganda
- O'Lenic, A.E., & Livezey, E.R., 1988: Notes and Correspondence: Practical considerations in the use of Rotated Principal Component Analysis (RPCA) in diagnostic studies of Upper air-height fields, *Monthly weather review*, vol.116.
- Ogallo L.J., Janowiak J.E. and Halpert M.S., 1988: Teleconnection between Seasonal Rainfall over East Africa and Global Sea Surface Temperature Anomalies, *Journal of the Meteorological Society of Japan* **66**, No.6
- Ogungbenro, S.B., Morakinyo, T.E., 2014: Rainfall distribution and change detection across climatic zones in Nigeria. *Weather and Climate Extremes* (2014), <http://dx.doi.org/10.1016/j.wace.2014.10.002>
- Omondi, A.P., Awange, L.J., Forootan, E., Ogallo, A.L., Barakiza, R., Girmaw, B.G., Fesseha, I., Kululetera, V., Kilembe, C., Mugunga, M.M., Kilavi, M., King'uyu, M.S., Omeny, A.P., Njogu, A., Badr, M.E., Musa, A.T., Muchiri, P., Bamanya, D., & Komutunga, E., 2013: Changes in temperature and precipitation extremes over the Greater Horn of Africa region from 1961 to 2010. *International Journal of Climatology*. DOI: 10.1002/joc.3763
- Omondi, P., Awange, J.L., Ogallo, L.A., Okoola, R.A., & Forootan, E., 2012: Decadal rainfall variability modes in observed rainfall records over East Africa and their relations to historical sea surface temperature changes, *Journal of Hydrology* 464-465 (2012) 140-156
- Ongoma, V., Chen, H., & Omony, G.W., 2016: Variability of extreme weather events over the equatorial East Africa, a case study of rainfall in Kenya and Uganda, *Journal of Theoretical and Applied Climatology* DOI 10.1007/s00704-016-1973-9
- Ongoma, V., Guirong, T., Ogwang, B.A., Ngarukiyimana, J.P., 2015: Diagnosis of Seasonal Rainfall Variability over East Africa: A Case Study of 2010-2011 Drought over Kenya, *Pakistan Journal of Meteorology* **11**, Issue 22: Jan 2015

- Sanogo, S, Fink, A.H., Omotosho, A.J., Ba, A., Redl, R., & Ermert, V., 2015: Spatio-temporal characteristics of the recent rainfall recovery in West Africa. *International J. Climatol.*, 35, 4589–4605, DOI: 10.1002/joc.4309
- Sebaziga, N.J., 2014: Association between Madden Julian oscillations and wet and dry spells over Rwanda, *PGD Thesis*, University of Nairobi
- World Meteorological Organization (WMO), 2012: Standardized Precipitation Index User guide. WMO-N0.1090
- Wu, H., Hayes, J.M., Wilhite, A.D., Svoboda, D.M., 2005: the effect of the length of record on the standardized precipitation index calculation. *International Journal of Climatology* 25 (2005), pp. 505–520; doi: 10.1002/joc.1142
- Wu, H., Svoboda, D.M., Hayes, J.M., Wilhite, A.D., & Wen, F., 2007: Appropriate application of the standardized precipitation index in arid locations and dry seasons. *International Journal of Climatology*. 27: 65–79 DOI: 10.1002/joc.1371
- Zhang X., Lisa, A., Hegerl, C.G., Jones, P., Tank, K.A., Peterson, C.T., Trewin, B., & Zwiers, W.F., 2011: Indices for monitoring changes in extremes based on daily temperature and precipitation data. *WIREs Clim. Change* 2: 851–870, doi: 10.1002/wcc.147.

APPENDICES

STATISTICAL TECHNIQUES

A: Homogeneity and Normality Tests of Climate Data

A.1: The double Mass curve Method

This study used the double mass curve method to test the homogeneity of rainfall data in the data quality control process. This method is based on the concept of two cumulative quantities during the same period that must feature a straight-line graph as long as the proportion between the two remain constant. The slope of the line express the proportion (Gonzalez-Rouco *et al*, 2000; Mugume *et al*, 2016).

Let Y and X be two datasets where:

$$Y = y_1, y_2, y_3, \dots, y_n \text{ And } X = x_1, x_2, x_3, \dots, x_n \quad (\text{A1-1})$$

Such that the cumulative values of y denote Y and the cumulative values of x denote X as follows:

$$Y_i = \sum_{i=1}^n y_i \text{ and } X_i = \sum_{i=1}^n x_i \quad (\text{A1-2})$$

A double mass curve is known as the graph of a curve passing through the couple of points(Y_i, X_i).

A.2 The Shapiro-Wilk's (w) Normality test

The test of normality using the Shapiro-Wilk's statistics assumes a null hypothesis of the rainfall data to be normally distributed (Mugume *et al*, 2016) along the mean rainfall for a given period.

Let the seasonal rainfall amount be: $R_1, R_2, R_3, \dots, R_n$ for each station where the subscript represents the order of data.

The Shapiro-Wilk's test statistics were given by:

$$W = \frac{(\sum_{i=1}^n \alpha_i R_i)^2}{\sum_{i=1}^n (R_i - \bar{R})^2} \quad (\text{A2-1})$$

In Equation (A2-1), R_i is the smallest i^{th} seasonal rainfall value, \overline{R}_i represents the seasonal rainfall mean for a given location. The mean is computed as:

$$\overline{R}_i = \frac{1}{n} \sum_{i=1}^n R_i \quad (A2-2)$$

Moreover, α_i is the constant depending on expected value of order statistics from a standard normal distribution. The value of w is such that: $0 < w < 1$. The highest normality were achieved when $w \rightarrow 1$ for a given station.

B: Normalized departures

The normalized departure for any meteorological variable is calculated (Mugume *et al*, 2016) as:

$$N_D = \frac{X - \mu}{\sigma} \quad (B-1)$$

In Equation (B-1), N_D denotes the normalized variable; X is the observed value of the variable; μ is the long term mean for data over a station whereas the σ is the standard deviation for each station.

C. Procedure and Formula for computation of SPI

The Standardized Precipitation Index (SPI) is a normalized index, which means an index with transformed values (Kumar *et al*, 2009), so that:

- (i) The mean for a given period is adjusted to zero;
- (ii) The standard deviation of the observed precipitation becomes one (1.0); and
- (iii) The Skewness of the precipitation data is adjusted to zero.

The standardized Precipitation Index (SPI) was used to denote a mean rainfall that is null and a standard deviation of 1.0 in case the conditions (i); (ii) and (iii) were achieved.

The mean precipitation for any location is calculated as follows:

$$\bar{X} = \frac{\sum X}{N} \quad (C-1)$$

In Equation (C-1), N is the number of observed precipitation events; X is the precipitation value for each season.

The standard deviation of the precipitation for a given location is expressed as:

$$\sigma = \sqrt{\frac{\sum(X-\bar{X})^2}{N}} \quad (C-2)$$

The Skewness of the precipitation distribution is given by the equation (C-3):

$$Skewness = \frac{N}{(N-1)(N-2)} \sum \left(\frac{X-\bar{X}}{\sigma} \right)^3 \quad (C-3)$$

The precipitation data are converted into lognormal values and U statistics and later the shape and scale parameter of the gamma distribution are calculated as follows:

$$Logmean = \ln(\bar{X}) \quad (C-4)$$

$$U = \ln(\bar{X}) - \frac{\sum \ln(X)}{N} \quad (C-5)$$

The shape parameter is given by:

$$\beta = \frac{1 + \sqrt{1 + \frac{4U}{3}}}{4U} \quad (C-6)$$

The scale parameter is given by the expression (C-7):

$$\alpha = \frac{\bar{X}}{\beta} \quad (C-7)$$

The cumulative gamma probability of an observed precipitation event is given by the expression (C-8) below:

$$G(x) = \frac{\int_0^x x^{\alpha-1} e^{-\frac{x}{\beta}} dx}{\beta^{\alpha} \Gamma(\alpha)} \quad (C-8)$$

The gamma distribution is undefined at $x = 0$ due to zero in the observed precipitation. Hence, the cumulative probability becomes:

$$H(x) = q + (1 - q)G(x) \quad (C-9)$$

In Equation (C-9), q is the probability of zero.

The cumulative probability $H(x)$ is transformed into the standard normal random variable Z with mean zero and variance of one. According to Edwards and McKee (1997), the standard normal variable Z provides the value of SPI. The approximate conversion provided by Abramowitz and Stegun (1965) as an alternative give:

$$Z = \text{SPI} = - \left(t - \frac{C_0 + C_1 t + C_2 t^2}{1 + d_1 t + d_2 t^2 + d_3 t^3} \right)$$

For $0 < H(x) \leq 0.5$ (C-10)

And

$$Z = \text{SPI} = + \left(t - \frac{C_0 + C_1 t + C_2 t^2}{1 + d_1 t + d_2 t^2 + d_3 t^3} \right)$$

For $0.5 < H(x) \leq 1$ (C-11)

In Equation, C-10 and C-11,

$$t = \sqrt{\ln \left(\frac{1}{H(x)^2} \right)} \quad \text{For } 0 < H(x) \leq 0.5 \quad \text{(C-12)}$$

$$\text{And } t = \sqrt{\ln \left(\frac{1}{(1.0-H(x))^2} \right)} \quad \text{For } 0.5 < H(x) \leq 1 \quad \text{(C-13)}$$

In Equation, C-10 and C-11, constants, $C_0, C_1, C_2, d_1, d_2, d_3$ are given as: $C_0 = 2.51557$; $C_1 = 0.802583$; $C_2 = 0.010328$; $d_1 = 1.432788$; $d_2 = 0.189269$; $d_3 = 0.001308$ respectively.